SQT

Utility of Correlation Techniques in Gravity and Magnetic Interpretation

Val W. Chandler, John F. Koski,
Lawrence W. Braile, and William J. Hinze

Department of Geosciences
Purdue University
West Lafayette, Indiana 47907

January, 1977

Final Report of NASA Contract No. NAS5-22816

Prepared for

Goddard Space Flight Center
Greenbelt, Maryland 20771

Abstract (cont'd)

length anomalies, and isolating geomagnetic field removal problems. Thus, these techniques are useful in considering regional data acquired by satellites.

PREFACE

Correlation of gravity and magnetic anomaly data is useful in improving the interpretation of the common geological source of these anomalies and in isolating and identifying specific anomalies. The objectives of this study were: 1) to develop analytical techniques which can be used in combined analysis of these anomalies and to prepare computer codes for implementing these techniques and 2) to determine the range of validity, methods of implementation, application, and limitations of these procedures by applying them to both theoretical and observed anomaly data.

Two correlation techniques were selected for study on the basis of their potential to fulfill the requirements of the correlation analysis. Principal attention was given to a modification of a statistical correlation method known as internal correspondence. This method utilizes Poisson's theorem in a moving-window linear regression analysis performed between the anomalous magnetic data reduced to the pole and the first vertical derivative of the gravity anomaly. The regression parameters of the linear regression, correlation coefficient, slope and intercept provide information on the nature of the relation between gravity and magnetic anomalies that significantly contributes to geological and geophysical interpretation. Clustering is the other correlation technique studied in this investigation. Cluster analysis is a general pattern recognition scheme involving the classification of a data set into groups of similarity. The similarity is based on quantitative comparison of measured or derived gravity and magnetic variables. The internal correspondence and clustering methods have been investigated by application of the methods to theoretical test cases where the results could be checked against known anomaly source characteristics. These studies have been extended to several sets of observed regional gravity and magnetic anomaly data. Particular emphasis has been placed upon investigations and applications of the internal correspondence method.

Analysis of the internal correspondence results is an extremely useful quantitative method of correlating gravity and magnetic anomalies and the applicability of Poisson's theorem can be dramatically extended using this technique. Specifically, studies to date show that internal correspondence can be useful in identifying crustal provinces, providing information on horizontal and vertical variations of physical properties of the crust over province size areas, validating the presence of long-wavelength anomalies, and isolating problems of geomagnetic field removal from magnetic observations. The results of the clustering studies are encouraging, but not definitive. The method appears to have considerable potential in performing combined magnetic and gravity interpretation employing a large number of attributes of extensive data sets with a minimum of subjectivity. However, much work remains to be done in clustering. Determination of significant variables, subarea sizes and geological resolution must be further investigated utilizing both model studies and observed data over known geological terrains. The application of advanced pattern recognition techniques such as supervised learning and discrimination techniques should prove very helpful in these studies. Future studies in internal correspondence are needed to incorporate the signs of anomalies into the regression parameters, study the effects of remanent magnetizations, develop schemes for recognition of valid internal correspondence parameters, and correlate $\Delta J/\Delta\sigma$ ratio to geologic properties and lithology.

Both internal correspondence and clustering should be applied to a large two-dimensional data set where the geological sources of gravity and magnetic data are relatively well known. This step has been initiated by the synthesis and digitization of gravity and magnetic anomaly data centered around the state of Michigan. Additional studies are warranted on the application of these techniques to geophysical data acquired at satellite elevations by using data observed, projected, or modeled at these elevations. The interpretation of large data sets acquired by

satellites should be particularly enhanced by correlation techniques.

Computer codes unique to the techniques discussed in this report are available upon request from the Geophysics Branch, National Aeronautics and Space Administration, Goddard Space Flight Center, Greenbelt, Maryland 20771.

TABLE OF CONTENTS

LIST OF FIGURES

Figures cont'd page

Figures cont'd page

Figures cont'd page

Figures cont'd page

Figures cont'd page

List of Tables

CHAPTER I

INTRODUCTION

The geologic interpretation of magnetic and gravity anomaly data is ambiguous and subjective. It can be shown through an extension of Green's Theorem of Equivalent Layer that observed anomaly values can be reproduced by an infinite number of surface distributions shallower than the maximum possible source of the anomaly. Additional ambiguity is derived from interference of anomalies and inadequate isolation of anomalies. An important method of reducing this ambiguity is the correlation of magnetic and gravity anomalies. The basis of correlation techniques is the hypothesis, commonly validated by observation, that variations in lithology and physical properties of the crystalline crust are reflected in both their gross mineralogy which controls rock density, and thus gravity anomalies, and their minor mineral content, specifically magnetite, which is the primary cause of magnetic anomalies.

Despite the complex, non-linear, and non-universal relationship between the rock properties which cause magnetic and gravity anomalies, the correlation of these anomalies has become a standard aid to geological and geophysical interpretation. An important use of combined magnetic and gravity analysis is the identification of anomaly source lithology. Hinze et al. (1975) have reviewed literature showing the problems of specific source lithology identification, but many generalizations are possible, particularly within specific geologic terrains. These generalizations are based upon physical property studies and correlation of anomalies with direct geologic information. A related use of correlation of gravity and magnetic anomalies is the mapping and characterizing, both horizontally and vertically, of geologic provinces that reflect units of relatively homogeneous lithologic suite, tectonics, and geophysical parameters. An additional potential use of correlation of gravity and magnetic anomalies is in the isolation and identification of these anomalies. The separation and recognition of individual anomalies is difficult under even optimum conditions. The problem

becomes particularly troublesome where the signal to noise ratio is low or multiple processing stages which may alter the anomalies have been used in the analysis of the data. Such is the case in dealing with most long wavelength anomalies and particularly magnetic anomalies observed at satellite elevations. One procedure which can be used to validate the isolated anomalies is to correlate them with geological data or gravity data. A corollary of this latter application is the use of correlation of gravity and magnetic anomalies to isolate problems of elimination of the geomagnetic field from observed magnetic data. All of these potential applications of combined magnetic and gravity analysis take on particular importance with the need for interpretation of large geophysical data sets covering extensive areas that are rapidly becoming available from satellite and similar regional surveys.

Magnetic and gravity correlation analysis has been effected by a wide range of methodologies. A combined analysis flow chart shown in Figure 1 specifies these techniques and classifies them in terms of decreasing subjectivity from qualitative to quantitative methods. Correlation of these potential field anomalies has been accomplished largely by qualitative visual-spatial correlation over regional areas or by inverse modeling and quantitative Poisson's theorem methods restricted to one or at most a few well-isolated anomalies.

A study has been performed to investigate those methods which are capable of analyzing regional areas, like visual-spatial correlation, but yield a form of objective, quantitative information like Poisson's theorem. Two methods have been investigated and are illustrated by application to theoretical models and observed data. The internal correspondence method has been modified to incorporate Poisson's theorem. This method, which received primary attention, involves a moving-window linear regression analysis between the anomalous first vertical derivative of gravity and total magnetic intensity reduced to the pole. Cluster analysis was also studied as an approach to magnetic and gravity correlation. Cluster analysis is a pattern recognition technique that

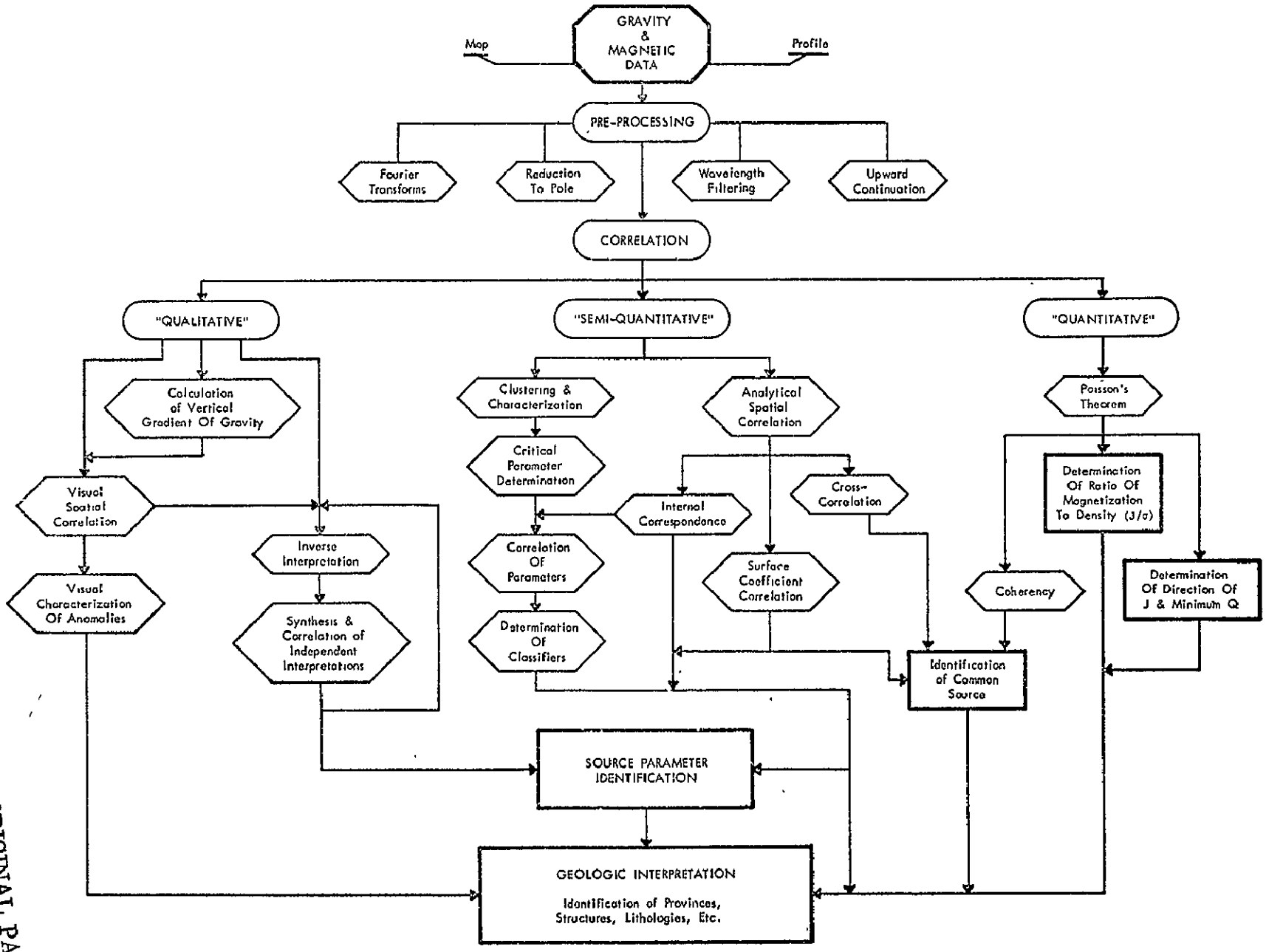

Figure 1. Combined gravity and magnetic analysis flow chart.

involves classification of a data set into groups of similarity based on correlation of measured or derived attributes.

The literature of combined magnetic and gravity analysis is reviewed by Hinze et al. (1975) and an annotated bibliography on the subject is presented.

CHAPTER II

PRINCIPLES OF INTERNAL CORRESPONDENCE

Effective correlation of gravity and magnetic data can be achieved by a method called internal correspondence analysis (ICA). A simplified form of the method was initially proposed by Robinson (1962) as a means of correlating two sets of contoured geographic data. Hinze et al. (1975) and Chandler et al. (1975) demonstrated the use of an improved method of ICA on gravity and magnetic data. This approach involved a moving-window linear regression analysis between sets of standardized gravity and magnetic profiles. Recent studies have indicated a more effective approach of ICA is between the first vertical derivative of gravity and the magnetics reduced to the pole. The advantage to this approach lies in consideration of Poisson's theorem.

The Incorporation of Poisson's Theorem into Internal Correspondence Analysis

The relationship between the gravitational and magnetic potentials arising from a common source was shown by Poisson (1826) to be

$$V = \frac{J}{\sigma G} \frac{\partial U}{\partial i}$$

where V = the magnetic potential

U = the gravitational potential

J = the source magnetization

i = the direction of source magnetization

σ = the source density

G = the universal gravitational constant.

In order for this relationship to be theoretically valid, it must be assumed that the source has a uniform distribution of density, magnetization, and direction of magnetization. Because of these assumptions, the geophysical applications of Poisson's theorem have been usually restricted to simple, well-isolated anomalies.

Recent studies, however, indicate that a more generalized form of Poisson's theorem, when used in conjunction with ICA, can often yield

significant results - even when the theoretical assumptions are clearly violated. If vertical magnetic polarization can be assumed, Poisson's theorem may be differentiated along the vertical direction z to yield

$$T_z = \frac{J}{\sigma G} \frac{\partial g_z}{\partial z}$$

where T_z = the total magnetic field reduced to vertical polarization

g_z = the vertical component of gravity acceleration (quantity measured in most surveys).

When dealing with gravity and magnetic anomalies a more useful equation is

$$T_z = A + \frac{\Delta J}{\Delta \sigma G} \frac{\partial g_z}{\partial z}$$

where ΔJ and $\Delta \sigma$ are magnetization density contrasts, respectively and A is an intercept term to account for constant anomaly base level. When an anomaly of interest is found to interfere with anomalies from nearby, dissimilar sources; the above relationship is incorrect. However, as further discussions will demonstrate, the relationship is often approximately correct within a small spatial segment of the anomaly of interest.

Preprocessing of Data

The methodology of ICA is summarized on the flow chart in Figure 2. Some of the steps presented in this illustration are optional and shall be discussed in the next chapter. The gravity and magnetic data, in either map or profile form, must be digitized at a constant interval and registered. All data must be observed at a common level. If this is not the case initially, reduction to a common level is accomplished by upward continuation. The first vertical derivative of gravity and magnetics reduced to the pole are calculated and it will be on these data that ICA will be conducted.

In this study the reduction to the pole as well as differentiation

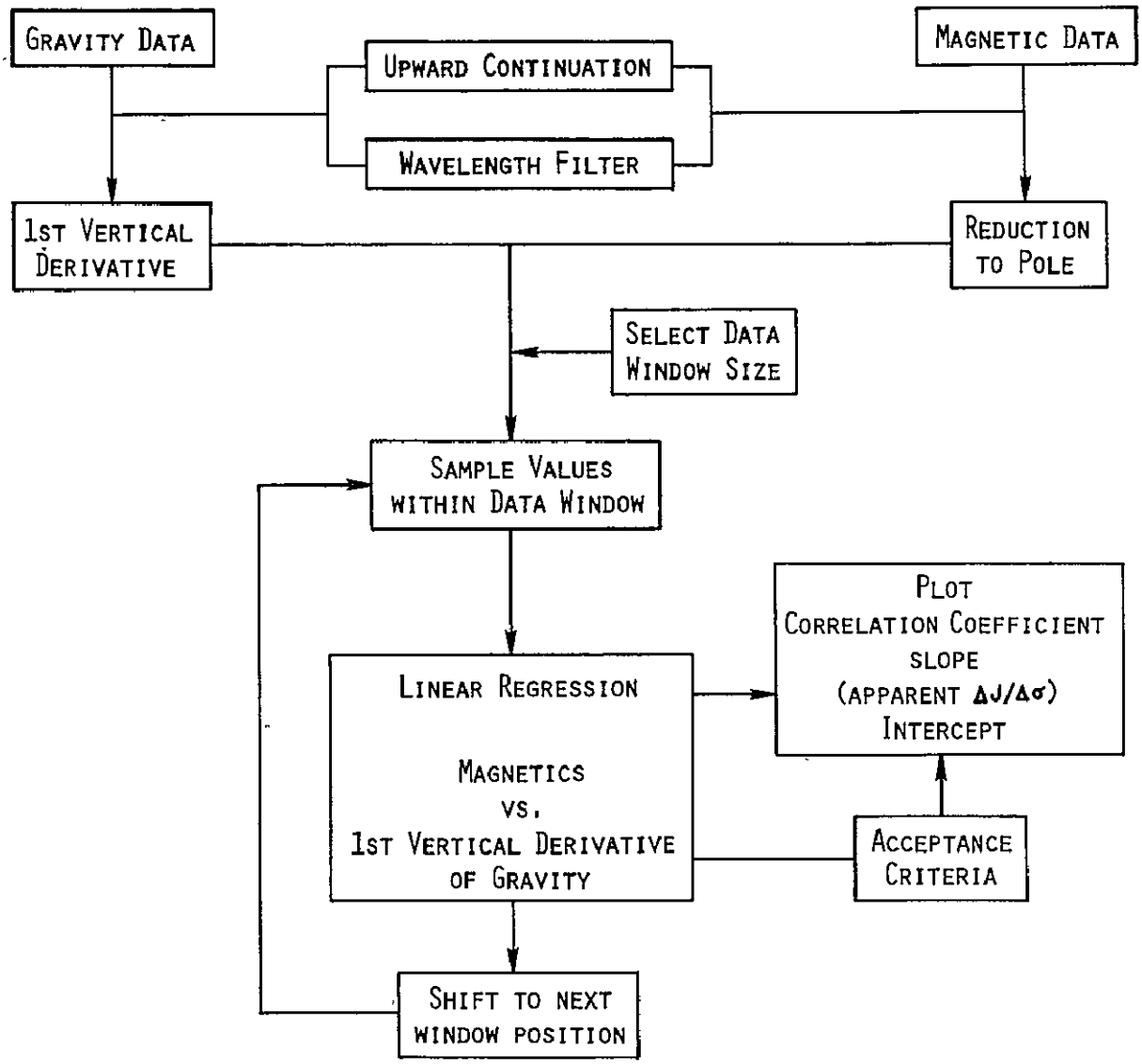

Figure 2. Internal correspondence analysis flow chart.

and continuation of gravity and magnetic data (Baranov, 1957; Bhattacharyya, 1965, 1972) are accomplished in the frequency domain. For simplicity of illustration, examples of the ICA method employ profile data associated with strike infinite sources. However, the ICA method can be easily applied to gridded map data by using a square moving window and two-dimensional preprocessing.

Internal Correspondence

Internal correspondence involves performing a least squares linear regression using reduced to pole magnetic anomaly values versus vertical gradient of gravity anomaly values within a moving data window.

The procedure carried out by internal correspondence analysis is demonstrated in Figure 3. A window size is specified by the user and initially positioned at the left margin of the data set. Guidelines for selecting a window size shall be discussed in the next chapter. Least squares linear regression is performed between data points within the window. The vertical derivative of gravity has been arbitrarily assigned as the independent variable for the regression. This choice is not critical because interpretation is limited to areas of high correlation coefficients. The regression yields three coefficients: correlation, slope, and intercept. The slope coefficient is corrected for the gravitational constant and converted into cgs units in order to yield an apparent $\Delta J/\Delta\sigma$ estimate. All three regression coefficients are assigned the spatial coordinate of the center of the window. The window is then shifted one digital position to the right and the process is repeated. This operation is carried out until the entire data set is analyzed and three regression coefficient profiles have been generated.

Significance of the Internal Correspondence Coefficients

The significance of the three ICA coefficients is clarified by

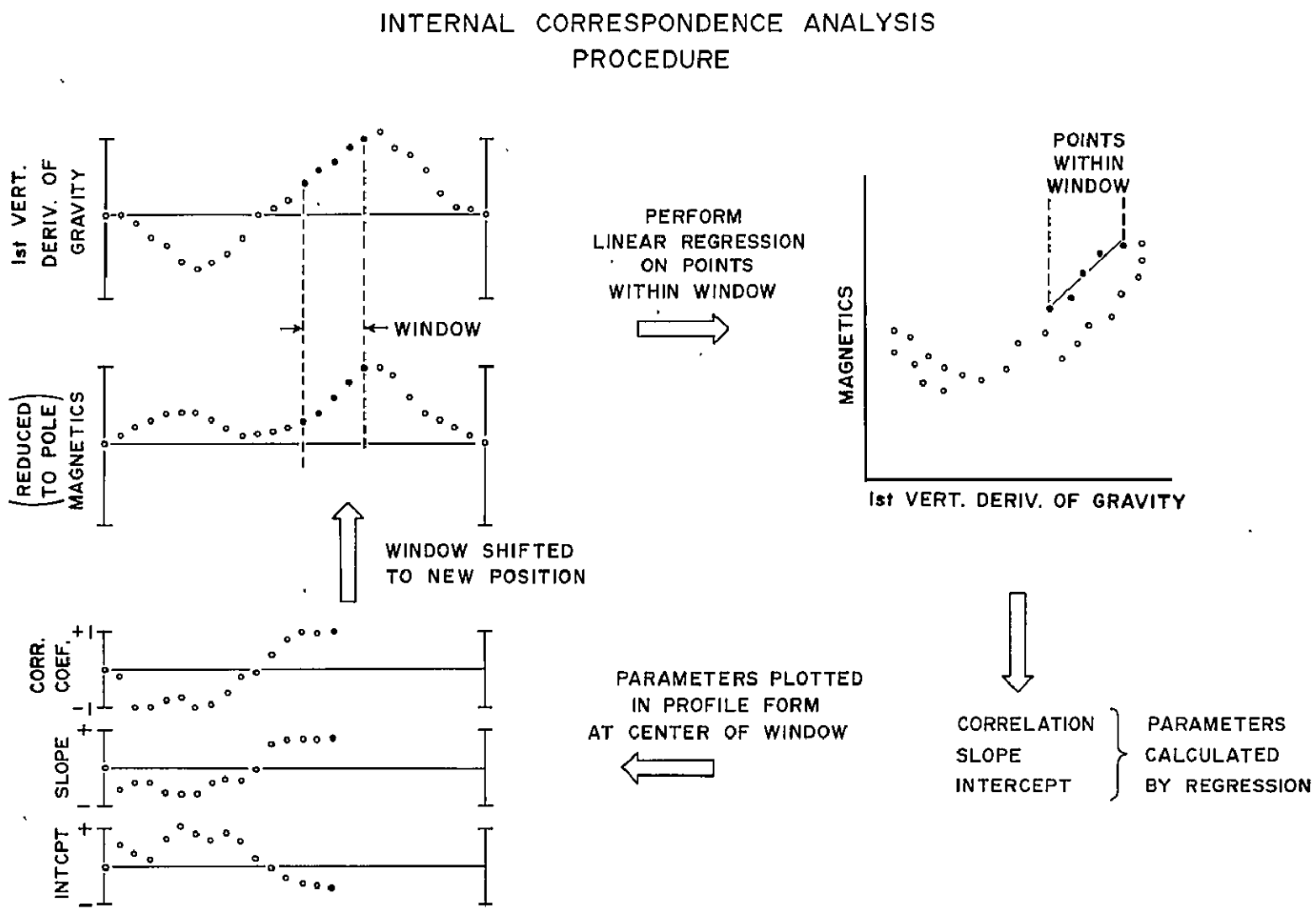

Figure 3. Internal correspondence analysis procedure.

considering the modified form of Poisson's theorem in Figure 4. This form of the theorem states that the vertical derivative of gravity and the magnetics reduced to the pole are linearly related by a slope $\Delta J/\Delta\sigma G$ and an intercept A. Similarly, the three ICA parameters represent a fitted linear relationship between the first vertical derivative of gravity and the magnetics reduced to the pole. Thus, several important analogies between the ICA coefficients and Poisson's theorem are readily apparent.

Each slope coefficient from ICA is corrected for the universal gravitational constant and converted into cgs units. In this form the slope coefficient is equivalent to the $\Delta J/\Delta\sigma$ ratio of the anomalous source considered in Figure 4. It will be demonstrated in the next chapter that this $\Delta J/\Delta\sigma$ estimate can be reasonably accurate, even when the assumptions inherent to Poisson's theorem are not strictly upheld.

An accurate estimate of $\Delta J/\Delta\sigma$ is not uniquely definitive of lithology and is a function of the country rock with which the anomalous source contrasts (Hinze et al., 1975). In addition, different combinations of density and magnetization contrasts yield the same ratio value. However, if the $\Delta J/\Delta\sigma$ estimate is considered along with the original anomalies, as well as with any other geophysical or geologic information, it can serve as a useful constraint on interpretation. Two extremes of source $\Delta J/\Delta\sigma$ are possible; a value of zero for a gravity anomaly with no magnetic expression and a value of infinity for a magnetic anomaly with no gravity expression.

The correlation coefficient generated by ICA expresses the significance of the linear fit for a given window position. The most significant linear regressions will have an associated correlation coefficient value near either -1.0 or 1.0. A negative correlation coefficient indicates an inverse relationship. A positive correlation coefficient indicates a direct relationship; either both anomalies are positive or negative. As a result, it is helpful to refer to the

$$T_z = A + \left(\frac{1}{G}\frac{\Delta J}{\Delta \sigma}\right)\left(\frac{\partial g_z}{\partial z}\right)$$

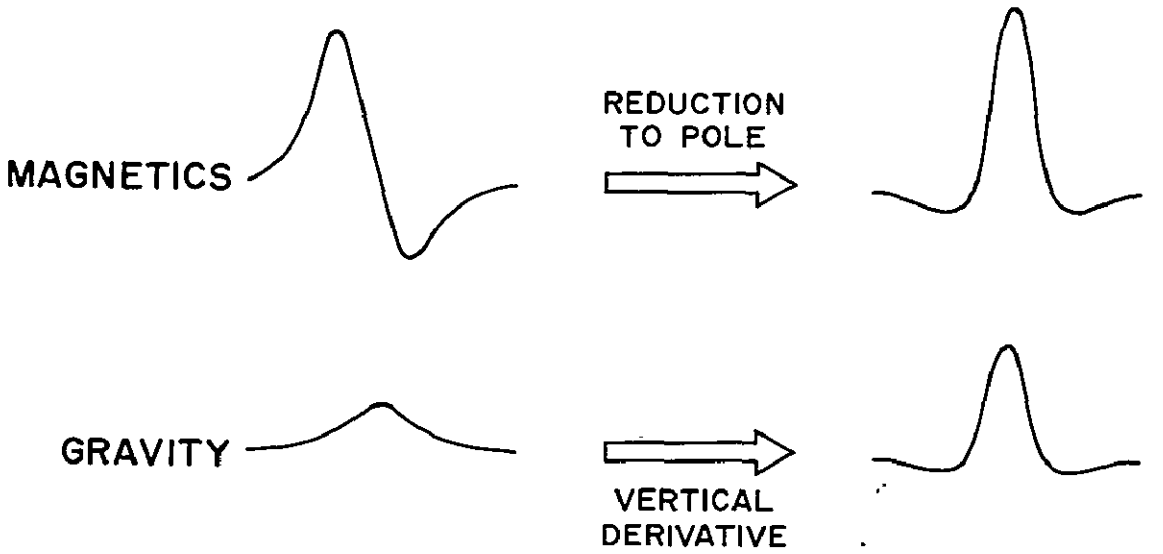

T_z = TOTAL FIELD MAGNETIC ANOMALY AT VERTICAL POLARIZATION

A = INTERCEPT

G = GRAVITATIONAL CONSTANT

g_z = VERTICAL COMPONENT GRAVITY

ΔJ = MAGNETIZATION CONTRAST

$\Delta \sigma$ = DENSITY CONTRAST

Figure 4. The generalized form of Poisson's theorem used in internal correspondence analysis.

original data in the interpretation process. The correlation coefficient also aids in the evaluation of the associated $\Delta J/\Delta\sigma$ estimates; a meaningful $\Delta J/\Delta\sigma$ estimate is not likely to occur if the regression indicates a poor linear correlation.

The intercept coefficient should be zero or at a constant base level value if the assumptions inherent to Poisson's theorem are upheld. Therefore, the presence of fluctuating ICA intercept coefficients reflect violations to these assumptions. Accordingly, the behavior of the intercept profile serves as another evaluation criteria for associated $\Delta J/\Delta\sigma$ estimates; regions of erratic intercept behavior are generally not associated with valid $\Delta J/\Delta\sigma$ estimates.

In order to demonstrate the method, internal correspondence analysis was performed on the theoretical gravity and magnetic profiles due to an isolated source (Figure 5). For simplicity all models illustrated in this study assume that individual anomaly-producing sources possess uniform properties. It is also assumed that all sources are polarized by a vertical magnetic field with an intensity of 58,000 gammas.

The internal correspondence results of the isolated anomaly profiles in Figure 6 have a correlation coefficient of essentially 1.0, or nearly perfect positive correlation and a correct estimate of $\Delta J/\Delta\sigma$ over the source. The intercept is less than one part in one thousand of the amplitude of the magnetic anomaly, and can be considered zero for practical purposes. The linearity of the magnetics versus vertical gradient of gravity relation is illustrated in Figure 7.

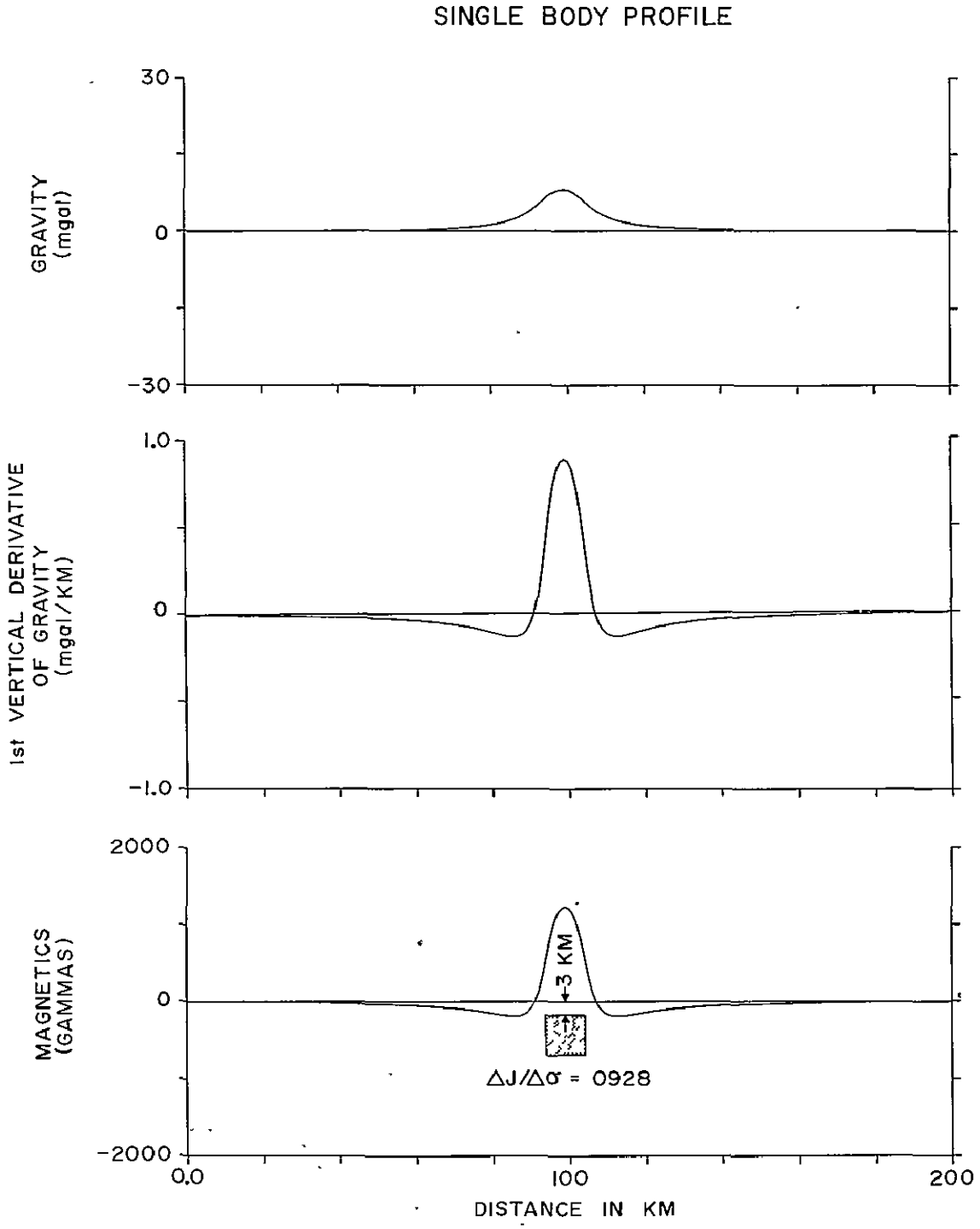

Figure 5. Isolated source: gravity, first vertical derivative of gravity, and magnetic anomaly profiles.

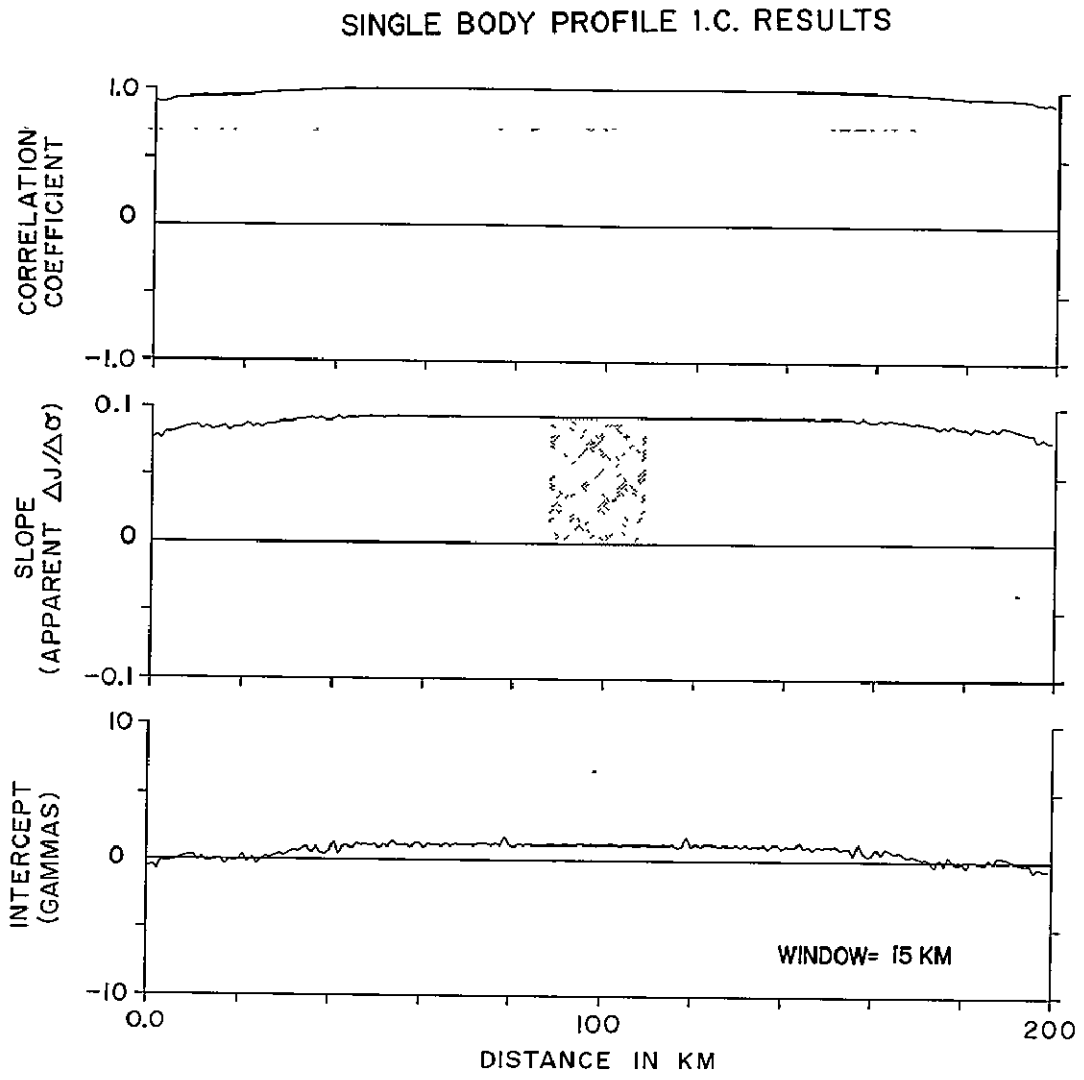

Figure 6. Isolated source: internal correspondence results. Level of the stippled bar equals the source body $\Delta J/\Delta\sigma$, 0.0928.

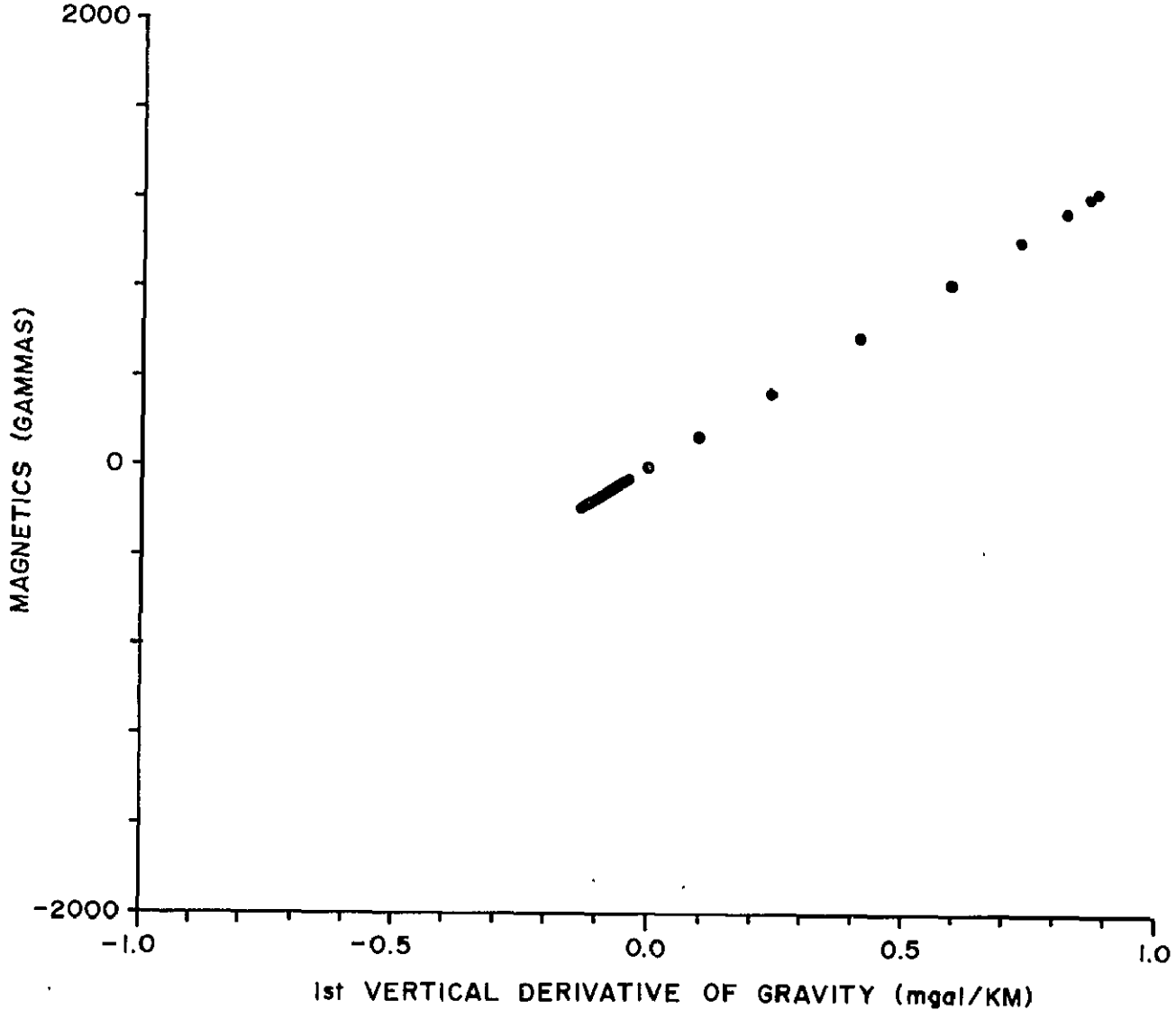

Figure 7. Magnetics versus first vertical derivative of gravity for an isolated source.

CHAPTER III

IMPLEMENTING INTERNAL CORRESPONDENCE ANALYSIS

Poisson's theorem and internal correspondence analysis (ICA), as described in the previous chapter, are independent of the wavelength of the anomaly and thus, theoretically, the analysis may be applied to long or short wavelength anomalies, at any elevation, and over the flanks of anomalies as well as over the central areas. The validity of the ICA results is limited only by the assumptions implicit in the application of Poisson's theorem and the accuracy of the necessary processing steps of reduction to the magnetic pole and taking the first vertical derivative of gravity data. It will be assumed that these preprocessing steps can be performed satisfactorily, and in this chapter we will study the effects of various types and amounts of anomaly interference which are violations of the conditions implied in Poisson's theorem. Model studies will be used to analyze the validity of $\Delta J/\Delta\sigma$ estimates derived from ICA. The enhancement of results by preprocessing of the data and effects of window length will be investigated.

Anomaly Superposition

Significant results can be obtained from internal correspondence analysis in certain cases of superimposed anomalies despite violation of the assumptions of Poisson's theorem. The combined gravity and magnetic anomalies resulting from two sources are shown in Figure 8. The lower source at a depth of 13 km has a $\Delta J/\Delta\sigma$ one-half that of the upper source which is at a depth of 3 km. The internal correspondence results shown in Figure 9 have a high correlation over the main portion of the anomalies. The nonzero intercept and the spikes in the slope and intercept plots indicate that interference of anomalies is present. These spikes occur in the transition zone between the outer limits of the anomalies where the amplitude effect of the anomaly due to the upper source gives way to the effect of the lower sources. The slope parameter over the central portion of the anomaly yields a $\Delta J/\Delta\sigma$ estimate which is not representative of either source, but is a weighted average

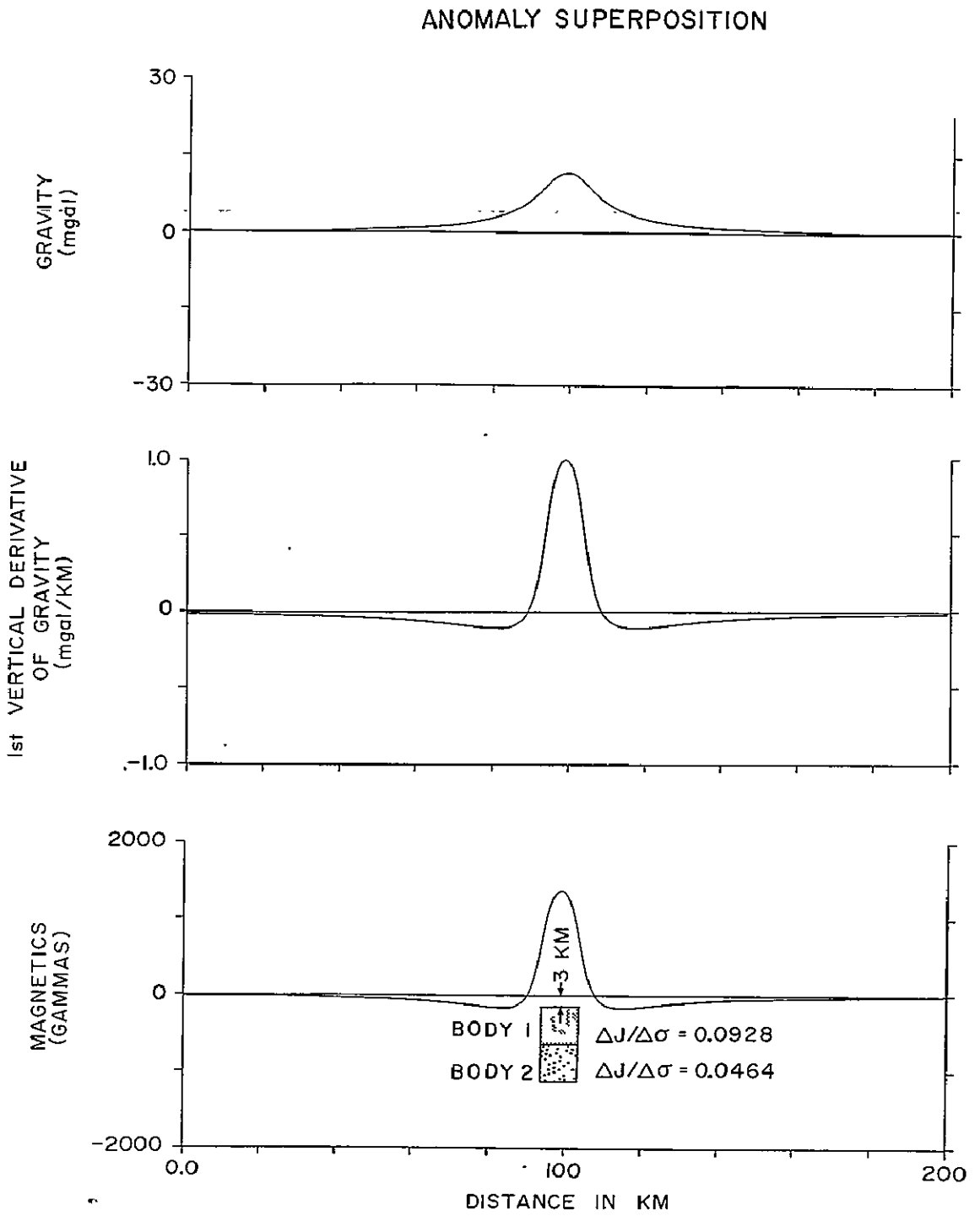

Figure 8. Gravity, first vertical derivative of gravity and magnetic anomaly profiles due to two superimposed sources with different $\Delta J/\Delta\sigma$ values.

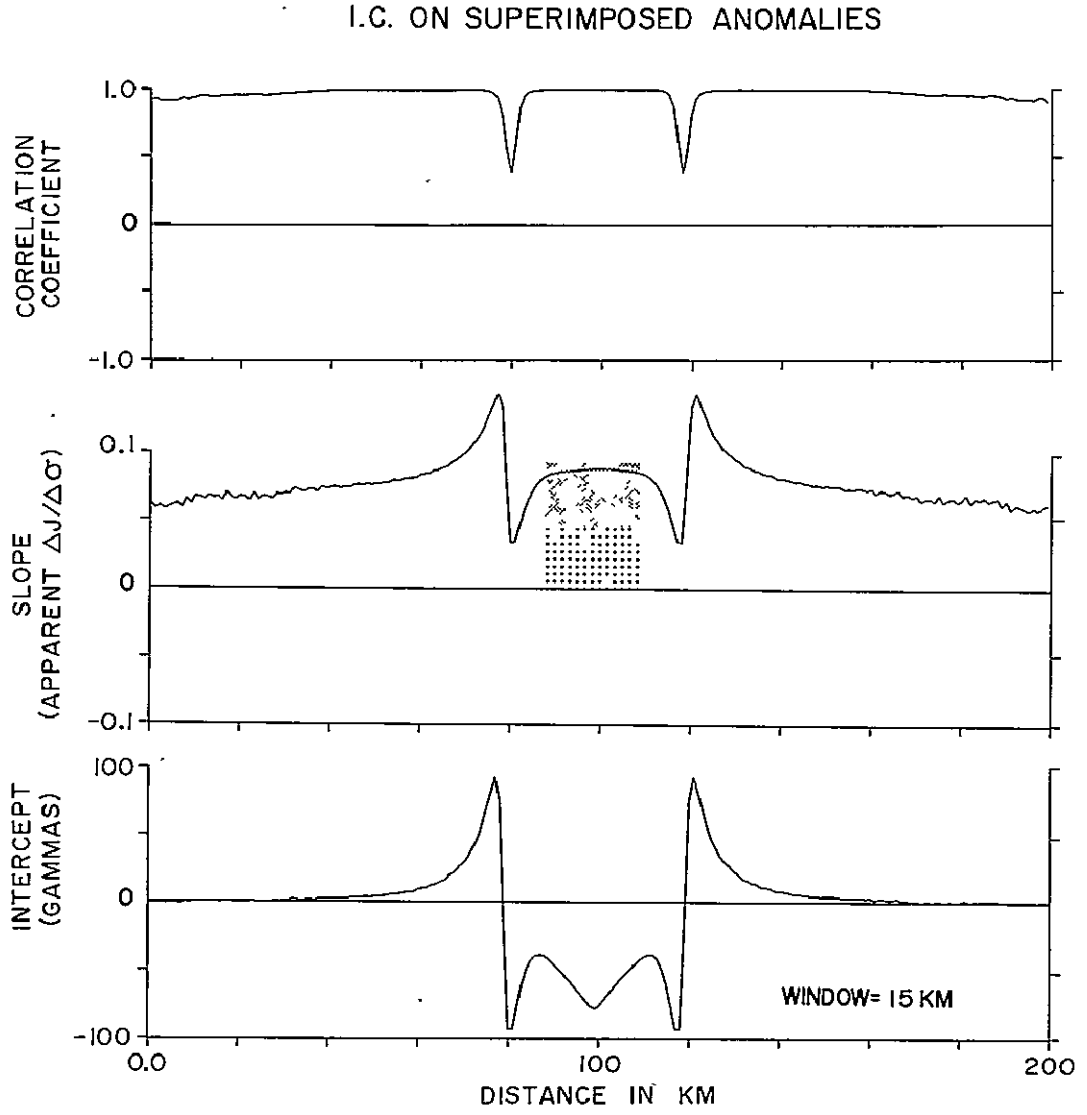

Figure 9. Superimposed anomaly sources: internal correspondence results. The level of the fine stippled bar equals the $\Delta J/\Delta\sigma$ of the upper source, 0.0928, the bold of the lower source, 0.0464.

of the effects of the two sources. The $\Delta J/\Delta\sigma$ estimate in this case is most heavily weighted by the shallower source.

The $\Delta J/\Delta\sigma$ estimate of interfering anomalies is a resultant of the vector sum of magnetic versus vertical gradient of gravity values due to the two sources as illustrated in Figure 10. Magnetic versus first vertical derivative of gravity values due to the two sources are shown individually as well as combined. Note that the superposition of two ideal sources with individual linear magnetic versus first vertical derivative of gravity correlations yields a relation that is in this case almost linear and has a nonzero intercept. The slope of the resultant is most heavily weighted by the source producing the largest range of values within a given window, in this case the shallower source. Thus, in areas where anomaly interference is present or suspected, apparent $\Delta J/\Delta\sigma$ values may not be representative of any single source body and must be interpreted with caution. However, the nonzero intercept and the spike patterns in the three coefficients (Figure 9) are indications of the presence of interference. Furthermore, since the apparent $\Delta J/\Delta\sigma$ value is the resultant of the true $\Delta J/\Delta\sigma$ values of the individual sources it may be possible to minimize interference effects and reliably estimate $\Delta J/\Delta\sigma$ for a given source. Methods for minimizing interference effects by varying window size and by filtering are discussed below.

Effect of Window Size

The choice of a data window size for internal correspondence analysis depends on the wavelength of anomalies of interest, sampling interval, and the resolution desired. Experience indicates that a window of approximately 0.5 to 1.0 times the half-maximum width of anomalies of interest is desirable. The change of internal correspondence results utilizing different sized windows provides information on the wavelengths of interfering anomalies and acts as one acceptance criterion

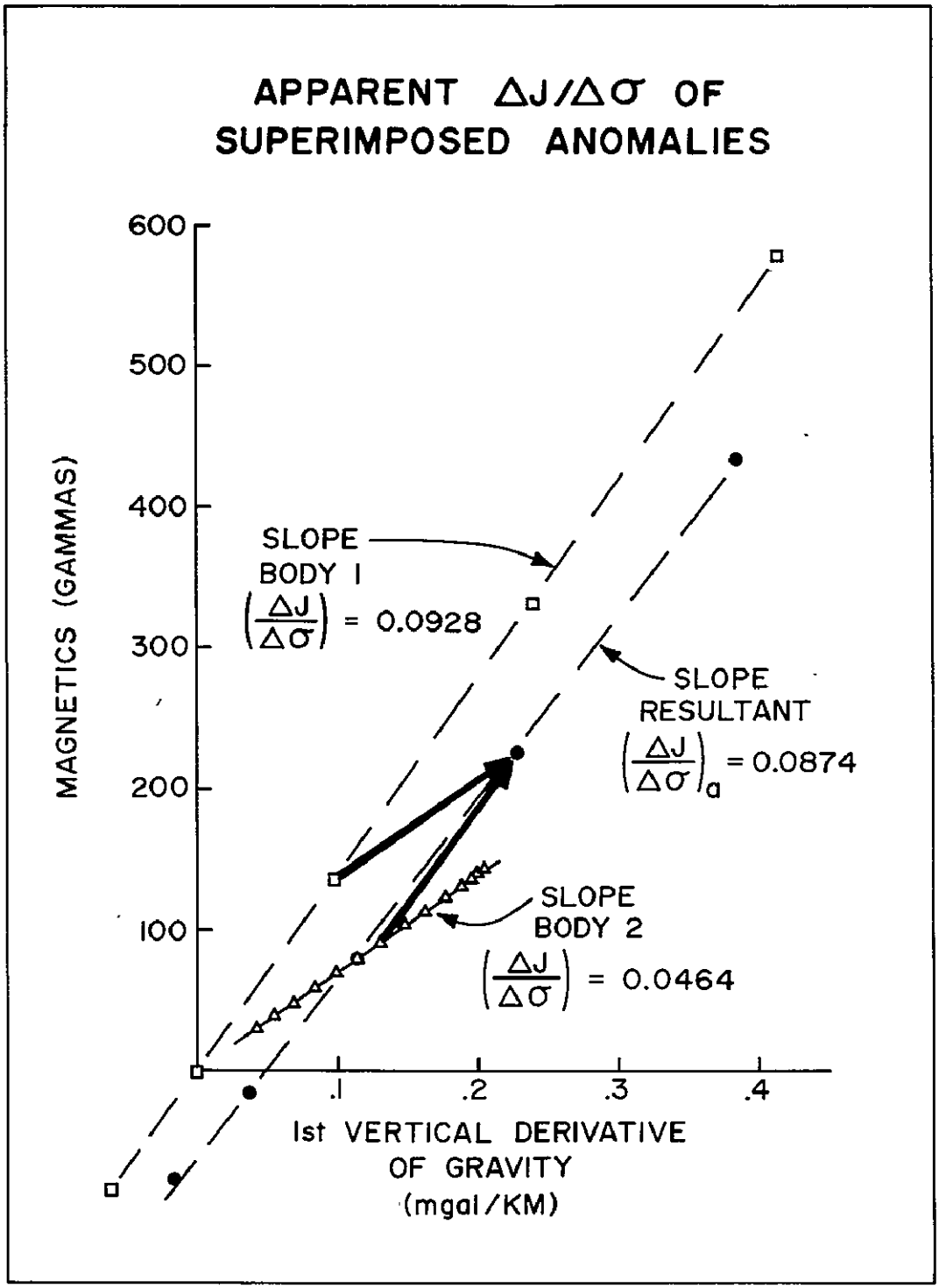

Figure 10. The vector sum of magnetics versus first vertical derivative of gravity relations resulting in an apparent $\Delta J/\Delta\sigma$.

for apparent $\Delta J/\Delta\sigma$ values.

Magnetic and first vertical derivative of gravity anomalies of differing dominant wavelengths are represented schematically in Figure 11. Assuming both sets are sampled at the same interval, the indicated five data point window samples a wider range of values on the narrow wavelength magnetic and first vertical derivative of gravity anomaly set than on the broad wavelength set at the top of the diagram. The five point window is approximately the half-maximum width of the narrow wavelength anomalies, and is better "tuned" to yield significant internal correspondence results for these anomalies.

Observed gravity and magnetic data will always contain effects of interfering anomalies. From the standpoint of resolution, an internal correspondence window should include a minimum number of data points from neighboring anomalies.

Figure 12 shows the gravity and magnetic data calculated for four pairs of equivalent sources, with decreasing distances of separation. The right hand source of each pair has a $\Delta J/\Delta\sigma$ one-half of that of the left. The extreme case is at the right of the diagram where the sources are in contact and the anomalies produced appear to have a single source.

A window size of five data points (5 km) was chosen for internal correspondence analysis of the anomalies shown in Figure 12. This corresponds in length to approximately one-half of the half-maximum width of the magnetic or vertical gradient of gravity anomalies produced by the combined sources at the right of the diagram.

The internal correspondence results shown in Figure 13 demonstrate that even for the case where two sources are in contact, two approximately correct apparent values of $\Delta J/\Delta\sigma$ are obtained. The spikes on the slope and intercept profiles indicate interference at the transition zone from a region of one dominant $\Delta J/\Delta\sigma$ influence to another. They aid in recognizing boundaries between these regions. The magnetics versus first vertical derivative of gravity plot of the data of Figure 12 is shown in Figure 14. Two sets of slopes, corresponding to the two different

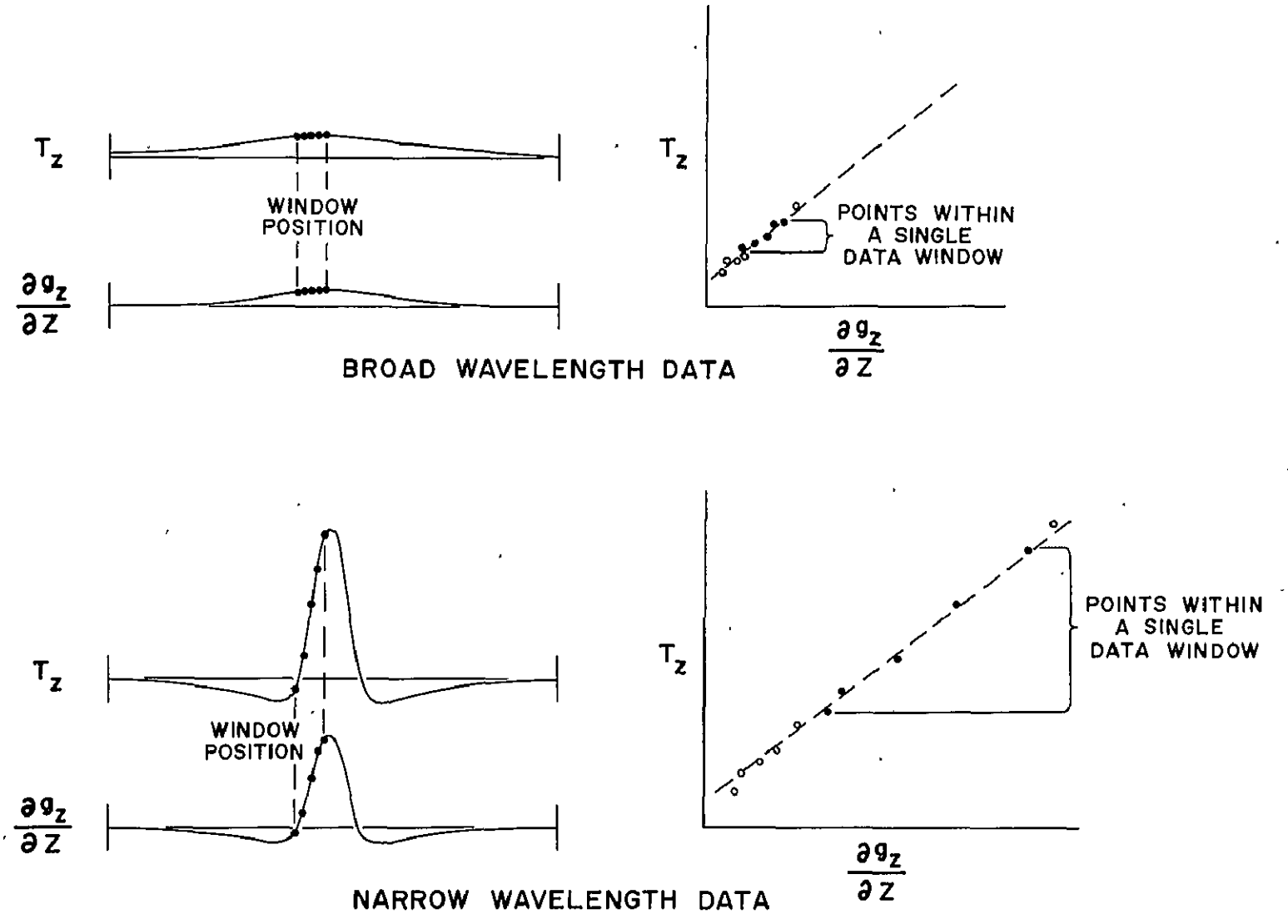

Figure 11. The effect of window size on the range of magnetic versus first vertical derivative of gravity values used in each regression.

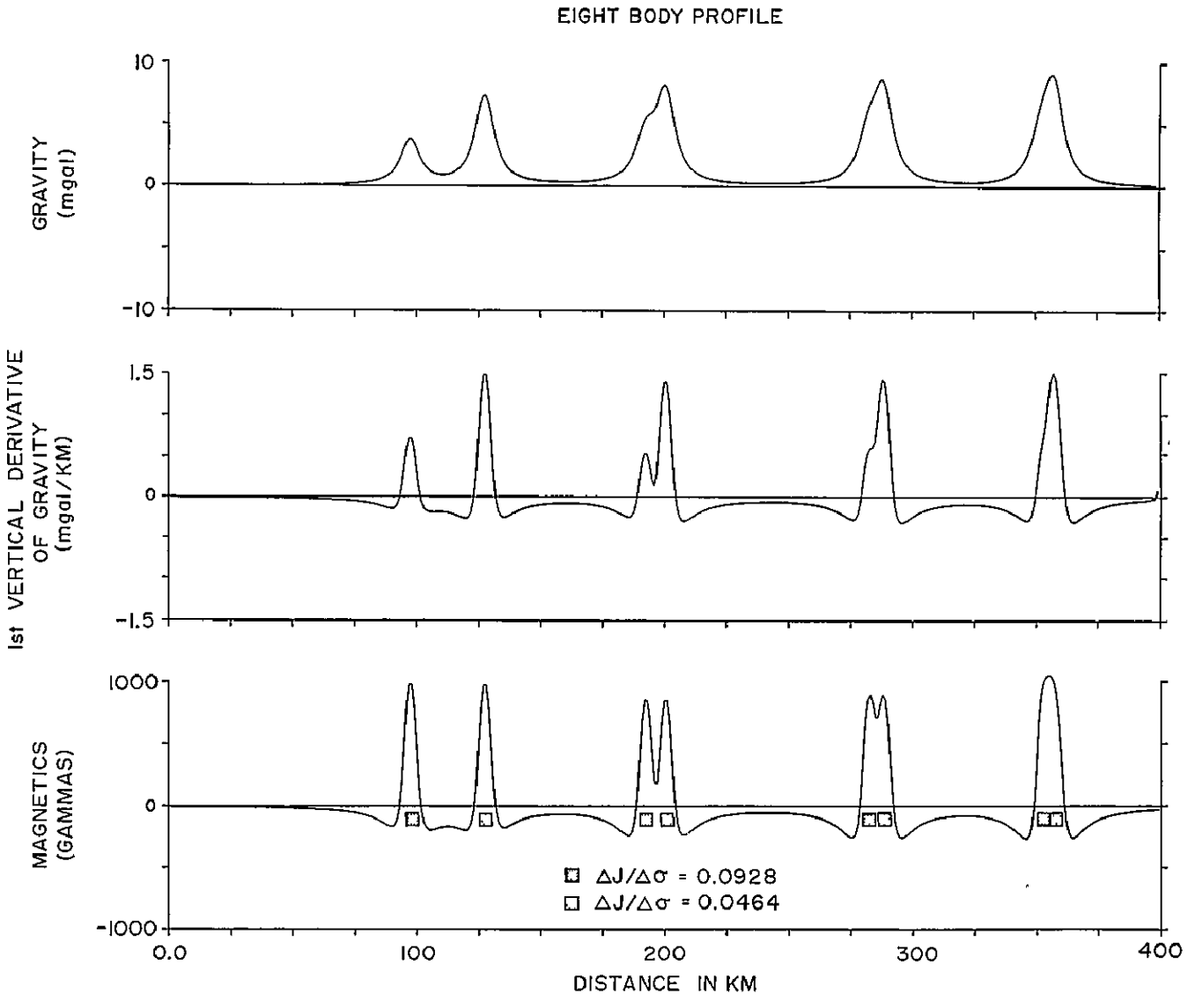

Figure 12. Eight body profile: gravity, first vertical derivative of gravity, and magnetic anomaly profiles due to four pairs of equivalent sources at decreasing distances of separation. Sampling interval is 1 km.

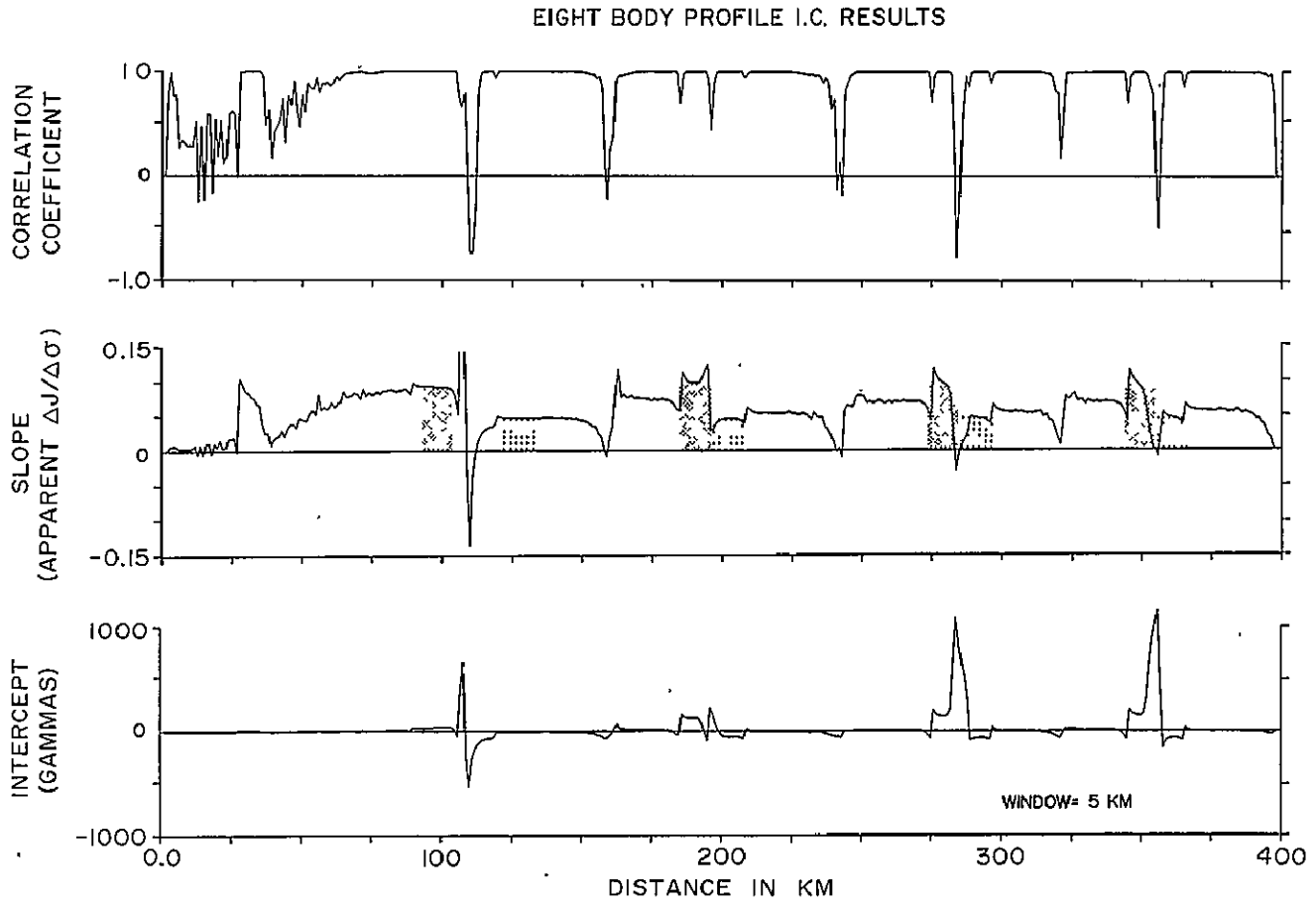

Figure 13. Eight body profile: internal correspondence results. The level of the fine stippled bar equals the left hand source $\Delta J/\Delta\sigma$ of each pair, 0.0928; the bold equals the $\Delta J/\Delta\sigma$ of each right hand source, 0.0464.

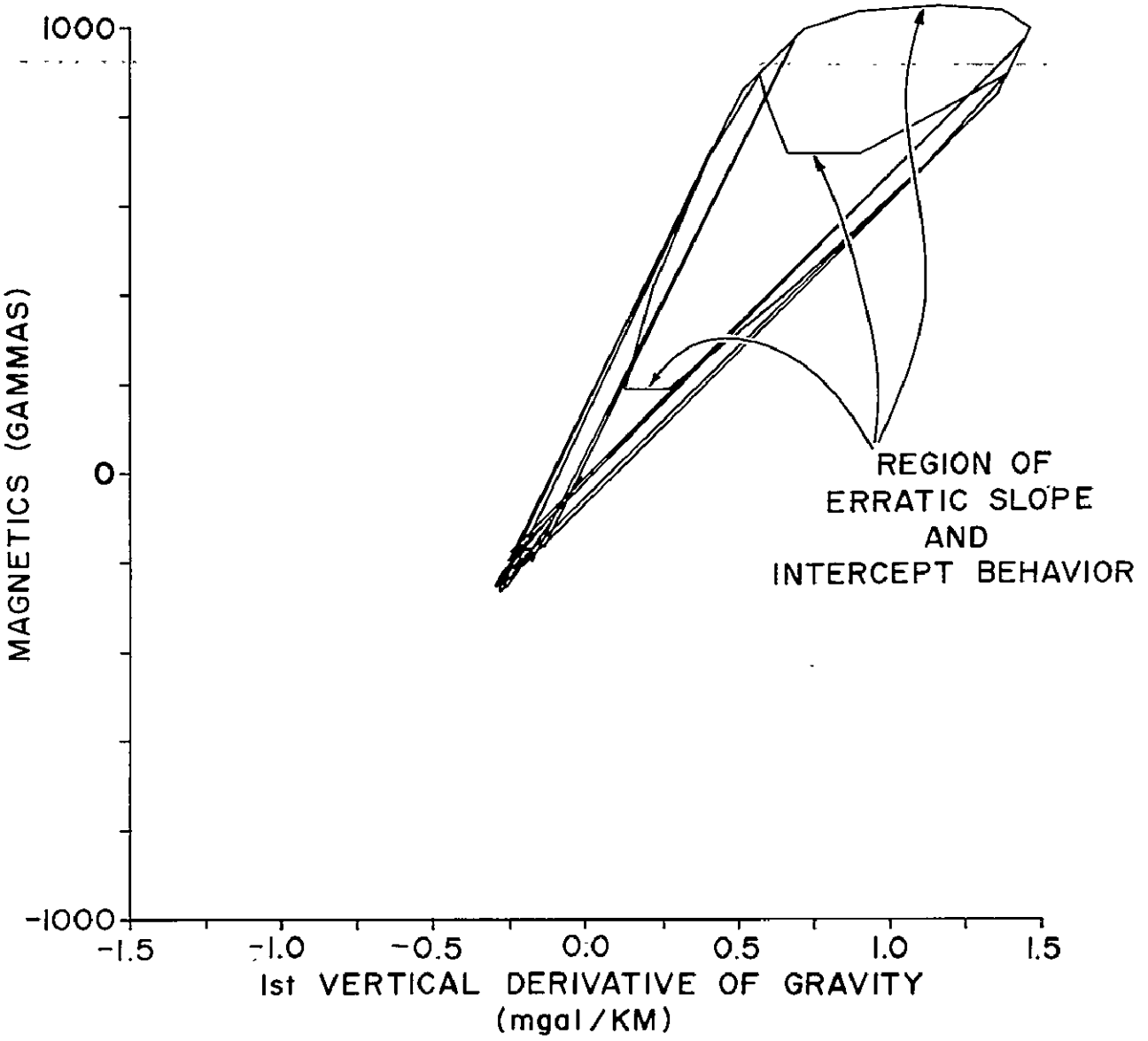

Figure 14. Eight body profile: magnetics versus first vertical derivative of gravity relation.

$\Delta J/\Delta\sigma$ values, are present. The erratic zones on the slope and intercept plots of Figure 13 correspond spatially to the values indicated between the two different slope sets.

One method of resolving the internal correspondence parameters due to anomalies of varying spectral characteristics is to perform ICA using several window sizes. Large correlation coefficients corresponding to areas of constant slope and intercept parameters that do not vary with changing window size indicate a high degree of confidence in the apparent $\Delta J/\Delta\sigma$ estimate. The variation of these parameters with changing window size is an indication of anomaly interference.

Enhancement of Internal Correspondence Results Through Preprocessing

Interference caused by the superposition of anomalies can lead to confusing or erroneous internal correspondence results. Upward continuation and wavelength filters can be used as preprocessing steps to enhance data components of interest, resulting in improved internal correspondence results.

A theoretical example of gravity and magnetic data made up of anomalies of two different wavelengths is shown in Figure 15. The longer wavelength components of the data are due to two 5 by 20 km two-dimensional sources at a depth of 20 km. Above the long wavelength source on the left are three 1.0 by 1.0 km two-dimensional bodies at a depth of 1.0 km which is the principal source of the short wavelength component of the data.

Assuming that the short wavelength components are of interest, internal correspondence analysis was performed with results shown in Figure 16. A five point data window was used, 2.5 km in width, which is approximately the half-maximum width of the narrow magnetic and first vertical derivative of gravity anomalies. The erratic character of the internal correspondence parameters over the superimposed region on the left is the effect of interference. The apparent $\Delta J/\Delta\sigma$ values

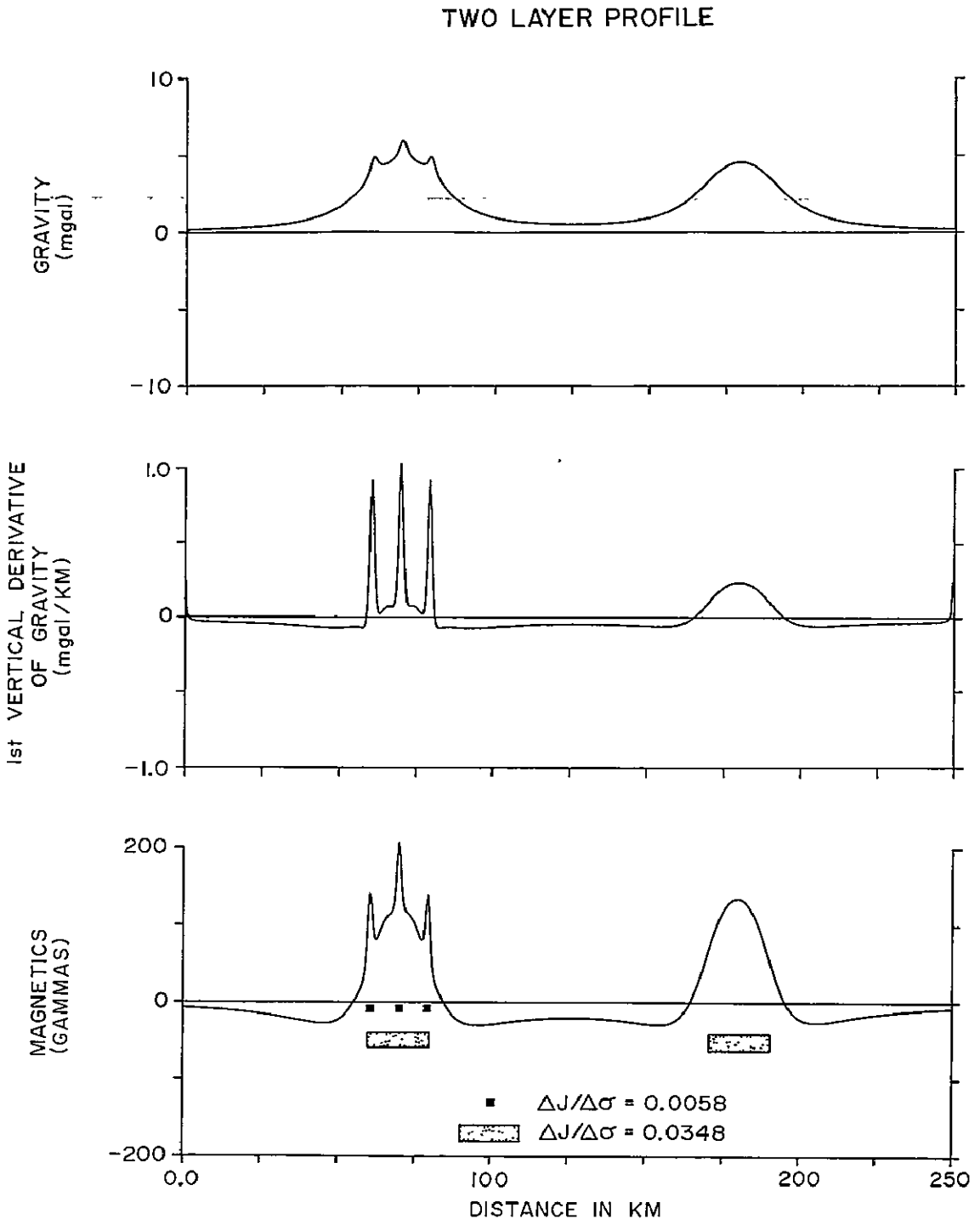

Figure 15. Two layer profile: gravity, first vertical derivative of gravity, and magnetic anomaly profiles due to two sets of equivalent sources producing different dominant wavelength anomalies. Sampling interval is 0.5 km.

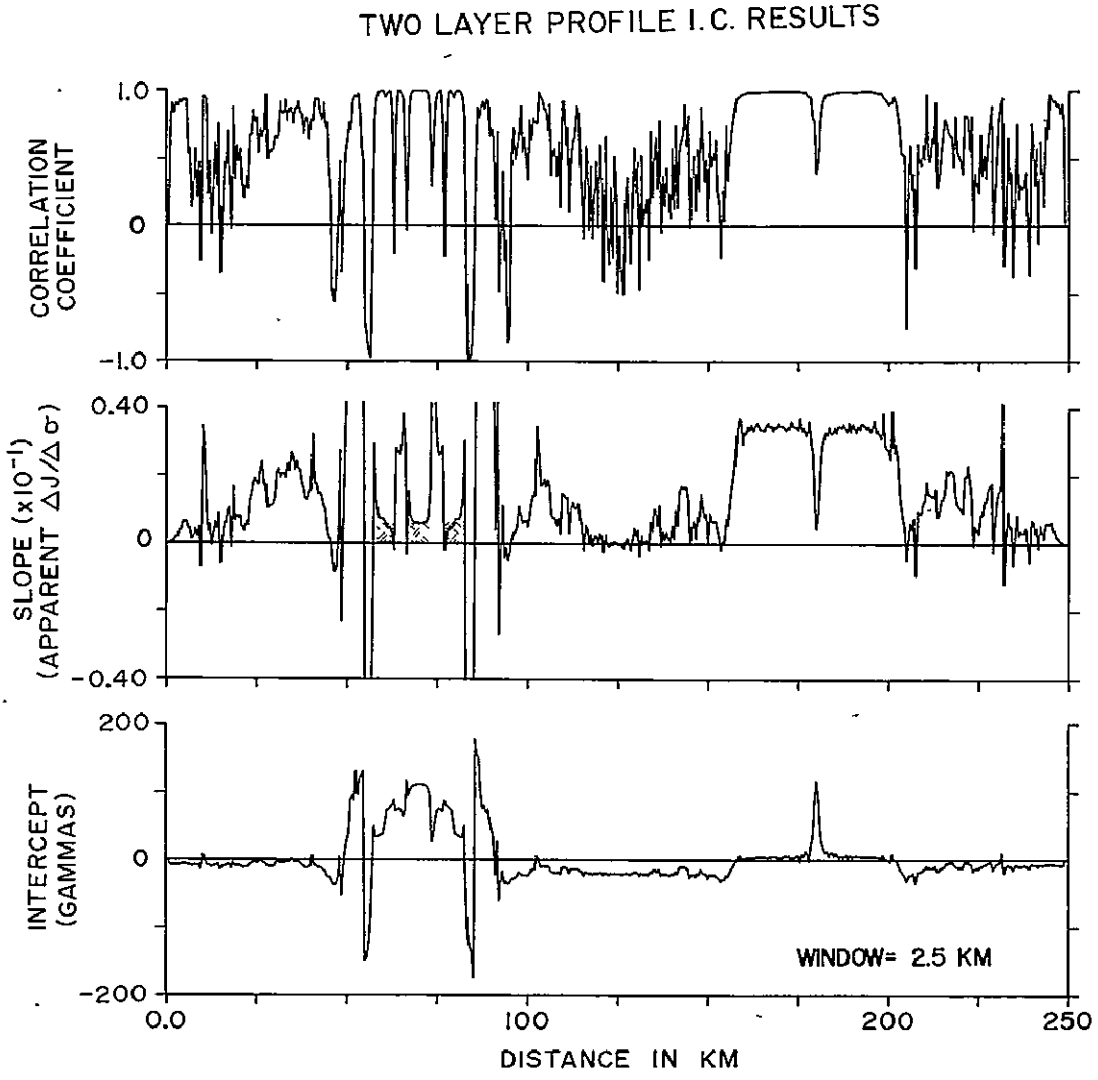

Figure 16. Two layer profile: internal correspondence results using a five data point window. The level of the stippled bars equals the narrow wavelength source $\Delta J/\Delta\sigma$, 0.0058.

for the narrow anomaly sources are obscured by this interference. The slope plot over the broad wavelength data at the right is noisy because the window size is tuned to narrow anomalies.

In order to enhance the short wavelength data the original gravity and magnetic data were filtered to pass wavelengths less than 4 km. The filtered data in Figure 17 demonstrate that the long wavelength energy has been greatly attenuated. The internal correspondence results for the high pass filtered data (Figure 18) show that significant results are obtained only for the region over the narrow anomalies. Over the short wavelength sources, a high correlation coefficient and accurate estimates of the true $\Delta J/\Delta\sigma$ values are obtained.

Assuming that the broad wavelength components are of interest the original gravity magnetic data were analyzed using an internal correspondence window of 35 data points, approximately the half-maximum width of these anomalies. The slope plot in Figure 19 shows that the apparent $\Delta J/\Delta\sigma$ values obtained for the anomaly at the right is correct for the source body. The interference caused by superposition of anomalies at the left leads to erratic internal correspondence results.

The original gravity and magnetic data were upward continued 15 km to enhance the long wavelength components. Upward continuation is a form of wavelength filtering with very smooth filtering characteristics. High frequencies are attenuated, emphasizing the long wavelength components of the data. In effect the level of observation of the data is increased. The upward continued gravity and magnetic profiles (Figure 20) demonstrate that the narrow anomalies have been attenuated.

The internal correspondence analysis of the upward continued data (Figure 21) show that the apparent $\Delta J/\Delta\sigma$ values for the region of interfering anomalies on the left is most heavily influenced by the broad wavelength source. Values over the body are approximately 10 to 12 percent lower than the correct $\Delta J/\Delta\sigma$, a much improved estimate considering that no values were acceptable when analyzing the raw data.

These examples illustrate the important use of wavelength filters

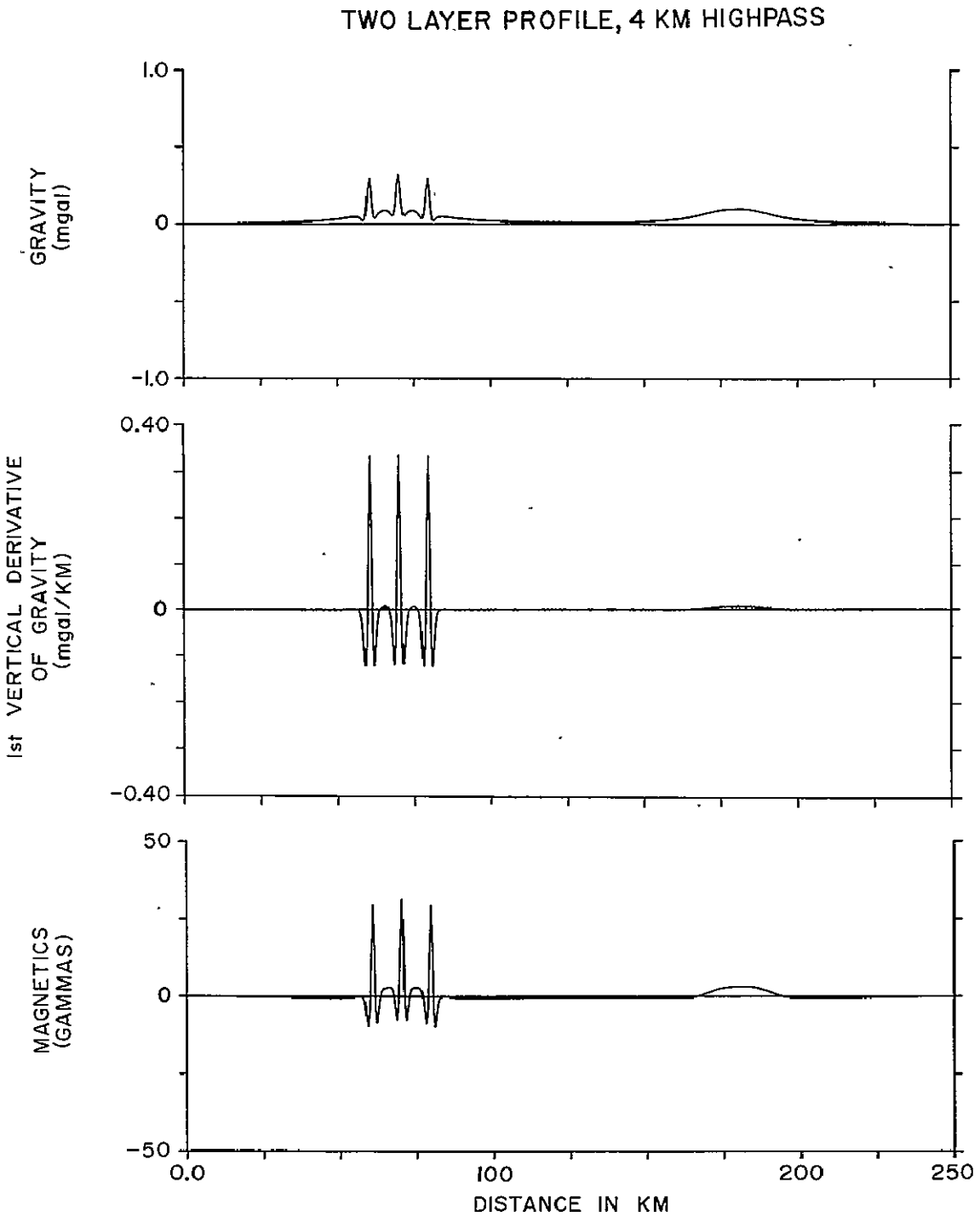

Figure 17. Two layer profile: anomalies filtered to pass wavelengths less than 4 km.

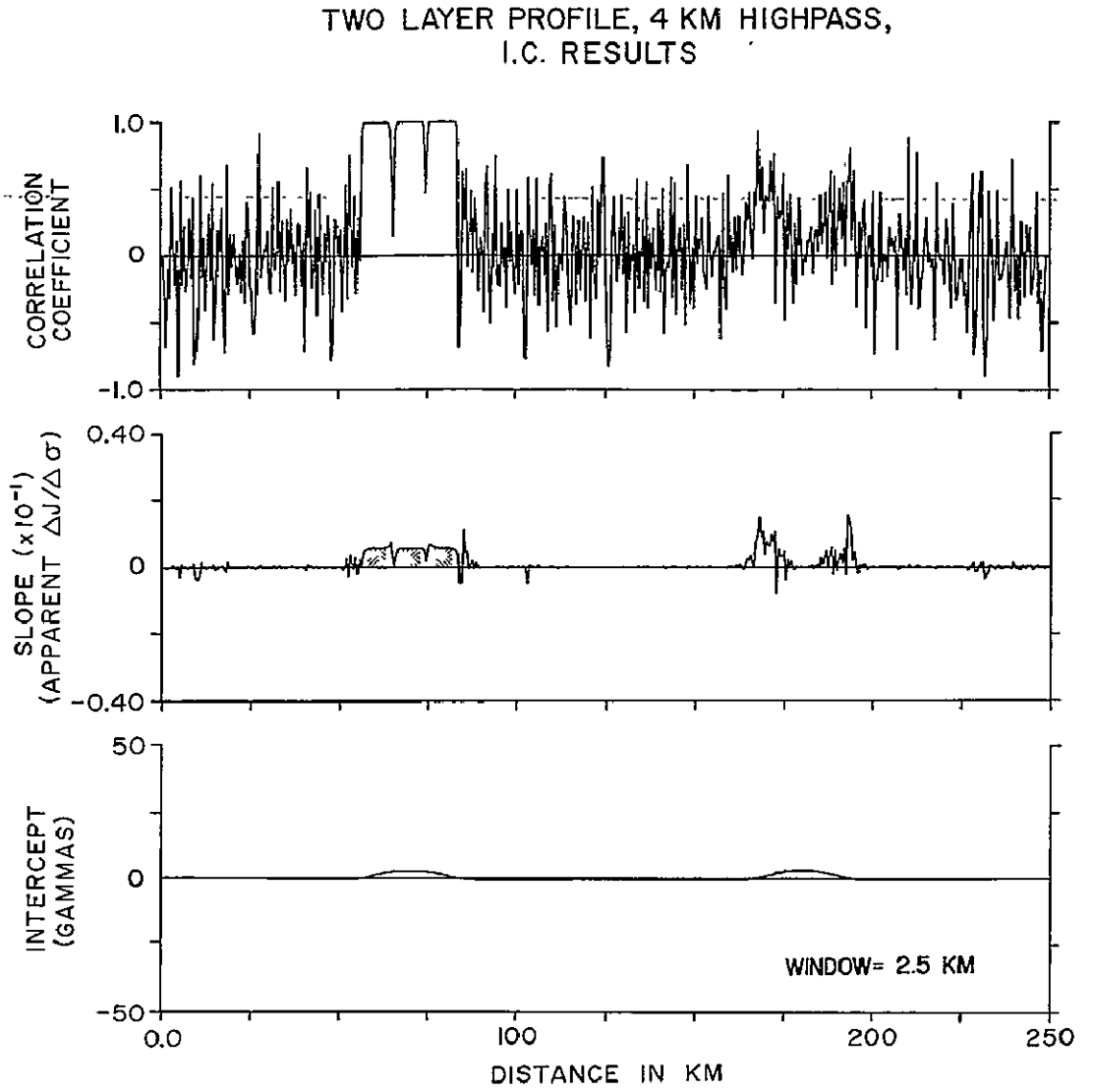

Figure 18. Two layer profile, 4 km high pass filtered: internal correspondence results. The level of the stippled bars equals the narrow wavelength source $\Delta J/\Delta\sigma$, 0.0058.

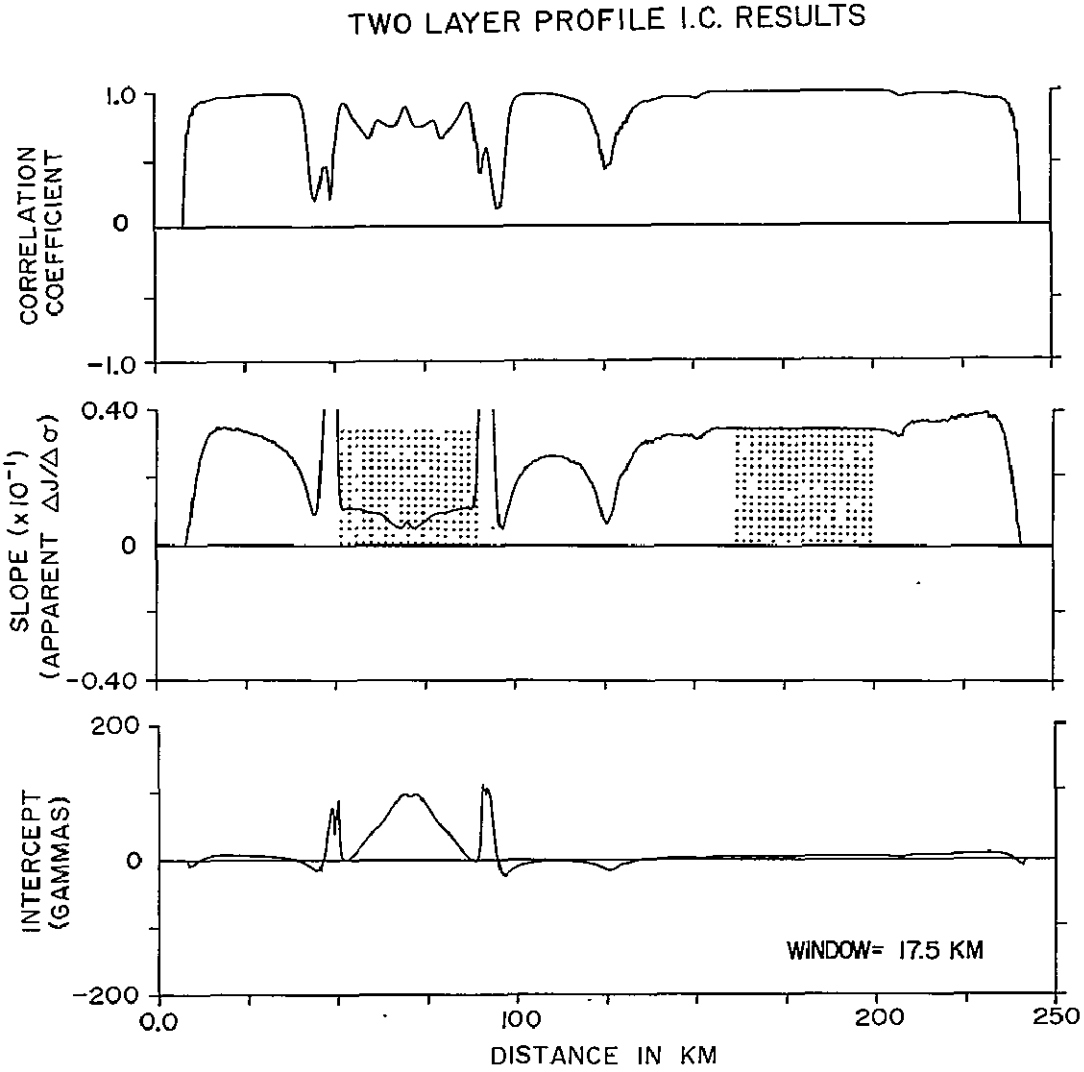

Figure 19. Two layer profile: internal correspondence results using a 35 data point window. The level of the stippled bars equals the broad wavelength source $\Delta J/\Delta\sigma$, 0.0348.

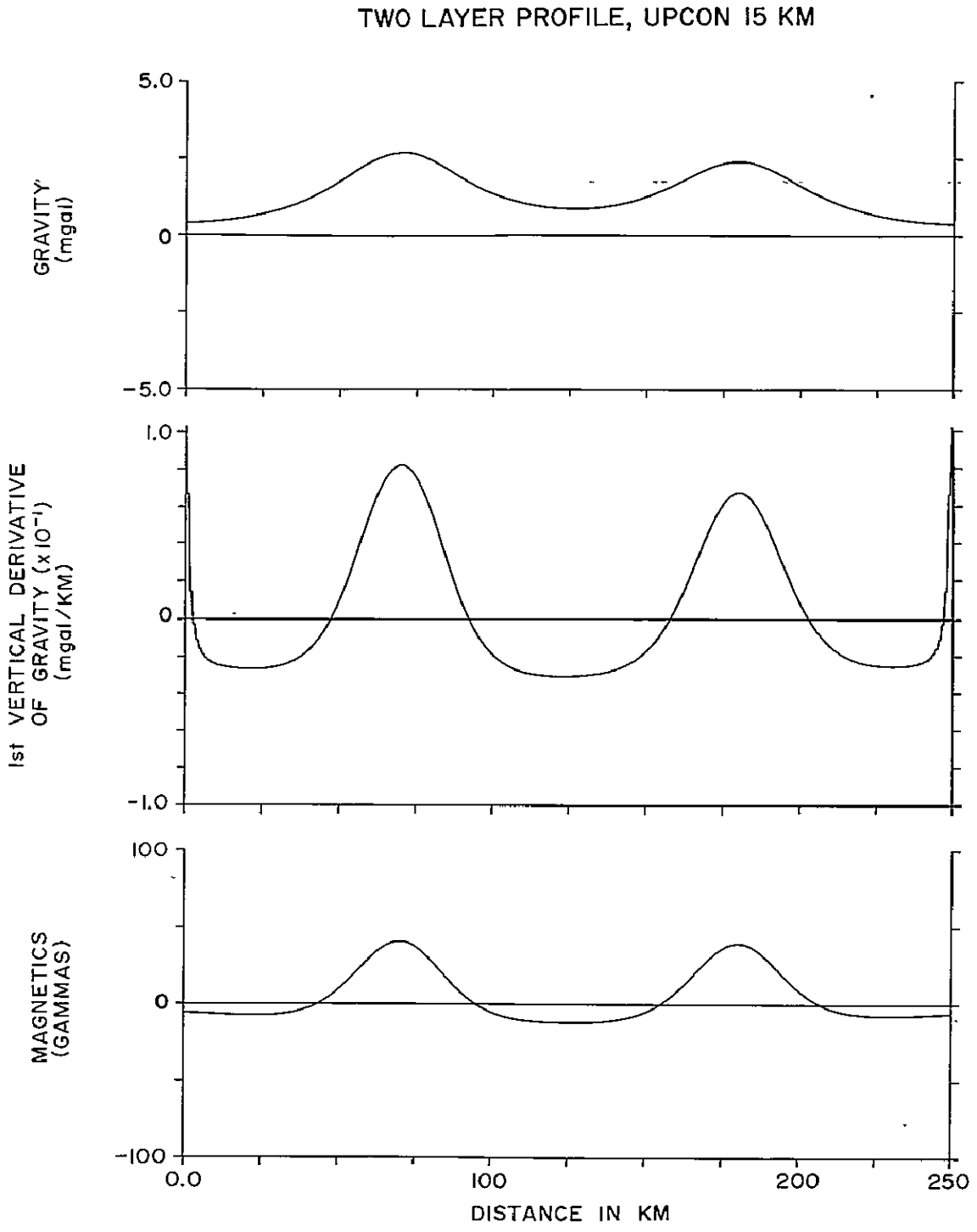

Figure 20. Two layer profile: gravity, first vertical derivative of gravity, and magnetic anomaly profiles upward continued 15 km.

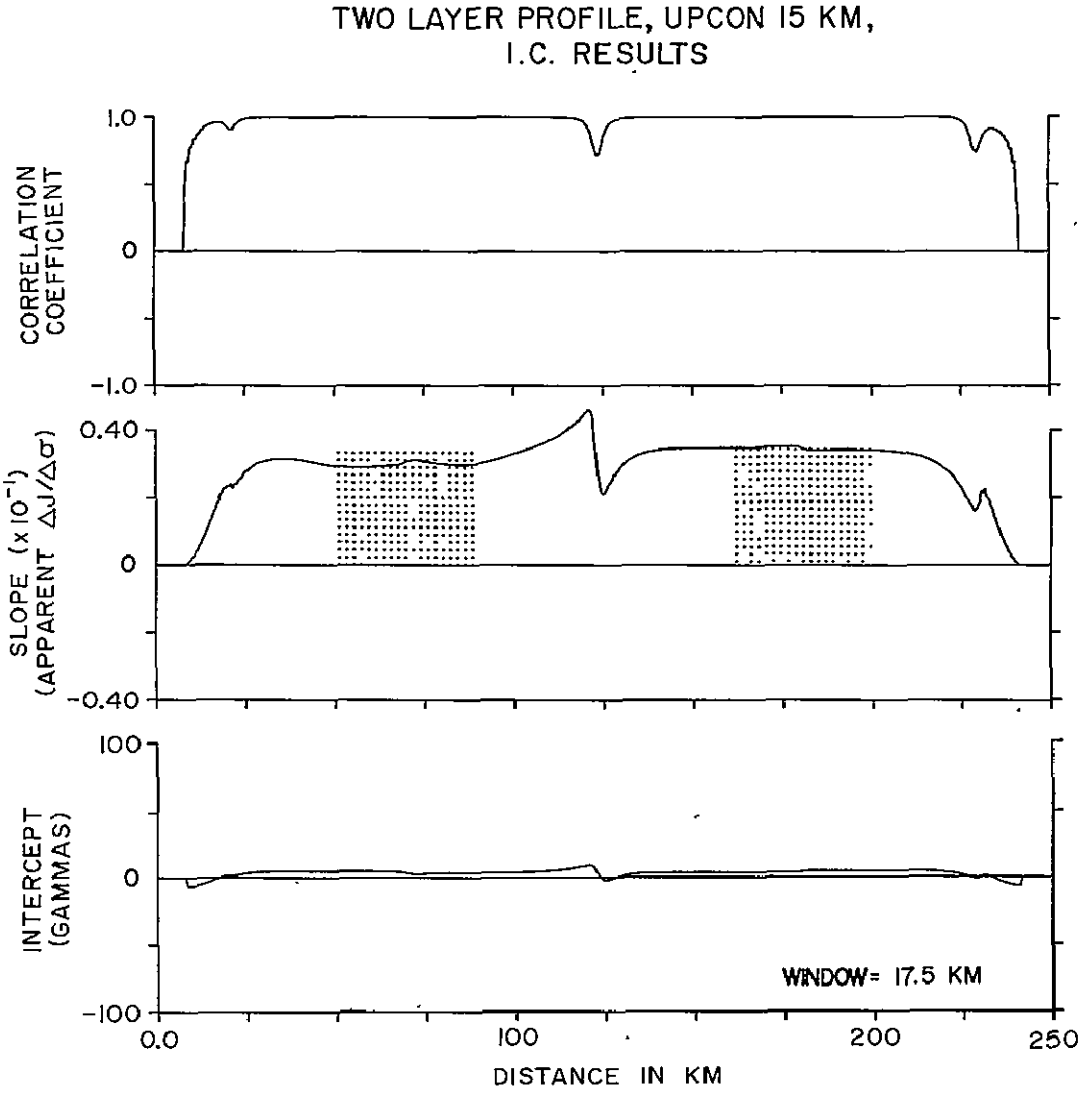

Figure 21. Two layer profile: internal correspondence results from anomalies upward continued 15 km. The level of the stippled bars equals the broad wavelength source $\Delta J/\Delta\sigma$, 0.0348.

and upward continuation in enhancing components of gravity and magnetic anomaly data for internal correspondence analysis.

Interpretation of Internal Correspondence Results

The determination of apparent $\Delta J/\Delta\sigma$ values is the principal objective of internal correspondence analysis. However, information is also present on regional relationships of the gravity and magnetic data, including indication of zones of interference and the presence of a regional base level.

A number of criteria can be established for selecting acceptable apparent $\Delta J/\Delta\sigma$ values. Constant slope and intercept parameters and a correlation coefficient approaching $\pm$ 1 are necessary conditions. A low correlation coefficient may be due to interference of several sources, inaccurate preprocessing, inappropriate window size in the ICA, or violation of the assumptions implicit in Poisson's theorem, particularly the presence of a significant remanent magnetization or the absence of "homogeneous" sources.

Perhaps the most useful criterion for evaluating the reliability of $\Delta J/\Delta\sigma$ values from ICA is the consistency of the apparent $\Delta J/\Delta\sigma$ value when derived from different dominant wavelength data. A consistent $\Delta J/\Delta\sigma$ value from a given anomaly determined from several levels of elevation or wavelength filter ranges is a direct indication of homogeneity of the source and therefore suggests an accurate $\Delta J/\Delta\sigma$.

Interanomaly areas yield apparent $\Delta J/\Delta\sigma$ subject to the same averaging process as the main portion of anomalies. Zones of good correlation can result in these areas. For example, the eight body profile gravity and magnetic data of Figure 12 have internal correspondence results shown in Figure 13 that exhibit large correlation coefficients, with level slope and intercept behavior over regions between anomalies. The apparent $\Delta J/\Delta\sigma$ values vary in a stepwise fashion between the

approximately correct value obtained over the anomalous sources. This potential source of error should be considered when analyzing observed data for acceptable apparent $\Delta J/\Delta\sigma$ values.

The geologic interpretation of acceptable $\Delta J/\Delta\sigma$ values is subject to a certain degree of ambiguity. Values of $\Delta J/\Delta\sigma$ deal with anomalous, not absolute, contrasts in magnetization and density. Sources exhibiting different absolute characteristics may yield similar $\Delta J/\Delta\sigma$ values in different regional settings. The fact that it is a ratio indicates that different combinations of magnetization and density contrasts can yield similar results.

Regional base levels or gradients will be apparent on intercept plots. The intercept is most sensitive to magnetic base levels since long wavelength gravity features are attenuated by the first vertical derivative process. A magnetic regional may have a geologic source or may indicate a problem involving geomagnetic field removal.

The character of all three regression parameter plots, when considered together, is useful in establishing regional patterns of correlation. Spike-like patterns in the internal correspondence parameters of the eight body profile of Figure 13 indicate regions of interference and clearly separate the areas of differing $\Delta J/\Delta\sigma$ values. A similar pattern occurs in Figure 9, the internal correspondence results of vertically superimposed anomalies. This diagnostic interference pattern serves as an aid in dividing gravity and magnetic data into regions of similar correlation characteristics.

In conclusion, the results of internal correspondence analysis, when combined with gravity and magnetic data, provide not only apparent $\Delta J/\Delta\sigma$ estimates, but also information on base level, anomaly interference, and resolution of subareas of similar correlation characteristics. This information is all of potential aid to the geologic interpretation of gravity and magnetic anomaly data.

A Simple Criterion for Isolating Valid $\Delta J/\Delta\sigma$ Estimates

In spite of its virtues, ICA will not yield a valid $\Delta J/\Delta\sigma$ estimate at every point in a multisource data space. Model studies have revealed that ICA actually yields a mixture of invalid as well as valid $\Delta J/\Delta\sigma$ estimates. Several criteria have been discussed in the previous section to aid in selecting valid $\Delta J/\Delta\sigma$ values. However, these criteria are based upon subjective observation and analysis. Thus, it is desirable to develop a criterion that is internally based and could be used in an automatic scheme adaptable to computer coding. The remainder of this section is concerned with a criterion which is based on two characteristics of the data; anomaly intensities and stability of the ICA profiles. Although this criterion has not been fully developed to where it can be used in isolating valid $\Delta J/\Delta\sigma$ values, it has been shown to be a statistically valid approach worthy of continued study.

Proposal of a Simple Criterion

Observation of the ICA profiles from model data indicates that two characteristics may aid in isolating regions that yield valid $\Delta J/\Delta\sigma$ estimates. It appears that an accurate $\Delta J/\Delta\sigma$ is most likely to occur in regions where anomalies approach maximum intensity and regions yielding invalid $\Delta J/\Delta\sigma$ estimates are commonly characterized by erratically behaved ICA profiles, especially the intercept. Therefore, a quantitative isolation criterion may be developed that uses parameters sensitive to anomaly intensities and ICA profile stability. Two variables are proposed and will be referred to as the internal covariance and gradient of combined intercept.

Internal covariance is calculated by the same moving window that is used in ICA. It is simply the sample covariance between the first vertical derivative of gravity and the magnetic intensity within a given window position. The internal covariance values comprise a profile

that attains large amplitudes over strong anomalies.

The gradient of combined intercept is calculated from the ICA coefficients. Each ICA window position involves a fitted line with intercepts onto both the magnetic and gravity gradient axes. The combined intercept is the product of these two intercepts and is calculated at each ICA window position. The horizontal gradient of combined intercept is then calculated by averaging two gradients existing between three successive combined intercept values. The averaged gradient is assigned to the center of the three points. The gradient of combined intercept profile attains large amplitudes in regions where the ICA parameters display erratic behavior.

It should be pointed out that it is the amplitude, not the sign of these two variables that is important. Thus, both the internal covariance and the gradient of combined intercept are expressed in absolute values.

Evaluation of Proposed Isolation Criterion

The selection of the internal covariance and gradient of combined intercept as a criterion is clearly based on qualitative observation. It is therefore necessary to evaluate the proposed criterion with a quantitative procedure. One approach is to test the criterion on model data where the $\Delta J/\Delta\sigma$ of the anomaly sources are exactly known. Two model profiles are tested with this criterion; the eight body profile (Figures 12 and 13) and a mixed body profile shown in Figures 22 and 23.

The internal covariance and the gradient of the combined intercept were calculated along with the standard ICA parameters of the profiles. The ICA computer program was modified to divide the points of each model profile space into two groups; a valid group and an invalid group. A particular point was classified as valid if its associated $\Delta J/\Delta\sigma$ estimate from ICA was within $\pm$ 10% of a $\Delta J/\Delta\sigma$ value known to exist in a profile; otherwise the point was classified as invalid. The two groupings in

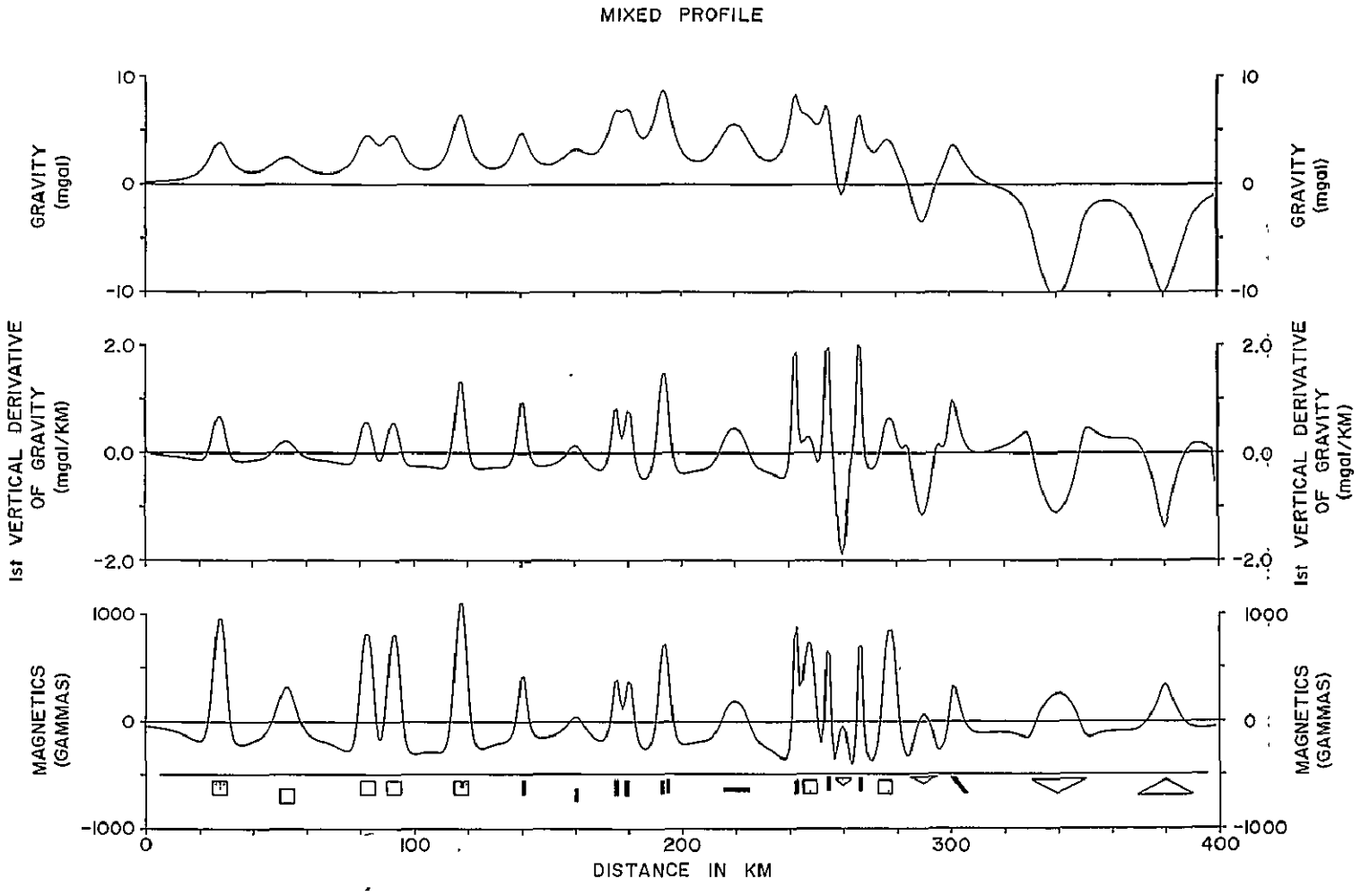

Figure 22. Mixed profile: gravity, first vertical derivative of gravity, and magnetic anomaly profiles due to various combinations of three source types. The square bodies have a $\Delta J/\Delta\sigma$ of 0.0928, the rectangular bodies have a $\Delta J/\Delta\sigma$ of 0.03248, and the triangular bodies have a $\Delta J/\Delta\sigma$ of -0.0174. Sampling interval is 1 km.

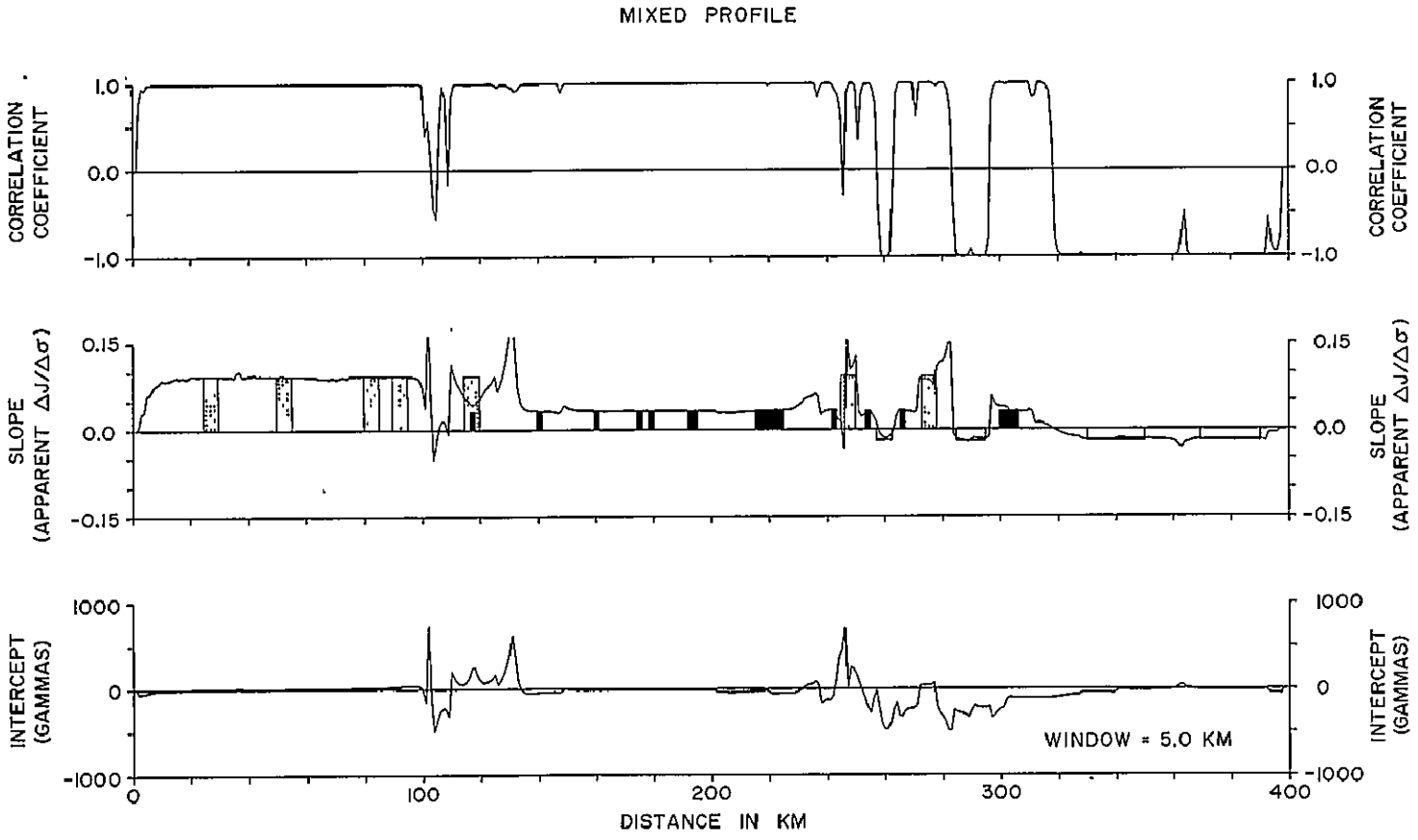

Figure 23. Mixed profile: internal correspondence results using a 5 km window. Position of shaded bars represent source positions and their levels represent actual source $\Delta J/\Delta\sigma$ values.

each model profile could then be used as a standard in evaluating the effectiveness of the internal covariance-gradient of combined intercept isolation criterion.

The use of scatter diagrams is one means of evaluating the internal covariance-gradient of combined intercept recognition criterion. Figures 24 and 25 are log-log internal covariance-gradient of combined intercept scatter diagrams of the mixed and eight body profiles, respectively. Valid points and invalid points are represented by pluses and zeros, respectively. In both models there is a marked tendency for the valid points to fall in the high covariance-low gradient of combined intercept regions of the diagrams. It, therefore, does appear that the proposed recognition criterion is related to the accuracy of a $\Delta J/\Delta\sigma$ estimate.

Discriminant analysis is a more quantitative means of evaluating the effectiveness of the proposed recognition criterion. This approach yields a statistical estimate of the separation of two groups of samples and is based on variables measured on each sample. In this case the two groups are the valid and invalid points and the variables are the internal covariance and gradient of combined intercept.

A simple linear discriminant analysis program from Davis (1973) was selected for this test. Two variations of the criterion were tried on each model, one using the absolute values of the two variables and the other using the base ten logarithm of the absolute values. In addition, two variations of each model profile were investigated; the original data and then a 20 km high pass of the data. The filtering was applied to determine if elimination of the highly interfering low frequency anomaly components would improve the discrimination between the two groups.

The results of all discriminant analyses are presented in Table 1. The λ_1 and λ_2 columns represent loading factors which collapse the bivariate (internal covariance-gradient of combined intercept) data into a univariate projection. The R_1 and R_2 values represent the

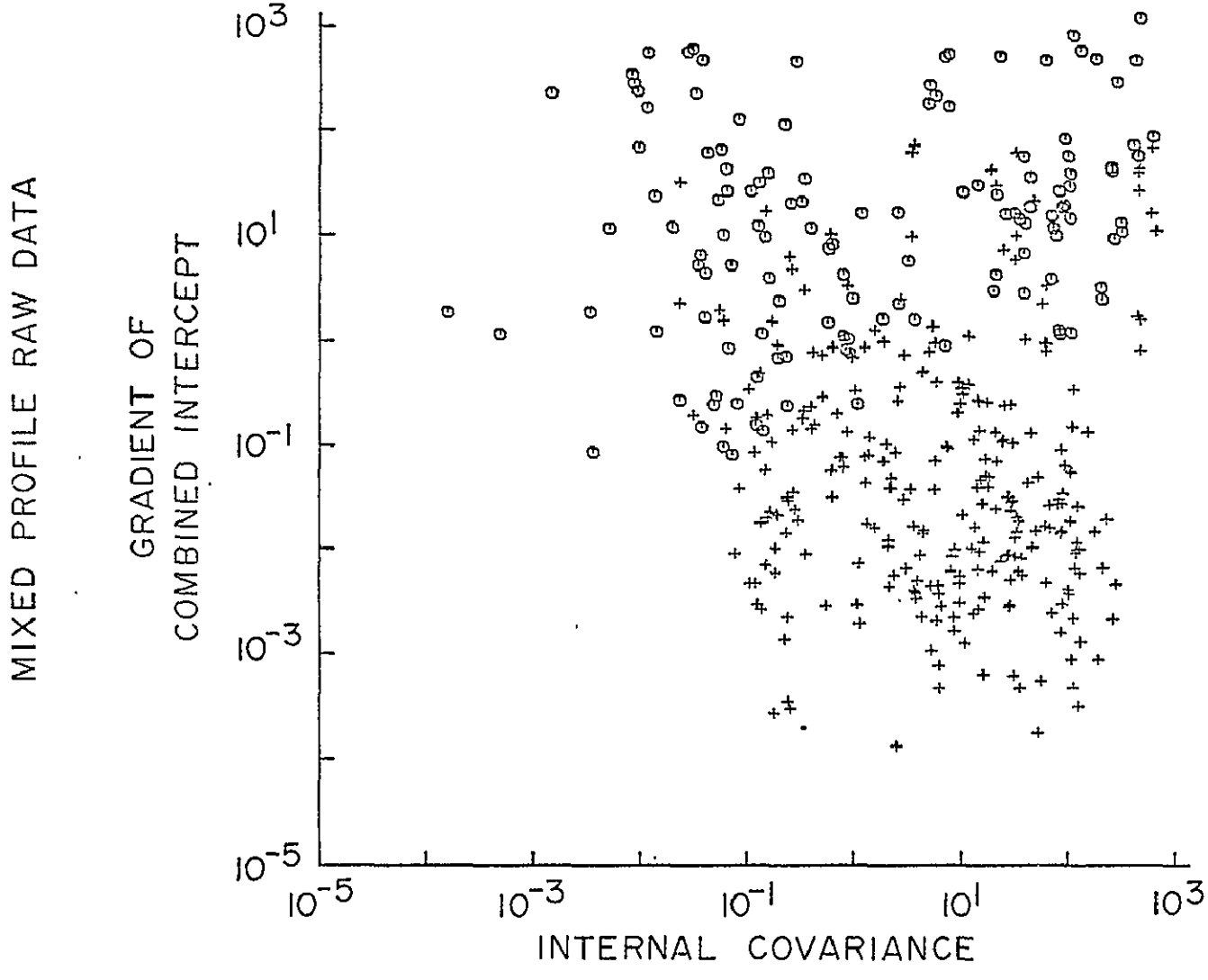

Figure 24. Log-log scatter diagram of the absolute values of internal covariance and gradient of combined intercept from mixed profile. Crosses represent window positions yielding $\Delta J/\Delta\sigma$ estimates within 10% of known values. Zeros represent window positions yielding $\Delta J/\Delta\sigma$ estimates that are outside of 10% range of known sources. Window size is 5 km.

Figure 25. Log-log scatter diagram of the absolute values of internal covariance and gradient of combined intercept from eight body profile. Crosses represent window positions yielding $\Delta J/\Delta\sigma$ estimates within 10% of known values. Zeroes represent window positions yielding $\Delta J/\Delta\sigma$ estimates that are outside of 10% range of known values. Window size is 5 km.

projected univariate means of the valid and invalid groups, respectively, and the R_o value is the midpoint between them. The R_o value is the boundary between the two sample groups as selected by the discriminant analysis. The percentage error value is the percentage of total points misclassified by the analysis.

The F test value is a statistical measure of how separable the valid and invalid groups are with respect to the proposed recognition criterion. The higher the F test value, the greater the discrimination between the two groups. Each model has 2 and 393 degrees of freedom which corresponds to a critical F value of approximately 4.6 at the 1% level of significance. In each case in Table 1 the internal covariance-gradient of combined intercept criterion demonstrates significant discriminant capabilities between the valid and invalid groups. The F test values and percentages of error suggest that the discrimination can be generally improved by using a logarithmic form of the criterion on high passed data.

Thus, it appears that an effective isolation criterion based on covariance and combined intercept is statistically feasible. The next logical step in developing the criterion is to establish a process that will automatically evaluate the validity of a particular $\Delta J/\Delta\sigma$ estimate. The basis for this decision would be upon the values of covariance and gradient of combined intercept at a given point relative to the total distribution of all covariance and gradient of combined intercept values. The nature of this problem suggests that the incorporation of automatic pattern recognition techniques would prove very helpful.

It should be pointed out that the criterion of covariance-gradient of combined intercept is not presented as being universally optimum. Further work may reveal that other combinations of variables yield more effective criteria. The major purpose of this section is to demonstrate that regions yielding accurate $\Delta J/\Delta\sigma$ estimates can be significantly isolated using internally based variables. The development of a fully automatic procedure that evaluates the $\Delta J/\Delta\sigma$ estimates from ICA is then a distinct possibility that warrants further study.

TABLE 1. Discriminant analysis of mixed and eight body profile using covariance-gradient of combined intercept criterion

Model	λ_1	λ_2	R_1	R_2	R_0	MD	F	total misclass	% misclass
ABSOLUTE VALUES									
Mixed Profile Raw Data	.0007	-.0080	.0143	-.7181	-.3519	.37	15.95	112	28.2
Mixed Profile 20 km high pass	-.0011	-.0206	-.0567	-.5568	-.3068	.25	10.53	88	22.2
Eight body profile raw data	.0295	.0000	1.6360	.0726	.8543	.78	31.14	72	18.2
Eight body profile 20 km high pass	.0201	-.0000	.3669	.0950	.2460	.15	6.44	126	31.8
LOG_{10} OF ABSOLUTE VALUES									
Mixed Profile Raw Data	.5181	-1.8287	2.8191	-1.987	.4610	2.36	102.70	56	14.1
Mixed Profile 20 km high pass	.4970	-1.7280	5.9356	.1670	3.0513	2.88	121.43	46	11.6
Eight body profile raw data	.7258	-.2977	.5279	-.9199	-.1960	.72	28.84	127	32.1
Eight Body Profile 20 km high pass	1.0094	-1.0855	3.1234	-1.4438	.8398	2.28	97.43	62	15.6

CHAPTER IV

CORRELATION OF GRAVITY AND MAGNETIC DATA BY CLUSTER ANALYSIS

Cluster analysis is a pattern recognition technique that classifies data into smaller groups of similar attributes. The similarity is based on a comparison of a set of variables that have been determined in each sample. The application of cluster analysis to gravity and magnetic data is schematically shown in Figure 26. A map or profile of gravity and magnetic data is divided into a number of subareas and treated as a collection of samples. A variety of traits describing the gravity and magnetic data are calculated within each subarea and used as variables in a cluster analysis program.

One of the advantages of the clustering approach lies in the large number of variables that can be integrated into the analysis. A particular combination of variables may discriminate between regions of significantly different gravity and magnetic data. These regions, as illustrated in Figure 26, may be of geological significance. In many respects, the application of cluster analysis resembles visual correlation of gravity and magnetic data. In both cases the interpreter attempts to delineate regions where the attributes of gravity and magnetic data are similar. However, the use of computerized cluster analysis has advantages in its objectivity and ability to handle large amounts of multivariate data rapidly and efficiently.

A simple hierarchical clustering program from Davis (1973) was selected for use in this study. Similarity between samples may be measured either by a correlation or distance coefficient and output is in the form of a line printer dendogram. The significance of each juncture on the dendogram is expressed in the same units as the selected coefficient of similarity. The interpreter must select a cutoff level of significance below which no further junctures form valid clusters.

Initial studies with cluster analysis on model and observed data was described in Hinze et al. (1975). A total of seven variables were calculated for each subarea; the averages of the gravity and magnetic values, the variances of the gravity and magnetic values, and three

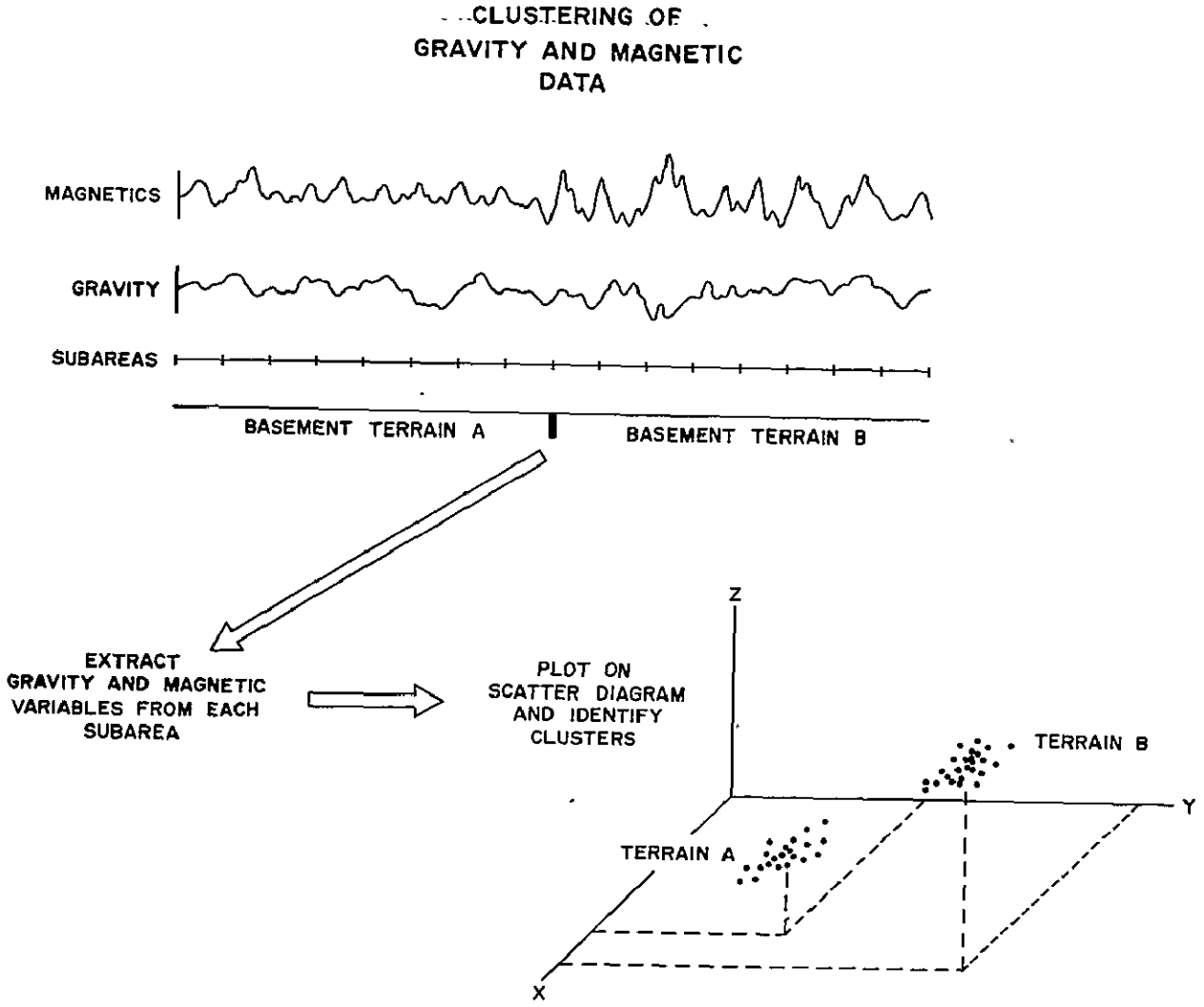

Figure 26. Schematic diagram illustrating the application of cluster analysis to gravity and magnetic data.

coefficients of a linear regression between the gravity and magnetic data. Shown in Figure 27 is the result of a cluster analysis on the mixed profile using the seven variables and a correlation coefficient similarity measure. The subareas are shown below the profiles and those bearing the same number define clusters at the 0.5 level of similarity. There is a tendency for certain clusters to favor certain lithologies. Cluster analysis with observed gravity and magnetic data (Hinze et al., 1975) indicated that clustering has a sensitivity to basement provinces.

Several new variables can now be calculated within each subarea of either a map or profile space; the averages of the gravity and magnetic horizontal gradients, the standard deviations of the gravity and magnetic horizontal gradients, and the three ICA coefficients. In the case of map data, the average of the horizontal gradient azimuths and the standard deviation of the horizontal gradient azimuths can be also calculated from the gravity and magnetic data in a subarea.

A particularly useful approach to clustering is simply using the three ICA coefficients within each subarea as variables. The results of this clustering approach are useful to ICA in delineating regional relationships between the coefficients not immediately apparent in the ICA profiles.

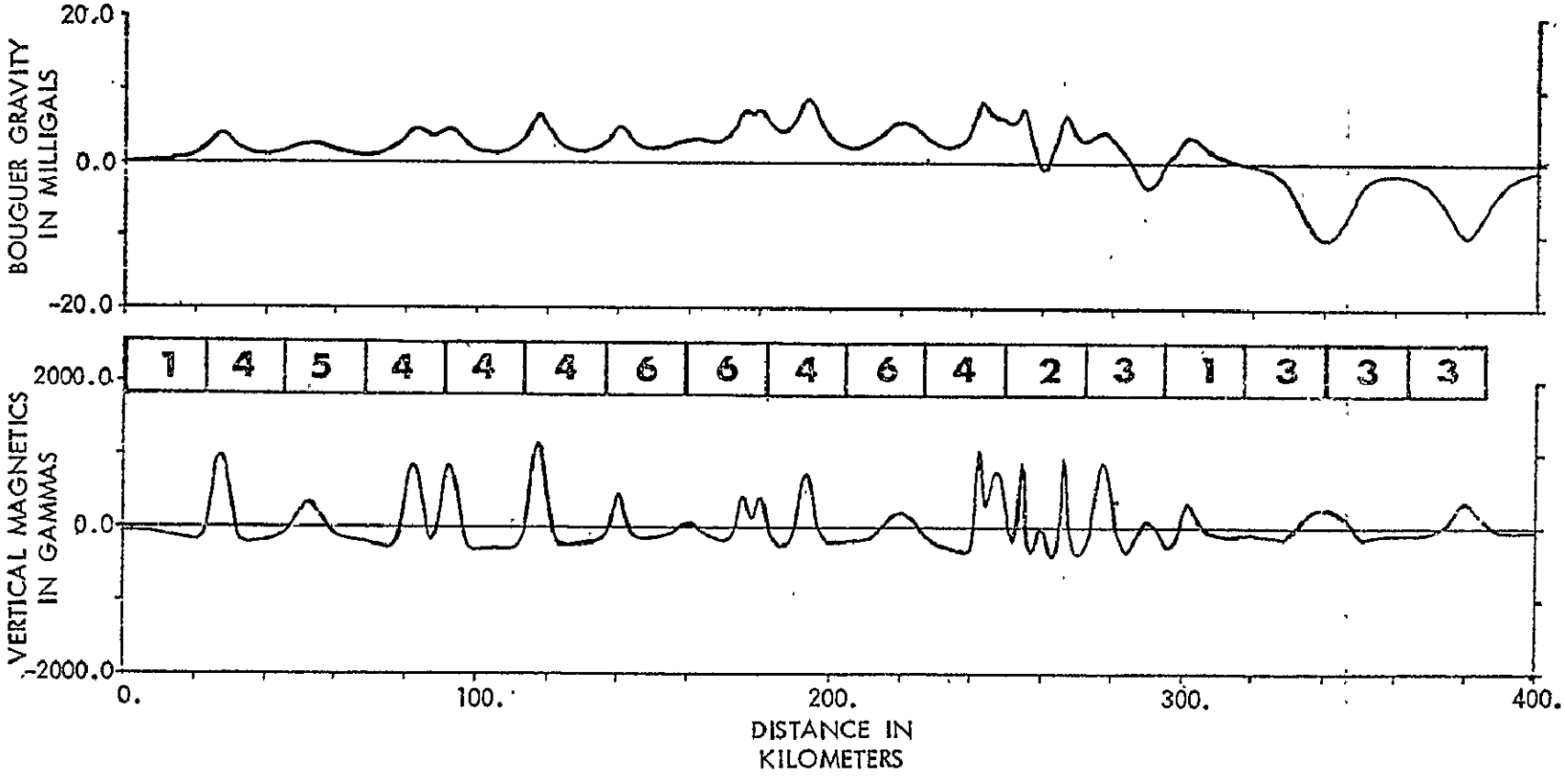

Figure 27. Results of cluster analysis on mixed profile. Subarea is 22.5 km and the variables are the means and variances of both gravity and magnetic data and three internal correspondence coefficients between the gravity and magnetics. Similarity coefficient is a correlation coefficient with a clustering cutoff at 0.5.

CHAPTER V

THE APPLICATION OF INTERNAL CORRESPONDENCE AND CLUSTER ANALYSIS TO OBSERVED DATA

Transcontinental Gravity and Magnetic Profiles of the 37th Parallel

Gravity and magnetic anomaly profiles across the North American continent along the 37th North parallel of latitude were prepared for and subjected to combined analysis for the purpose of investigating the correlation of magnetic and gravity features of a geologic province scale. A transcontinental profile was chosen to provide a manageable data set covering several geologic provinces. The 37th parallel profile was selected because it coincides with the Upper Mantle transcontinental profile and thus relatively recent and consistent magnetic, gravity and geologic information are available. Most major geologic provinces transect this profile at a high angle and have a long length in contrast to width, which is a significant criteria in the consideration of the two-dimensional assumption of profile analysis.

Data Acquisition and Preprocessing

Gravity data along the 37th parallel were obtained from the U.S. Geological Survey "Transcontinental Geophysical Survey (35^{o}-39^{o}) Bouguer Gravity Map Series I-531-B to I-535-B." These maps were compiled from local and regional surveys which incorporate a variety of station intervals.

A total intensity aeromagnetic anomaly profile of the 37th parallel was obtained by personal communication from Isidore Zeitz and J.R. Kirby of the U.S. Geological Survey. This profile is the original data used in the preparation of U.S. Geological Survey Map GP-597, "Aeromagnetic and Gravity Profiles of the United States along the 37th Parallel." The data, which were observed in 1965, consist of two segments flown at different barometric elevations. The segment west of 104.2^{o}W longitude was observed at 14,500 feet (4.42 km), and the eastern segment at 6,500 feet (1.98 km). The magnetic anomaly data,

as received, had the effect of the earth's geomagnetic field removed using U.S. Coast and Geodetic Survey 1955 epoch data (Zeitz and Kirby, 1967), but the specific values that were used were unavailable. Both the magnetic and gravity profiles were digitized at an interval of 1/20th of degree of longitude, which is approximately 4.48 km along the 37th parallel. This spacing is adequate to define the anomalies of primary interest.

These data were differentially upward continued to 6 km in two segments joined at 104.2°W longitude to produce a quasi-consistent data set compatible with the broad gravity station intervals over portions of the profile and the purposes of the analysis. The magnetic data at 6 km elevation were reduced to the pole using mean declination and inclination values over 12° of longitude overlapping segments of data. The overlap was 4° on either end of the segments, with values in these regions averaged to provide the smoothest join. Both the upward continuation and reduction to the pole calculations were performed in the frequency domain assuming two-dimensional sources.

Upward Continuation of the Transcontinental Profile

The 37th parallel gravity and magnetic data at 6 km were upward continued at increasing intervals to 500 km to emphasize the longer wavelength components (Figures 28 and 29). Errors are imposed upon these results in an absolute sense because of the violation of the two-dimensional assumption in the upward continuation to the higher elevations and the lack of adjustment to the curvature of the earth, but these errors are minor because the primary purpose was to filter out the higher frequency components which upward continuation achieves with a smooth filter. The magnetic profiles (Figure 29) include a satellite magnetic anomaly profile derived from even degree values at an average elevation of 450 km as obtained by private communication from M.A. Mayhew of the NASA's Goddard Space Flight Center. These values are not reduced to the pole.

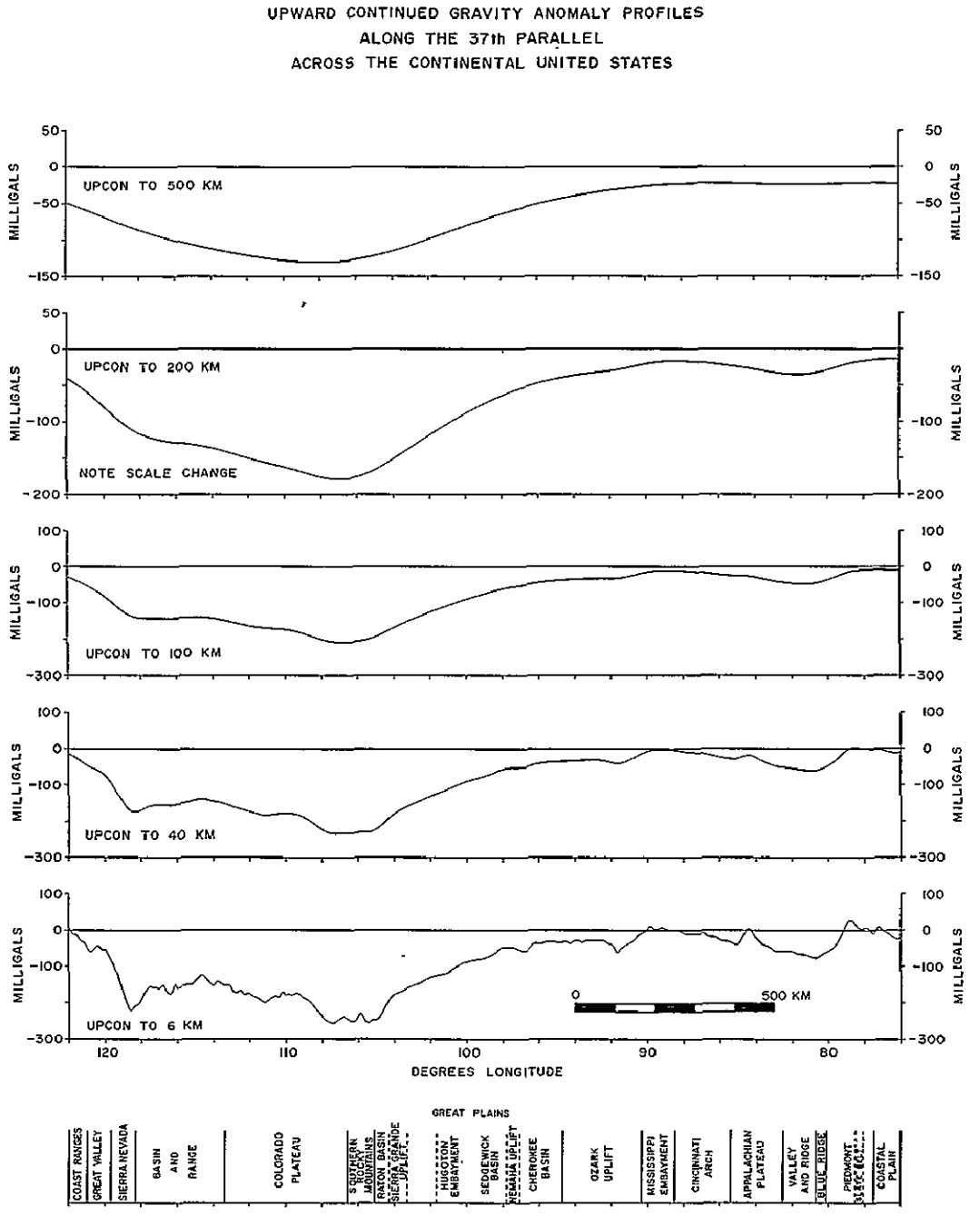

Figure 28. Gravity anomaly profiles along the 37th parallel of latitude across the continental United States, upward continued to 6, 40, 100, 200, and 500 km elevations.

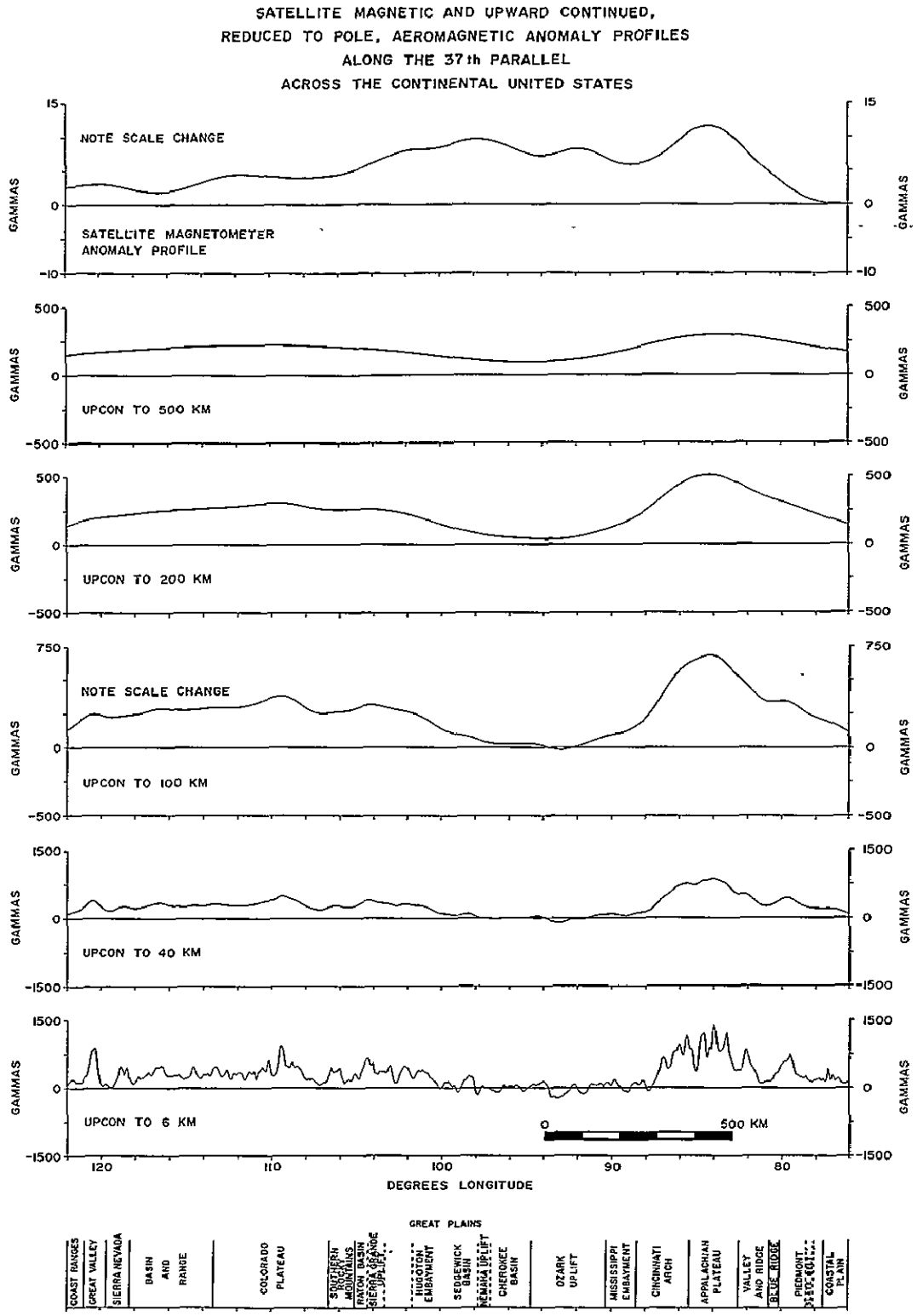

Figure 29. Aeromagnetic anomaly profiles, reduced to the pole, and a satellite magnetic anomaly profile along the 37th parallel of latitude across the continental United States. Aeromagnetic profiles are upward continued to 6, 40, 100, 200, and 500 km elevations.

The magnetic profiles show significant long wavelength anomalies even at the highest elevation. However, there is a lack of correlation and considerable difference in amplitudes of 500 km upward continued and magnetic satellite data. A portion, but not all of these differences can be explained by the two-dimensional and flat-earth assumptions. Tests of the upward continuation procedure shown in Figure 30 demonstrate the accuracy of the process. The upward continued values shown by the continuous profile line compare very well with anomaly values indicated by the dots which were calculated directly from the models. The discrepancies between upward continued and satellite anomaly profiles may result from differing geomagnetic field removal schemes. The results from internal correspondence analysis presented later in this section will provide evidence for this supposition. The 1955 epoch geomagnetic field which was used to reduce the 37th parallel data is compared to the 1965 International Geomagnetic Field (IGRF) in Figure 31. The 1965 IGRF is probably a better approximation to the actual geomagnetic field that existed when the data were observed. The effect of using the 1955 field rather than the 1965 IGRF is to remove too large of a field from data over the eastern U.S. with respect to the west. If the fields are correlated in a relative sense as in Figure 32, anomaly data of the western U.S. would include a long wavelength base level of approximately 200 to 400 gammas relative to the eastern U.S. Thus, the observed differences in western U.S. can be explained, but the considerable difference in amplitude of the positive magnetic anomaly east of 90°W longitude is unaccounted for. Is it possible that the geomagnetic field used in the reduction of the satellite magnetic data has removed some of the crust derived magnetic anomaly? Another significant question is - are the long wavelength magnetic anomalies observed in both the upward continued and satellite magnetic data caused by the superposition of the long wavelength components of the near-surface, upper crustal sources as observed in the eastern U.S. portion of the 6 km upward continued anomaly profile, or are they derived from deep crustal sources or both? The answers to these important questions remain unanswered

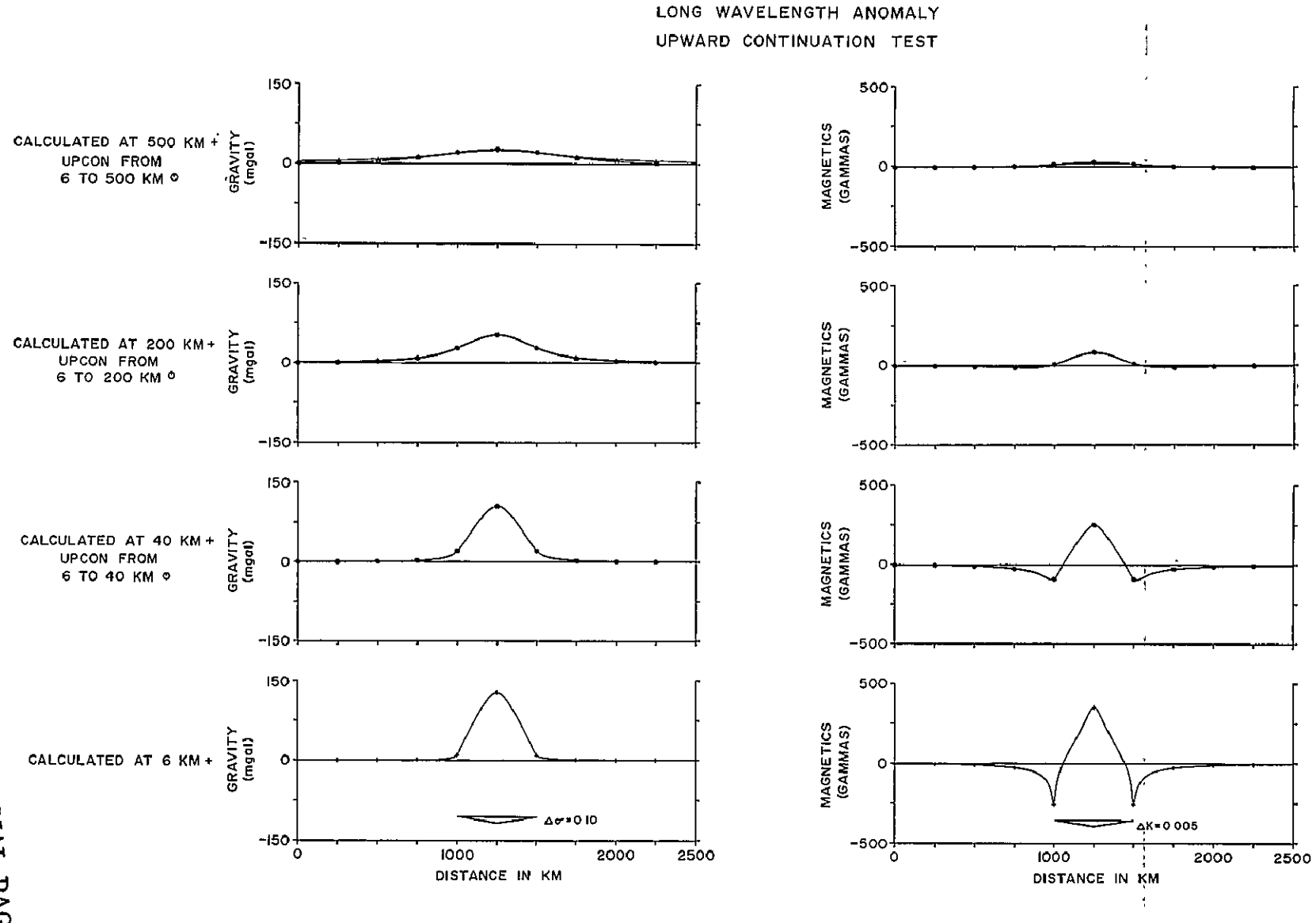

Figure 30. Long wavelength anomaly upward continuation test.

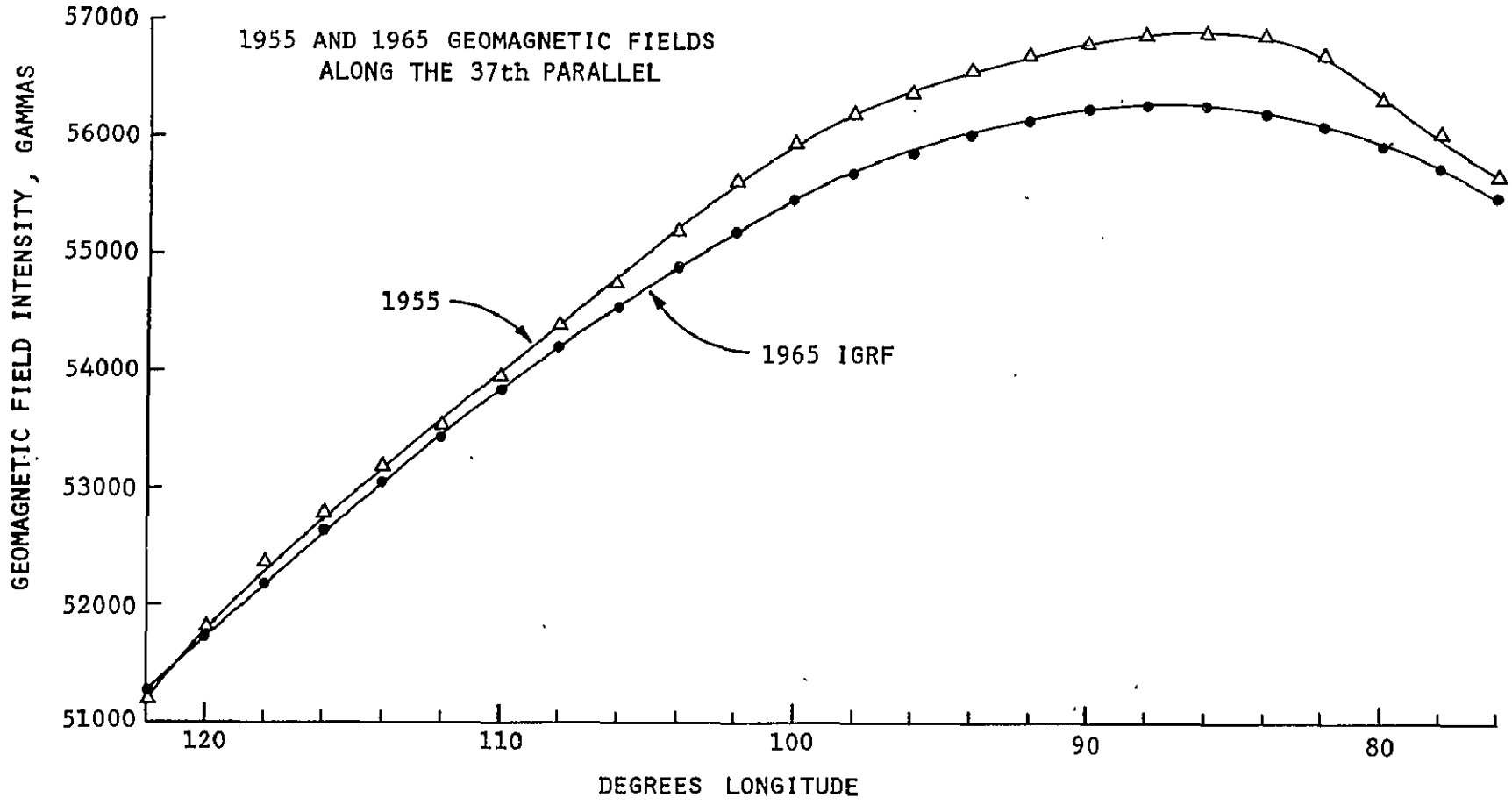

Figure 31. The U.S. Coast and Geodetic Survey's 1955 geomagnetic field and the 1965 International Geomagnetic Reference Field along the 37th parallel of latitude across the continental United States.

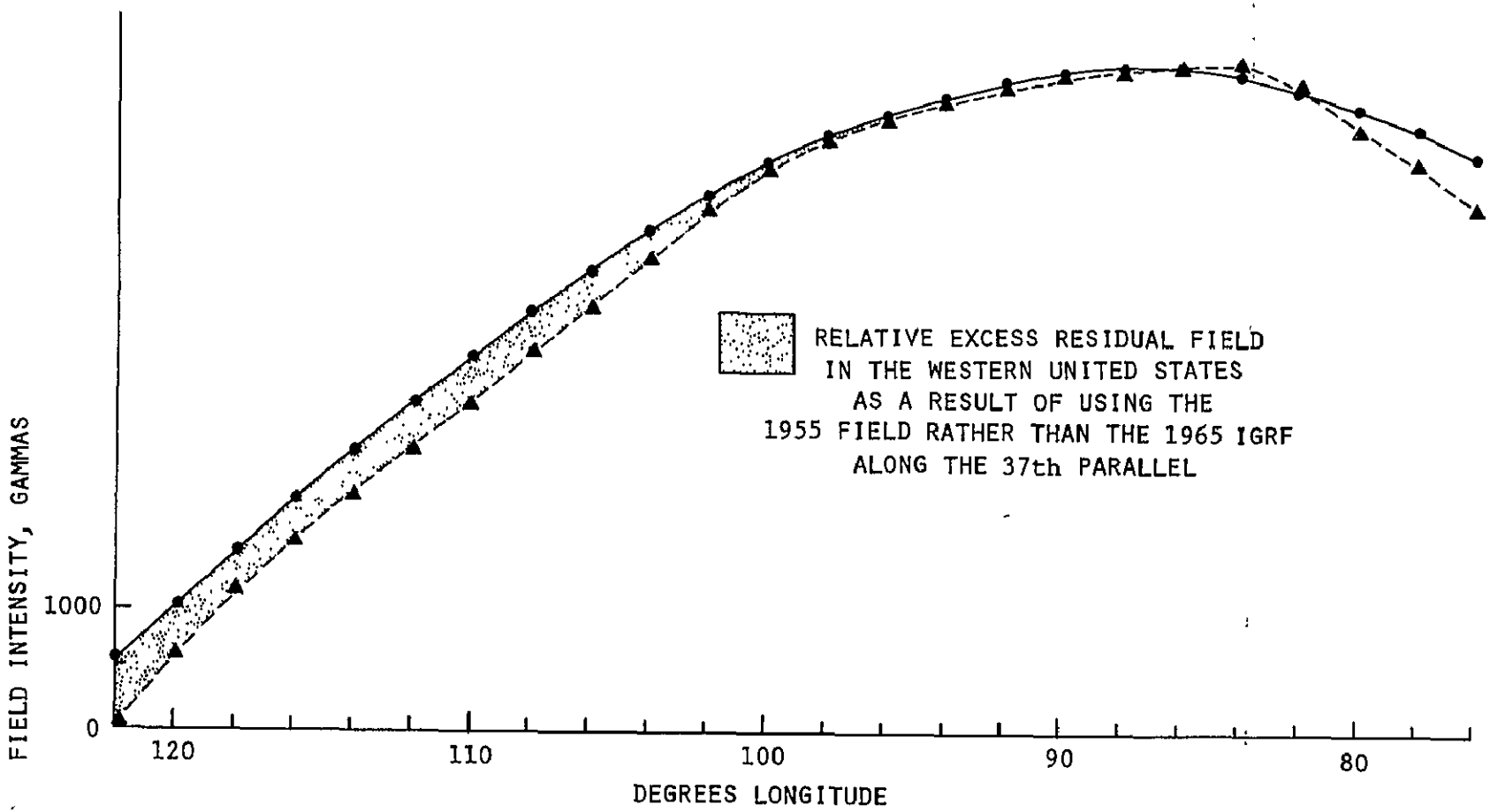

Figure 32. The relative difference between the 1955 and 1965 geomagnetic fields along the 37th parallel of latitude with the fields correlated in the eastern United States.

from the present data and analysis.

To eliminate the very long wavelength anomalies which are a large portion of the discrepancy between the upward continued and satellite magnetic data and that may be core derived, the gravity and magnetic data at a 6 km elevation were filtered to reject energy contained in wavelengths greater than 500 km. The frequency response characteristics of the filter, as shown in Figure 33, indicates that all wavelengths of less than 200 km are passed and 20% of the amplitude of 1000 km wavelengths. The filter is smooth to avoid ringing, but as a result there is some leakage of wavelengths greater than 200 km. These filtered data were upward continued with the results presented in Figures 34 and and 35. Obviously some long wavelength energy is leaking through. The amplitude of the filtered upward continued magnetic data at 500 km is approximately of the same order of magnitude as the satellite magnetic data, but the comparison of the data west of 90^{o}W longitude has not improved.

The upward continuation of the 37th parallel magnetic anomaly data indicates that long wavelength anomalies - anomalies of several hundreds of kilometers wavelength - are present. However, it is unclear whether these anomalies have an independent source from the near-surface anomalies or whether they are the superposition of long wavelength energy from multiple upper crustal magnetic sources. In addition, the upward continued magnetic data at 500 km, even when subjected to a very long wavelength reject filter, does not duplicate the magnetic satellite data. Whether this is a problem of the profile data set and the assumptions used in filtering the data or some other cause, remains to be answered. These questions are significant to consider because they bear on the interpretation and even the existence of these anomalies. It is therefore important to further compare near-surface, preferably two-dimensional, magnetic data upward continued to satellite elevations with magnetic satellite data.

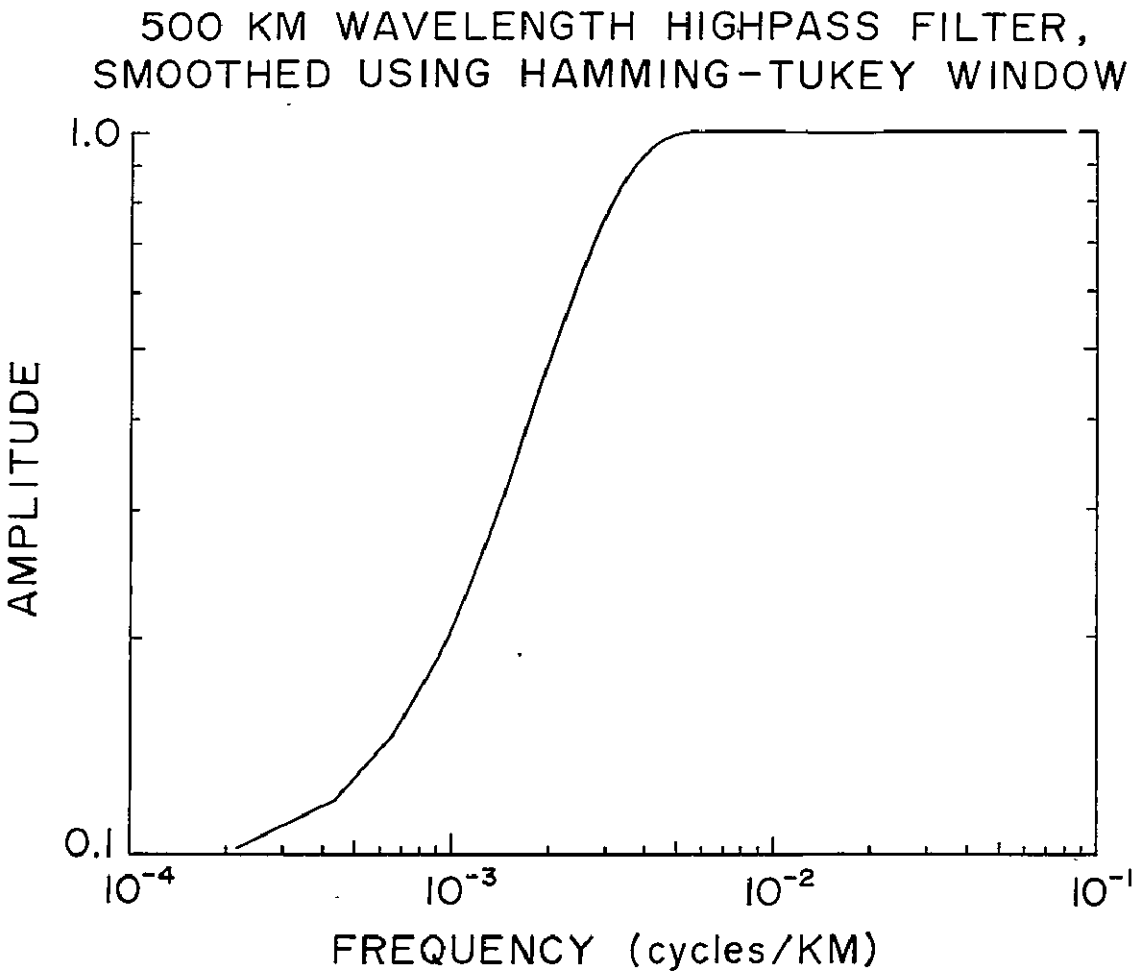

Figure 33. Frequency domain representation of smoothed 500 km highpass wavelength filter.

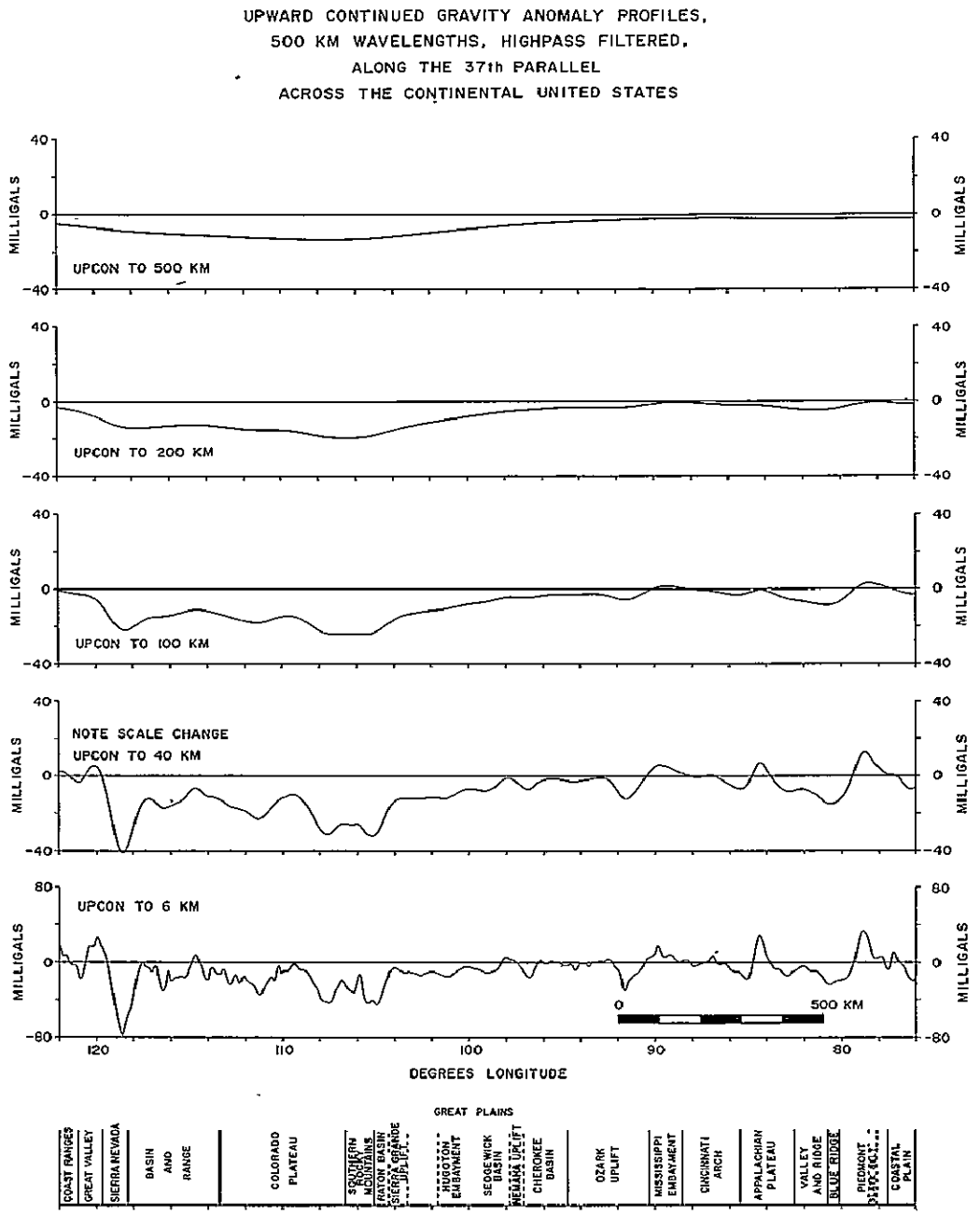

Figure 34. Gravity anomaly profiles, 500 km highpass filtered, along the 37th parallel of latitude across the continental United States, upward continued to 6, 40, 100, 200, and 500 km.

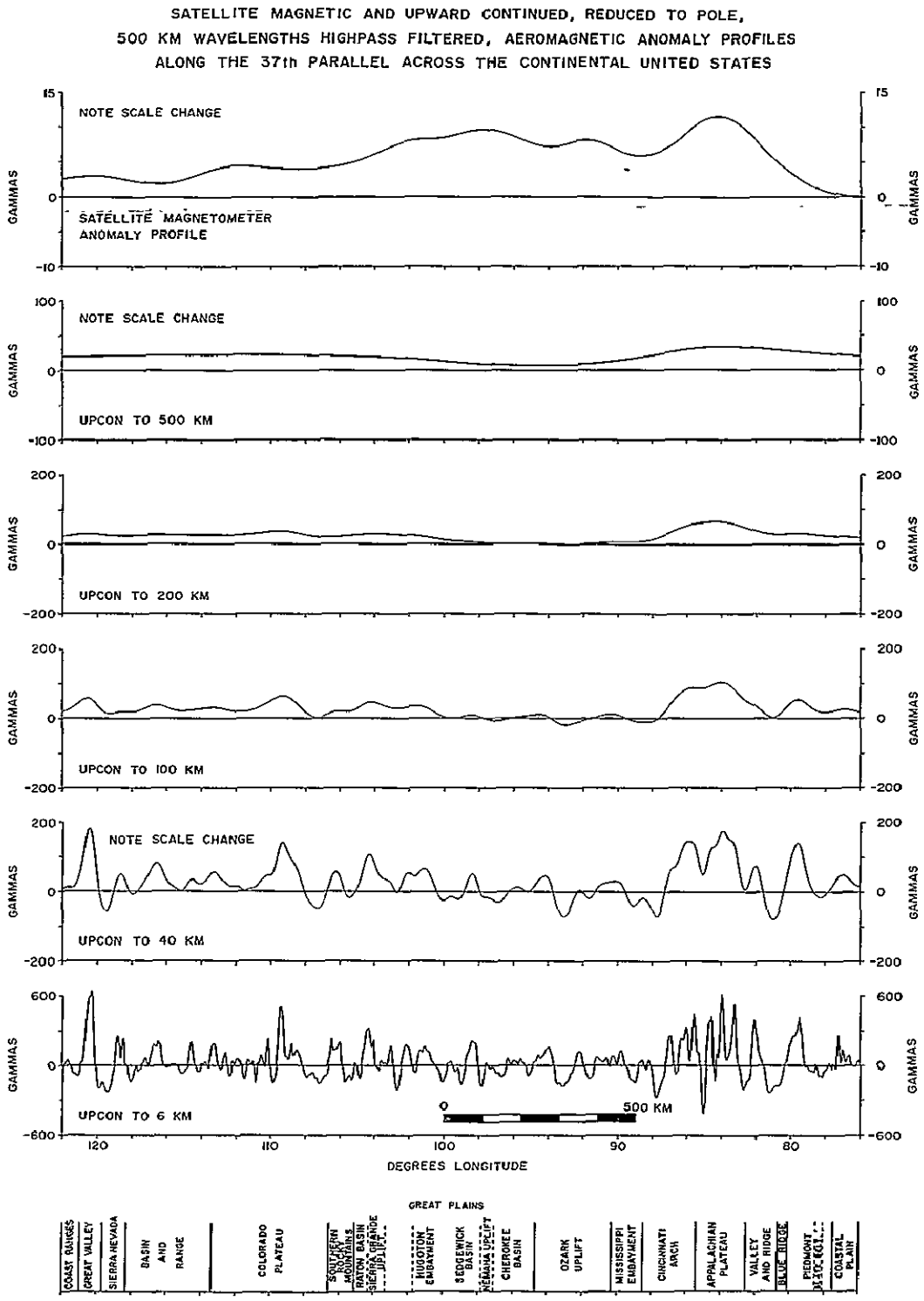

Figure 35. Aeromagnetic anomaly profiles, reduced to the pole and 500 km highpass filtered, and a satellite magnetic anomaly profile, along the 37th parallel across the continental United States. Aeromagnetic profiles are upward continued to 6, 40, 100, 200, and 500 km.

Internal Correspondence

Internal correspondence analysis of the 37th parallel gravity and magnetic anomaly data demonstrates the correlation of regional geophysical anomalies, validates the presence of long wavelength magnetic anomalies, and indicates a close relation between internal correspondence parameters and the transected geologic provinces which in turn shows that the method has potential for mapping boundaries and certain properties of the provinces.

The gravity, first vertical derivative of gravity and reduced to the pole magnetic anomaly data upward continued to 6 km are shown along with the major geologic provinces along the 37th parallel in Figure 36. The geologic provinces are after Fenneman and Johnson (1969) with subdivisions of the Great Plains Province after Riggs (1960). The internal correspondence parameters of this profile which are plotted in Figure 37 emphasize relatively short wavelength anomalies. There are no broad segments which have significant correlation coefficients near + 1 or - 1. The $\Delta J/\Delta\sigma$ and intercept values change over short distances indicating near surface sources dominant in the analysis. The internal correspondence parameters do not focus on individual sources because both short and long wavelength anomalies are reflected in the profile. As a result $\Delta J/\Delta\sigma$ values are difficult to interpret. However, several observations are of interest on this profile. First, the $\Delta J/\Delta\sigma$ values east of Rocky Mountains, whose eastern margin is at 105^{o}W longitude, are significantly greater than in the western U.S. This result is consistent with observations made by Pakiser and Zietz (1965) on crustal differences based on magnetic anomalies. There are strong concentrations of high $\Delta J/\Delta\sigma$ values centered around 85^{o} and 102^{o}W longitude which correlates with approximate peaks of positive satellite magnetic anomalies (Mayhew and Davis, 1976). Also, it can be observed that consistently large intercept values occur over the profile indicating the existence of considerable long wavelength energy. In the western portion of the profile the intercept is consistently positive

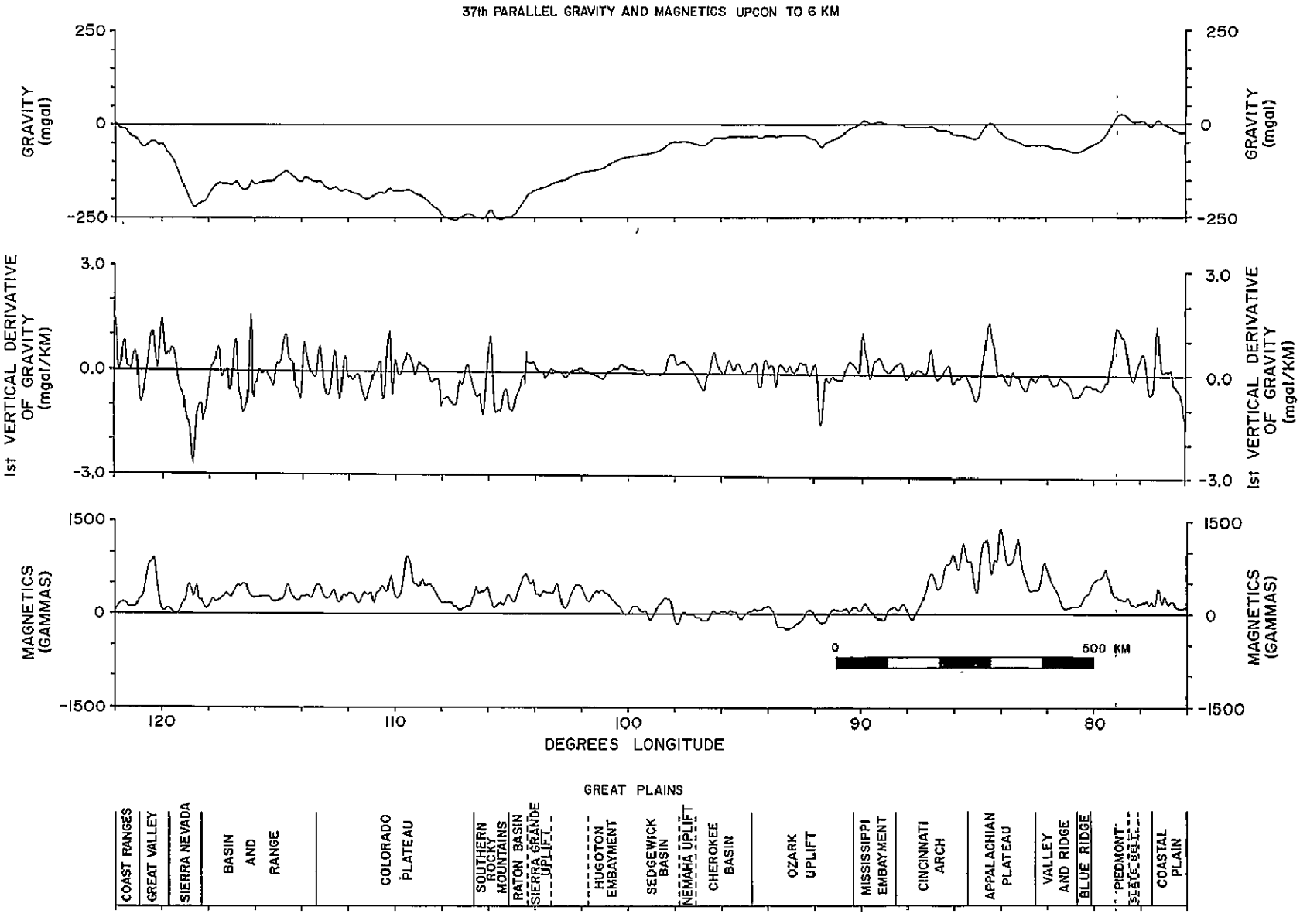

Figure 36. Transcontinental gravity, first vertical derivative of gravity, and reduced to pole magnetic anomaly profiles along the 37th parallel of latitude, upward continued to 6 km.

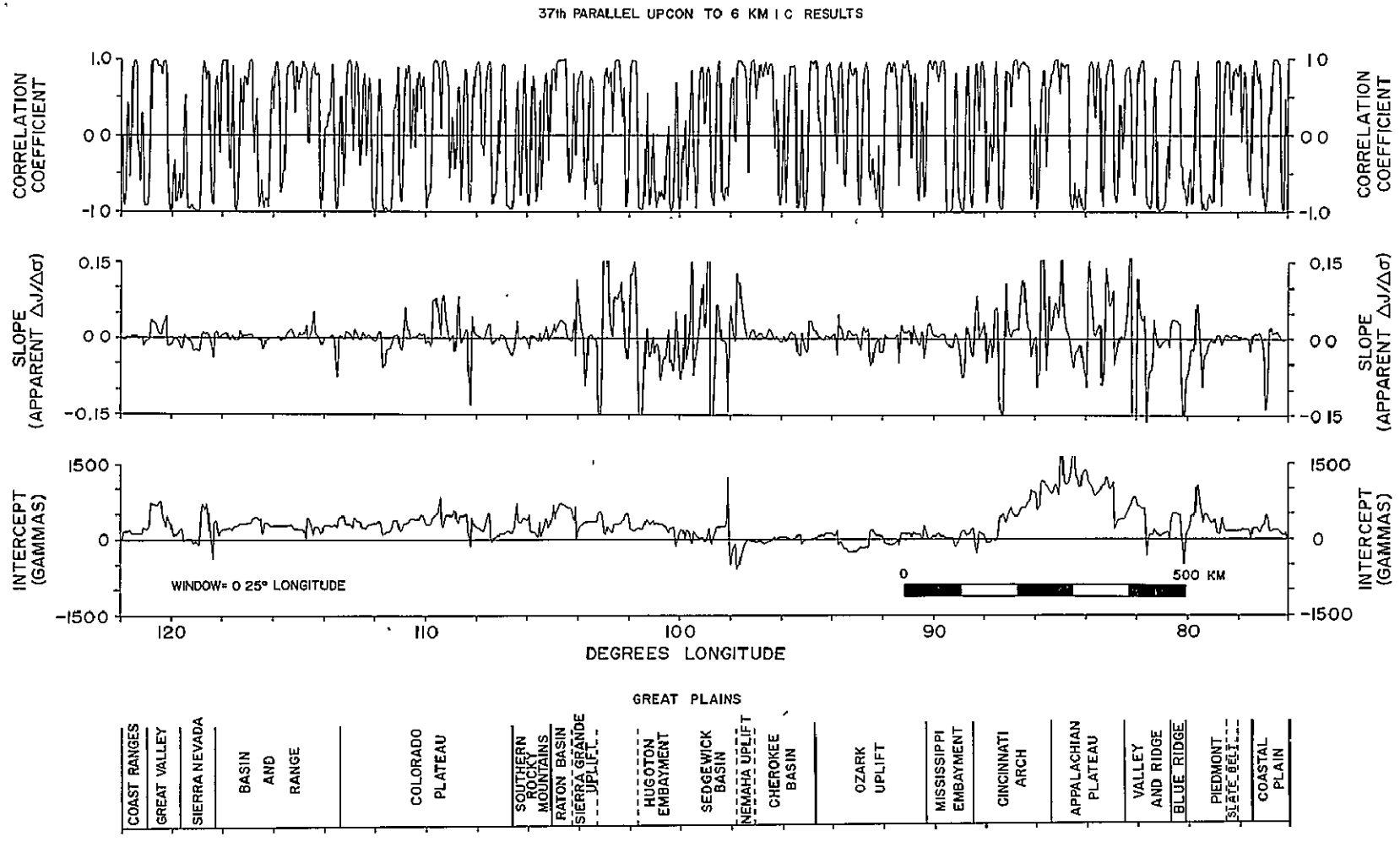

Figure 37. Internal correspondence results of 37th parallel anomaly data upward continued to 6 km.

supporting the previous hypothesis that the 1955 epoch geomagnetic field which was used to reduce these data resulted in erroneous excessive long wavelength magnetic energy in the anomaly field.

Internal correspondence analysis was performed on the 37th parallel anomaly data upward continued to several elevations to emphasize provincial scale anomalies. The data set upward continued to 40 km (Figure 38) was selected for more comprehensive analysis because it possesses minimum interference between anomalies while retaining significant anomalies, as evidenced by the strong correlation coefficients present in the internal correspondence results of Figure 39. Despite the magnetic base levels as indicated by the intercept profile, the parameters have a regional pattern that can be related to many of the geologic provinces transected by the 37th parallel. The regional patterns, as well as the strong correlation coefficients, indicate that a relatively high degree of homogenization of the gravity and magnetic anomaly sources has been achieved by the upward continuation process. Furthermore, margins of generally similar apparent $\Delta J/\Delta\sigma$ values are commonly marked by spike patterns that in model studies indicate approximate boundaries of anomalous bodies.

Although the geologic provinces are not necessarily directly related to basement geology which is mapped by gravity and magnetics, several segments of relatively consistent $\Delta J/\Delta\sigma$ values are correlative with geologic provinces. Examples are the Sierra Nevada, central Colorado Plateau, the Nemaha Uplift area, and the Atlantic Coastal Plain. These are illustrative of segments of high positive or negative correlation coefficients and relatively constant intercept values. The consistency of $\Delta J/\Delta\sigma$ values indicates, when considering longer wavelength anomalies that the related anomalies are due to a homogeneous source of province dimensions within the crust. The spike patterns in both the slope and intercept parameters indicate transitional regions between anomalies.

The central portion of the Sierra Nevada batholith province is one of the few regions on the profile which possesses a strong negative

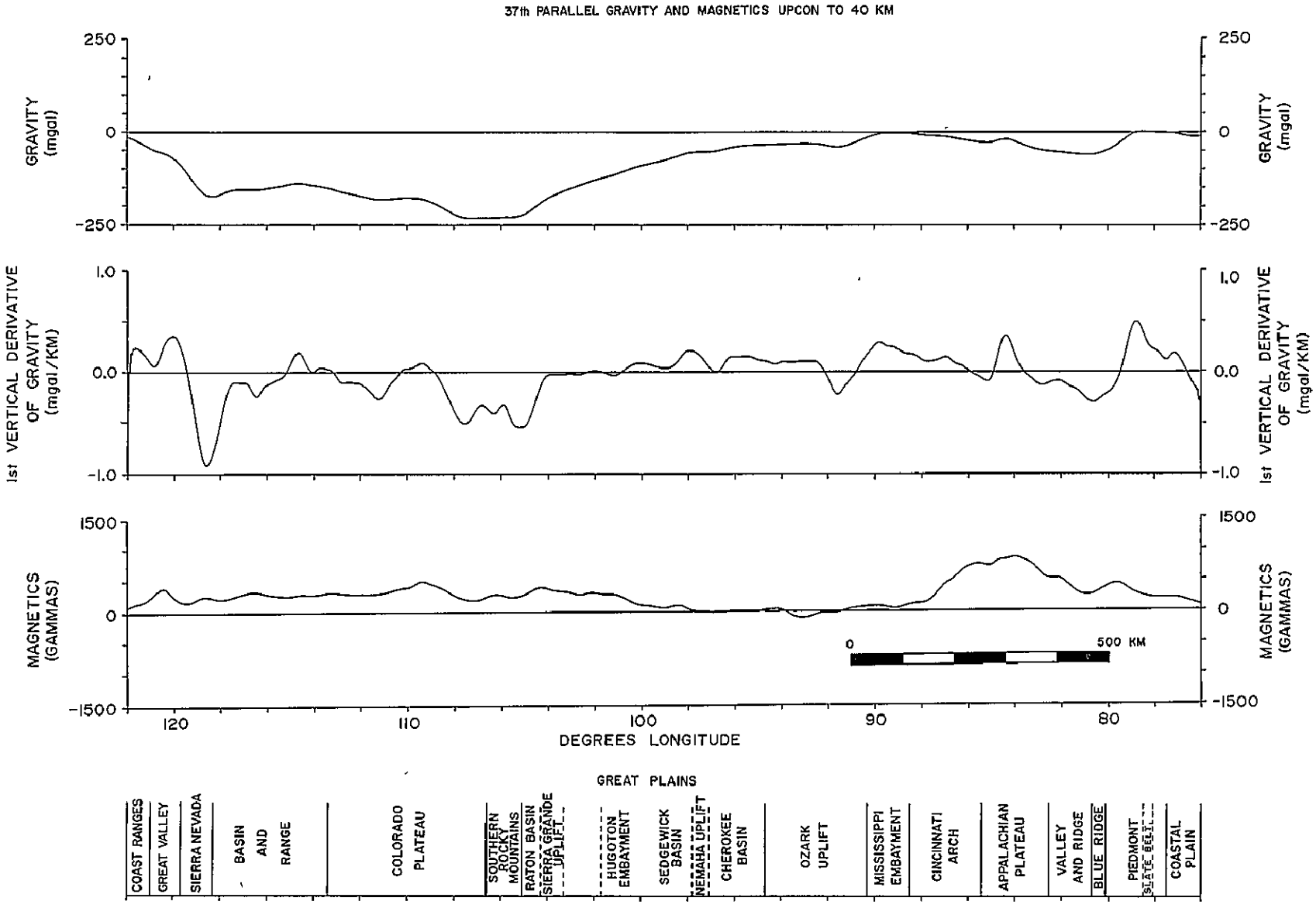

Figure 38. Transcontinental gravity, first vertical derivative of gravity, and reduced to pole magnetic anomaly profiles along the 37th parallel of latitude upward continued to 40 km.

Figure 39. Internal correspondence results of 37th parallel of latitude anomaly data upward continued to 40 km.

correlation. This is caused by a positive magnetic anomaly and a negative gravity anomaly. This segment has rather constant apparent $\Delta J/\Delta\sigma$ values between -0.0076 and -0.0093. Both eastern and western borders of this region are marked by strong interference patterns in the slope and intercept parameters. It is noteworthy that the internal correspondence parameters indicate a possible Sierra Nevada-Basin and Range boundary about one degree east of the physiographic boundary. The eastern extensions of the Sierra Nevada Province is evidenced by partially buried satellite intrusive bodies related to the Sierra Nevada batholith (Zietz et al., 1969). However, a small break in all three regression parameters does occur at the actual physiographic boundary.

The Colorado Plateau region between 107.5 and 111°W longitude is characterized by the widest zone of strong positive correlation along the profile. Positive gravity and magnetic anomalies are the source. Three major distinct zones of apparent $\Delta J/\Delta\sigma$ levels are evident on the slope plot with the central zone reaching values in excess of +0.1. The marginal areas of the Colorado Plateau are marked by weak and rapidly varying correlations and complex slope and intercept patterns.

The Nemaha Uplift-western Cherokee Basin subarea of the Great Plains Province between 96° and 98°W longitude exhibits strong positive correlation and constant apparent $\Delta J/\Delta\sigma$ values of approximately +0.0107. The positive correlation originates from negative anomalies. This segment also has the widest zone of constant negative intercept values on this profile.

The internal correspondence parameters of the Atlantic Coastal Plain Province show a close correlation with the province boundaries as in the case of the provinces of the Appalachian region to the west. The correlation coefficient is strongly positive due to positive anomalies and the intercept and slope parameters are constant. The apparent $\Delta J/\Delta\sigma$ is consistent at a value of approximately +0.016.

In general the gravity and magnetic anomalies of the 37th parallel across North America exhibit a greater percentage of strong positive

correlation than strong negative. In addition, the strong consistent positive intercept west of 100°W longitude suggests a magnetic base level shift due to improper geomagnetic field removal scheme as previously discussed.

Internal correspondence analysis was performed on the transcontinental profile continued upward to 200 km to emphasize very long wavelength anomalies (Figures 40 and 41). As evident on Figure 41, the percentage of the profile exhibiting strong negative correlation has increased appreciably with respect to the results obtained from the data at 40 km elevation (Figure 39). The absolute values of apparent $\Delta J/\Delta\sigma$ have increased with several regions showing extreme positive or negative values suggesting either neglible $\Delta\sigma$ values or high ΔJ values. The intercept values remain approximately the same as those obtained from the 40 km elevation profile. Several geologic provinces coincide with variations in the internal correspondence parameters. Also, the $\Delta J/\Delta\sigma$ values remain relatively consistent in certain regions such as the Sierra Nevada and eastern Colorado Plateau when considering the results of internal correspondence from data at 6, 40, and 200 km. This suggests that in addition to horizontal homogeneity that there is vertical homogeneity as well in these regions. In contrast, other regions such as the Great Plains and the Cincinnati Arch Provinces, for example, exhibit markedly different correlation coefficient and apparent $\Delta J/\Delta\sigma$ parameters at 40 and 200 km elevations, suggesting vertical changes in the physical properties of the crust.

The 500 km high pass filtered 37th parallel gravity and magnetic anomaly data set, upward continued to both 40 and 200 km, were subjected to internal correspondence analysis to compare effects of removing long wavelength components. The high pass filtered anomaly data at 40 km (Figure 42) yield internal correspondence results (Figure 43) with no regional intercept in the western U.S. This suggests the possible use of ICA in isolating geomagnetic field components in anomaly data. The regional intercept values are also significantly diminished in the eastern U.S. in the vicinity of 85°W. longitude. The apparent $\Delta J/\Delta\sigma$

Figure 40. Transcontinental gravity, first vertical derivative of gravity, and reduced to pole magnetic anomaly profiles along the 37th parallel of latitude, upward continued to 200 km.

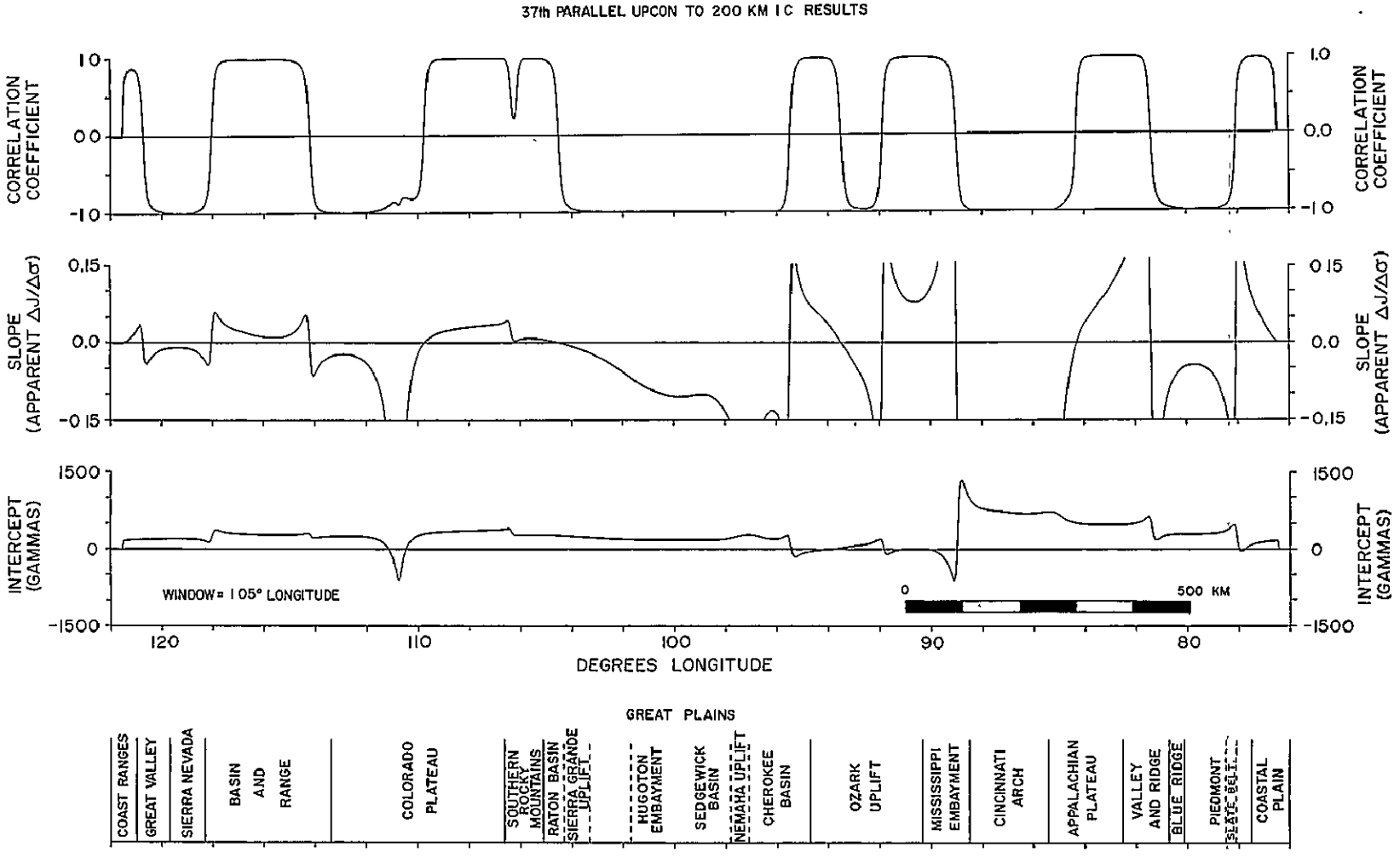

Figure 41. Internal correspondence results of 37th parallel of latitude anomaly data upward continued to 200 km.

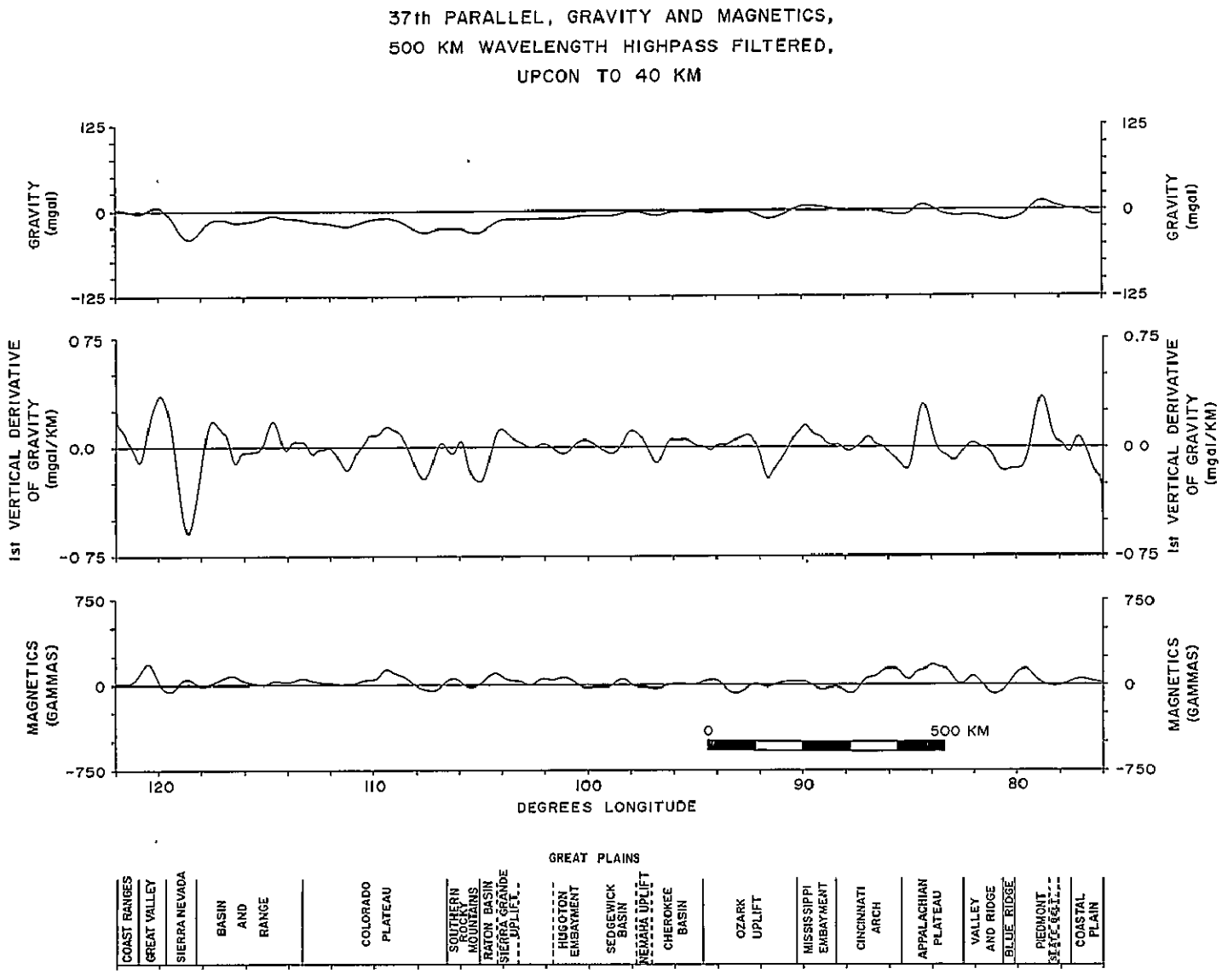

Figure 42. Transcontinental gravity, first vertical derivative of gravity, and reduced to pole magnetic anomaly profiles along the 37th parallel of latitude, 500 km highpass filtered and upward continued to 40 km.

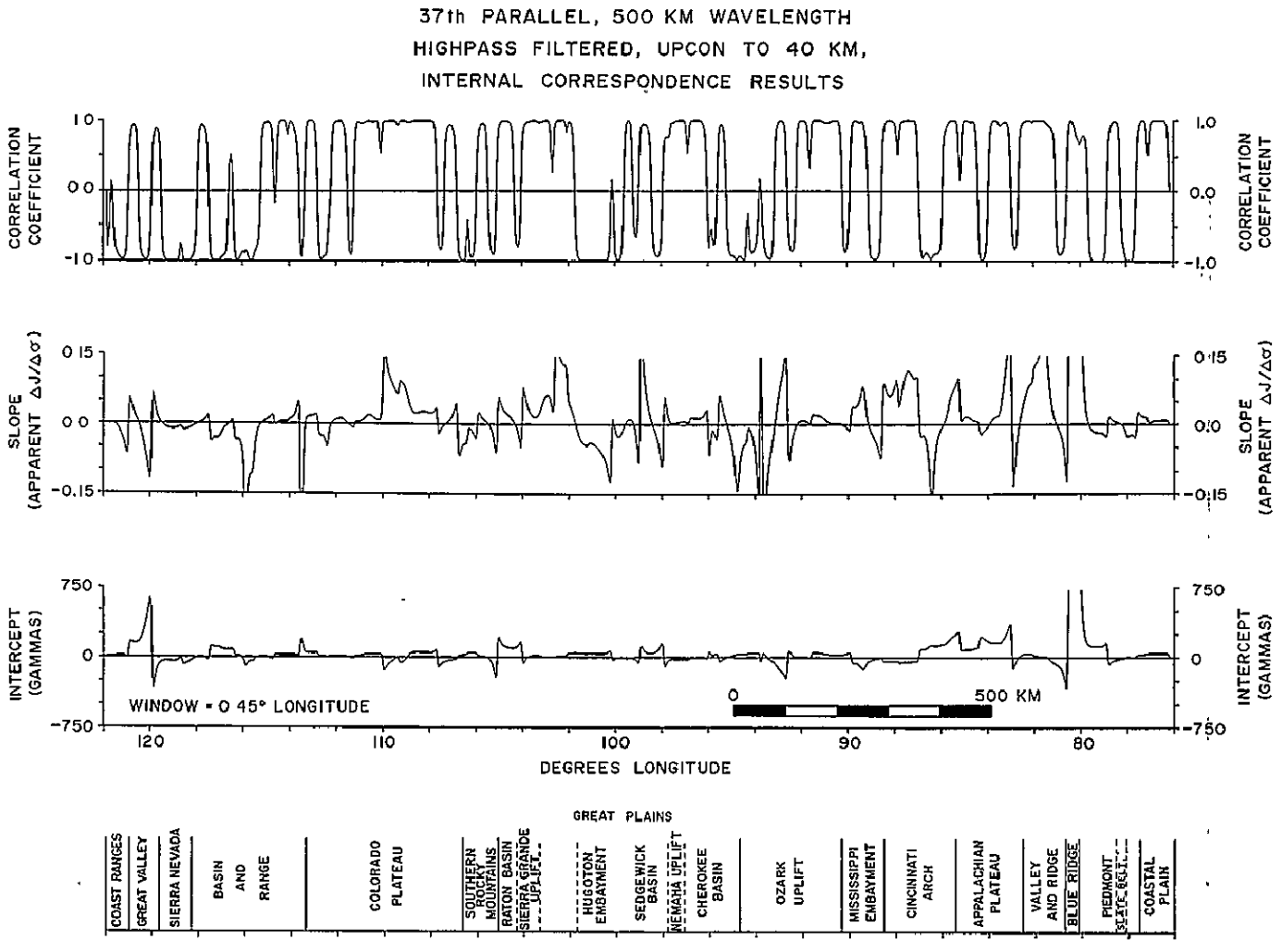

Figure 43. Internal correspondence results of 37th parallel of latitude anomaly data, 500 km highpass filtered and upward continued to 40 km.

values of much of the profile of Figure 43 are essentially unchanged with respect to the results from the nonfiltered data. This indicates that the longer wavelength magnetic and gravity components were not a major factor in determining the ICA results of the unfiltered 40 km elevation data.

The 500 km high pass filtered magnetic and gravity data at 200 km elevation and the results of internal correspondence on this profile are shown in Figure 44 and 45, respectively. Strong correlation coefficients are noted which are generally not as broad as in the unfiltered data (Figure 41) because of the elimination of the broader wavelengths. Further comparison of the results from the unfiltered (Figure 41) and filtered data (Figure 45) shows a decrease in the intercept and apparent $\Delta J/\Delta\sigma$ values from the unfiltered to filtered data. The former decrease is probably related to elimination of geomagnetic field components and the latter probably has a variety of causes. For example, it is interesting to note the essentially zero value of the $\Delta J/\Delta\sigma$ values across the Basin and Range Province. One hypothesis to explain this result is the presence of a shallow Curie isotherm which destroys the ferromagnetism of the rocks at depth and thus in effect reduces the $\Delta J/\Delta\sigma$ values of the anomaly sources represented by the wavelengths present in the profile.

The internal correspondence parameters of the transcontinental profile upward continued to 40 km were clustered to group similar parameter relationships. The results are presented in the form of patterned bars plotted against the original data (Figure 46) and the internal correspondence parameters (Figure 47). The results are clearly not definitive. However, some relationships are interesting, for example, the clusters specified by broad ruled lines (down to the right) are primarily related to negative correlation and $\Delta J/\Delta\sigma$ parameters and are relatively less common east of the Rocky Mountains. Also, the clusters represented by the blanks are restricted to the Colorado Plateau and environs. These areas are characterized by positive

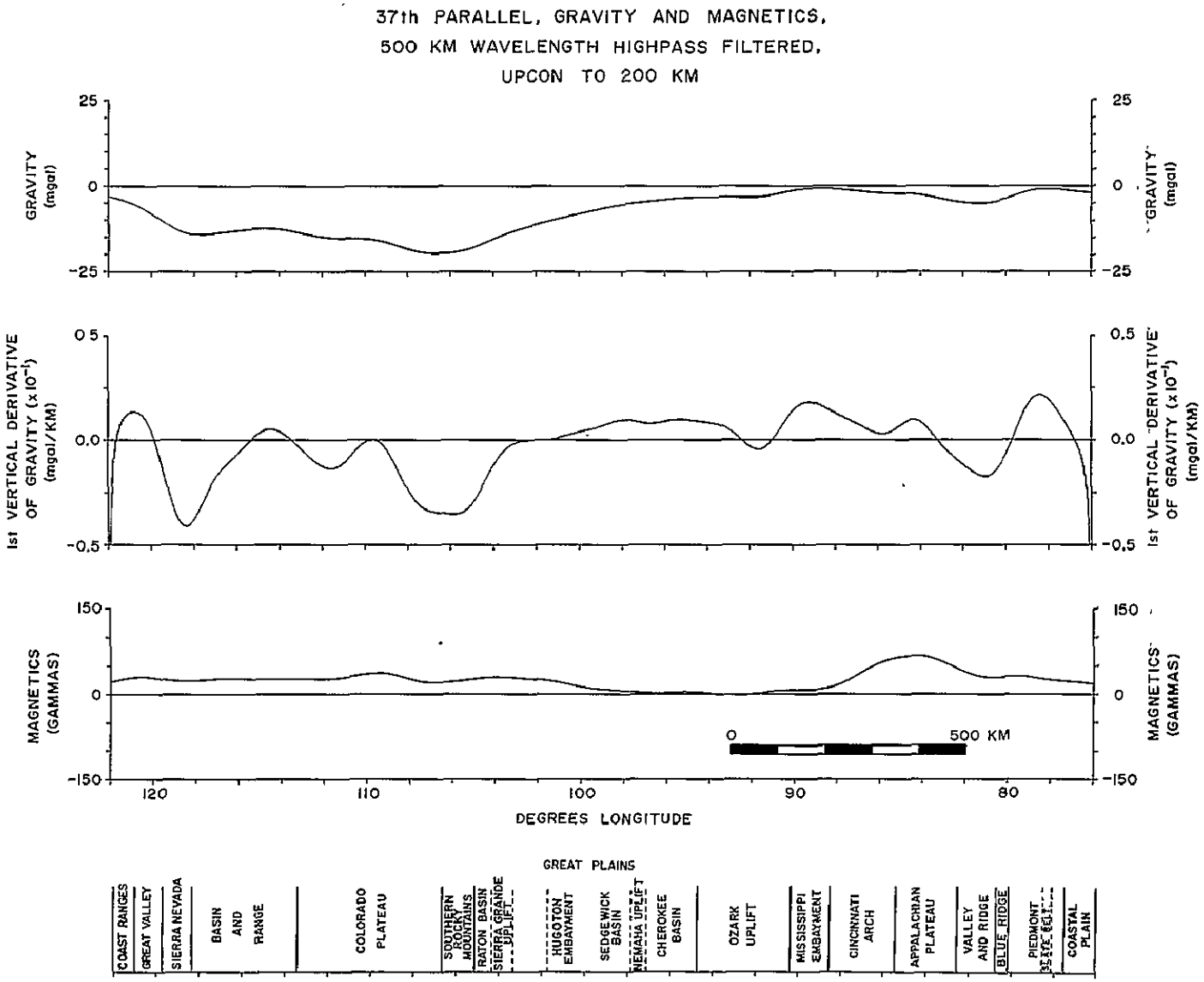

Figure 44. Transcontinental gravity, first vertical derivative of gravity, and reduced to pole magnetic anomaly profiles, 500 km highpass filtered and upward continued to 200 km.

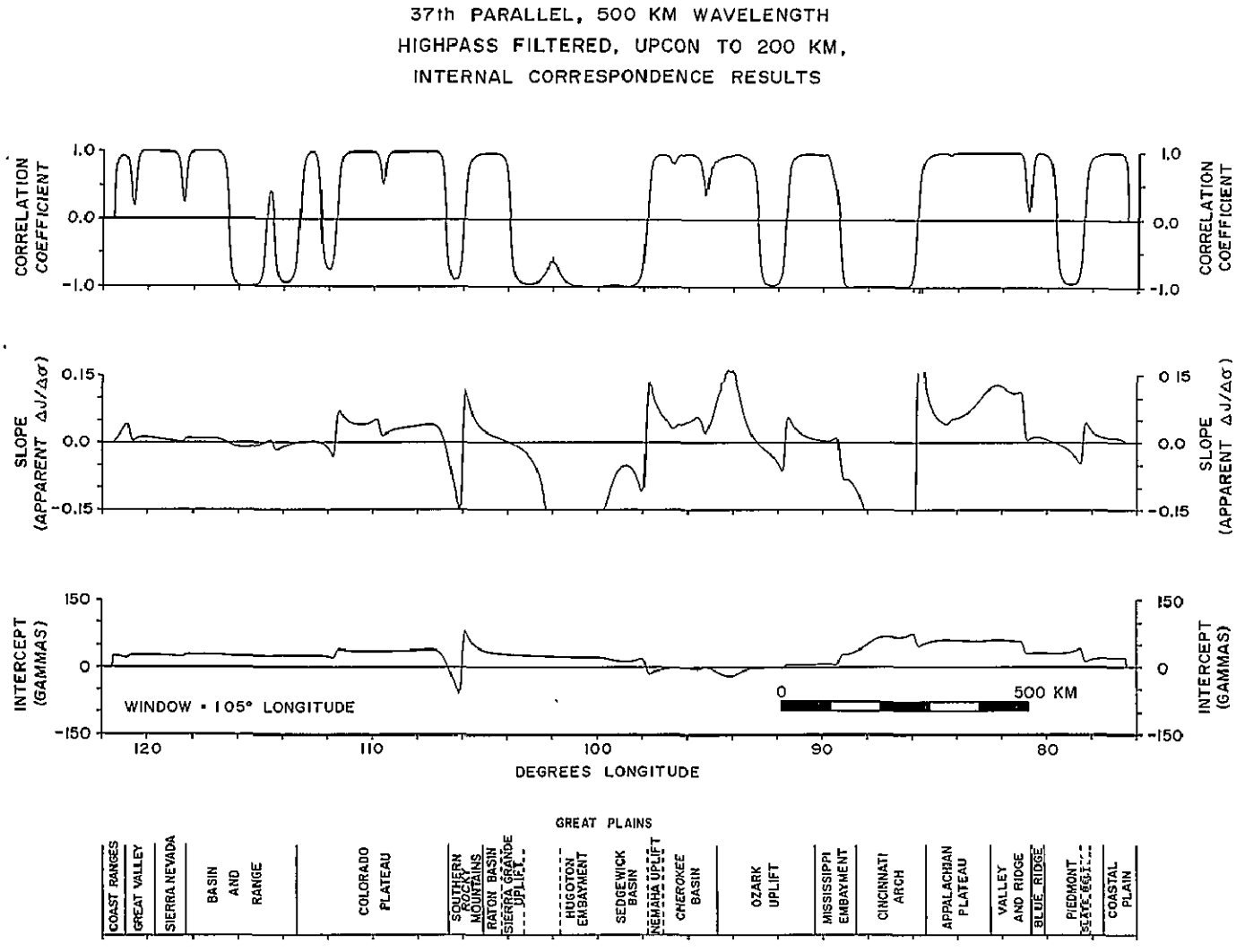

Figure 45. Internal correspondence results of 37th parallel of latitude anomaly data, 500 km highpass filtered and upward continued to 200 km.

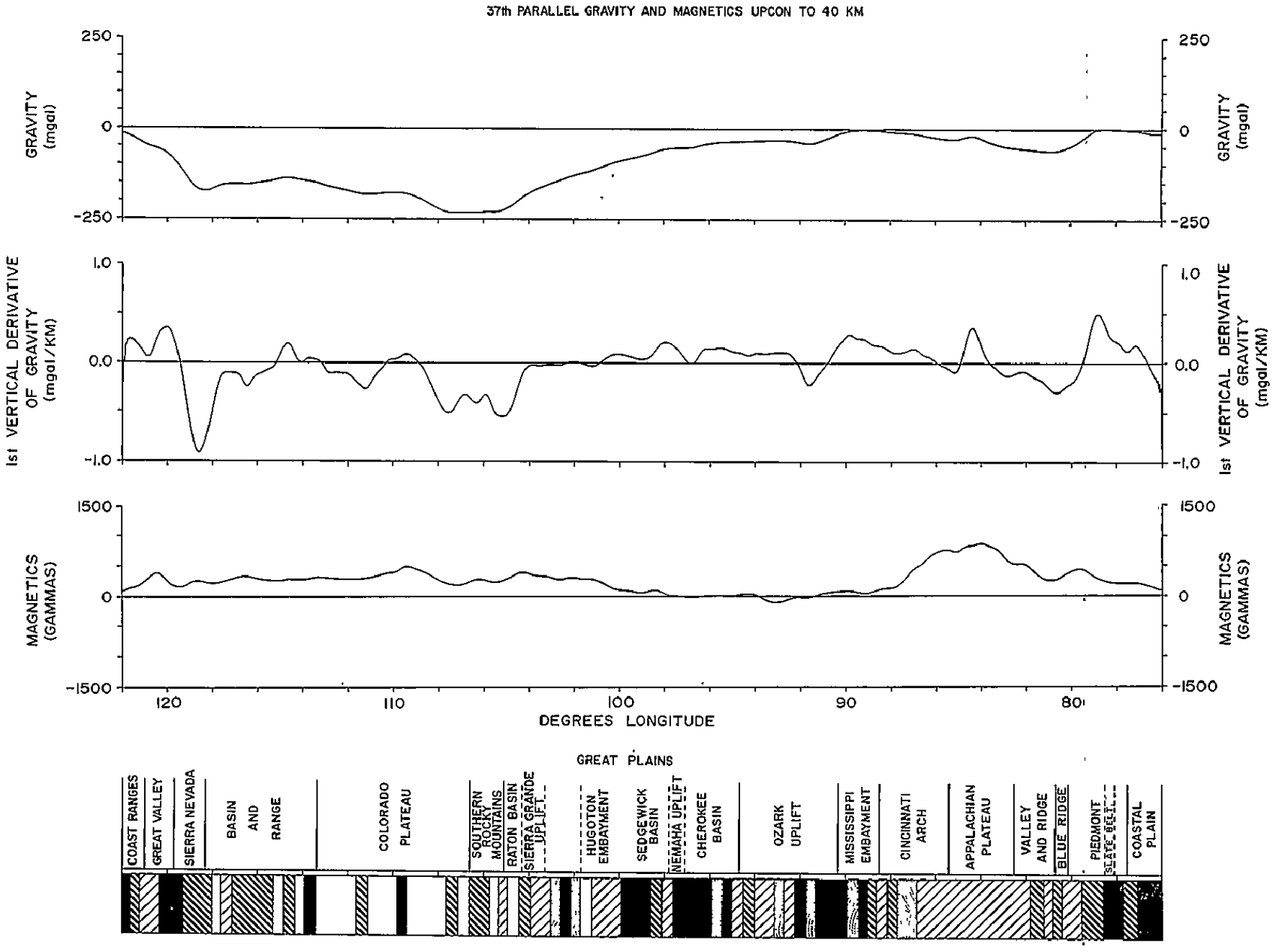

Figure 46. Results of cluster analysis on 40 km level data. Subarea size is 0.45° and the variables are the three internal correspondence coefficients. Presented above the cluster bar are the original 40 km level data. Similarity coefficient is a correlation coefficient with a clustering cutoff at 0.5.

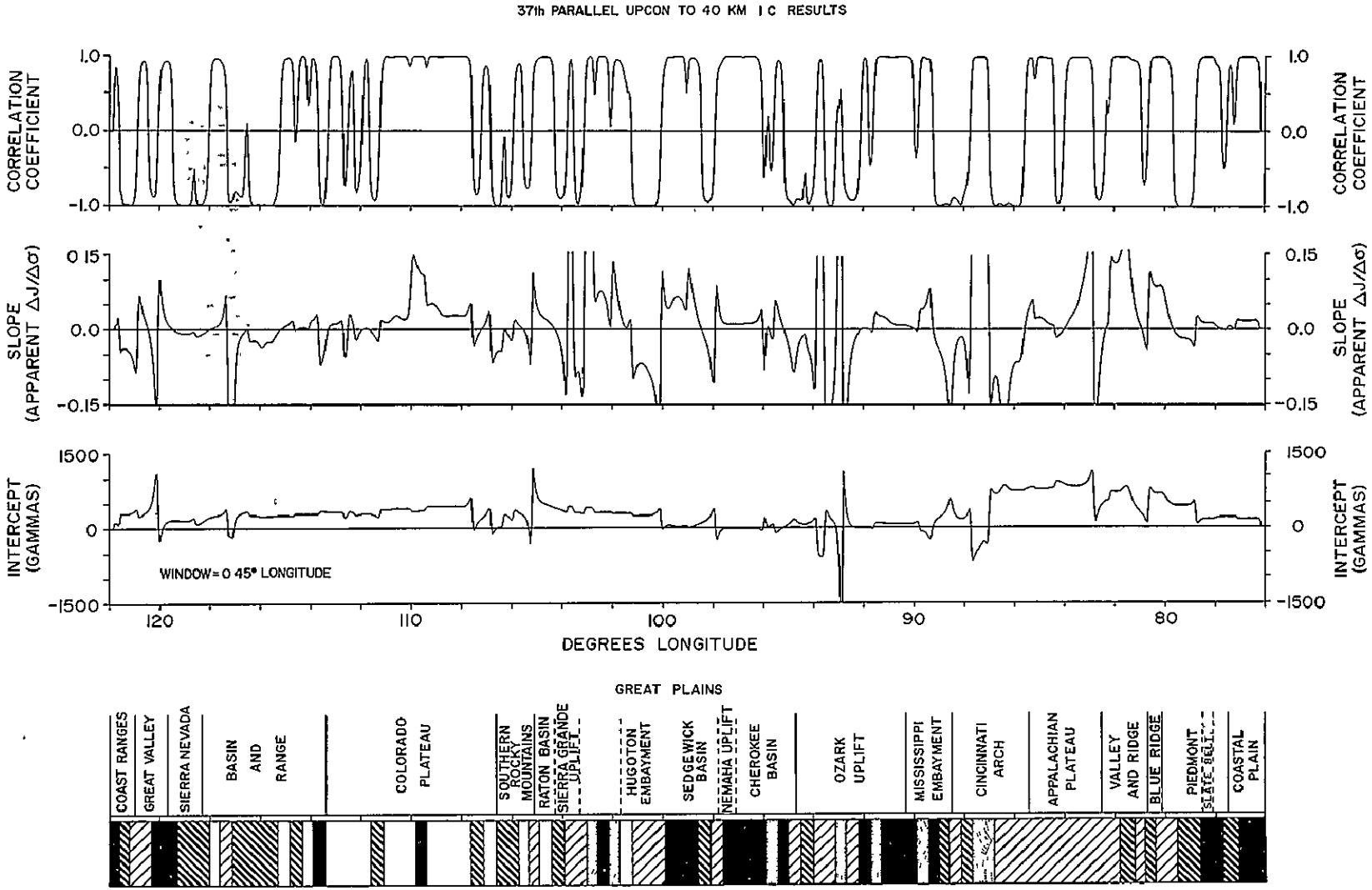

Figure 47. Results of cluster analysis on 40 km level data. Subarea size is 0.45° and the variables are the three internal correspondence coefficients. Presented above the cluster bar are the internal correspondence profiles. Similarity coefficient is a correlation coefficient with a clustering cutoff at 0.5.

correlation coefficients and low to intermediate positive $\Delta J/\Delta\sigma$ values. It is apparent that further clustering studies are warranted to determine their usefulness in the analysis of ICA results and correlation of gravity and magnetic anomalies in general.

Conclusions

Despite the limitations of the transcontinental data set, the results illustrate the usefulness of the correlation of magnetic and gravity anomalies using the ICA technique in validating the presence of long wavelength anomalies, isolating problems of geomagnetic field removal, providing information on the horizontal and vertical variations of the physical properties of the crust over province size areas, and identifying crustal provinces.

Western Minnesota Gravity and Magnetic Profile

Figure 48 shows gravity and magnetic data along a N14°W profile in western Minnesota which has its southern terminus at the Iowa-Minnesota border and 95°W longitude. The data were digitized from gravity (Craddock et al., 1970) and aeromagnetic (Zietz and Kirby, 1970) maps at an interval of 2.5 km. To account for the uneven control in the original data, the broader wavelength anomalies were emphasized by upward continuation of all data to a common elevation of 10 km. The magnetics were reduced to the pole assuming a declination of 2°W and an inclination of 73°. The heavy dark line in Figure 48 represents the boundary recently proposed by Morey and Sims (1976) as a major crustal discontinuity between a 2.6 billion year old greenstone-granite terrain to the north and a 3.6 billion year old gneissic terrain to the south. Internal correspondence analysis was conducted on the data using a window of 17.5 km.

Examination of the ICA profiles (Figure 49) in conjunction with the original data show that distinct regional differences exist in the correlation of the gravity and magnetic data. These regional differences can be in turn correlated with crustal features proposed by Morey and Sims. The ancient gneissic terrain is characterized by poorly matched gravity and magnetic anomalies and regionally low, erratically behaved intercept values. The region near the proposed Morey-Sims boundary has relatively well matched gravity and magnetic anomalies, extremely low and locally level intercept values, and large magnitude $\Delta J/\Delta\sigma$ estimates. The greenstone-granite terrain to the north is characterized by generally well matched anomalies, moderate intercept values, and moderate magnitude $\Delta J/\Delta\sigma$ estimates. When viewed overall, the ICA profiles suggest that a change in the basement lithologies does occur near the proposed Morey-Sims boundary.

Cluster analysis was conducted on the Minnesota profile data using a subarea size of 17.5 km and the three ICA coefficients as variables (Figure 50). The similarity measurement is a correlation coefficient and a clustering cutoff of 0.5 was selected. Although some overlap occurs, there does appear to be a general relationship between the cluster distributions and the proposed Morey-Sims boundary. The cluster

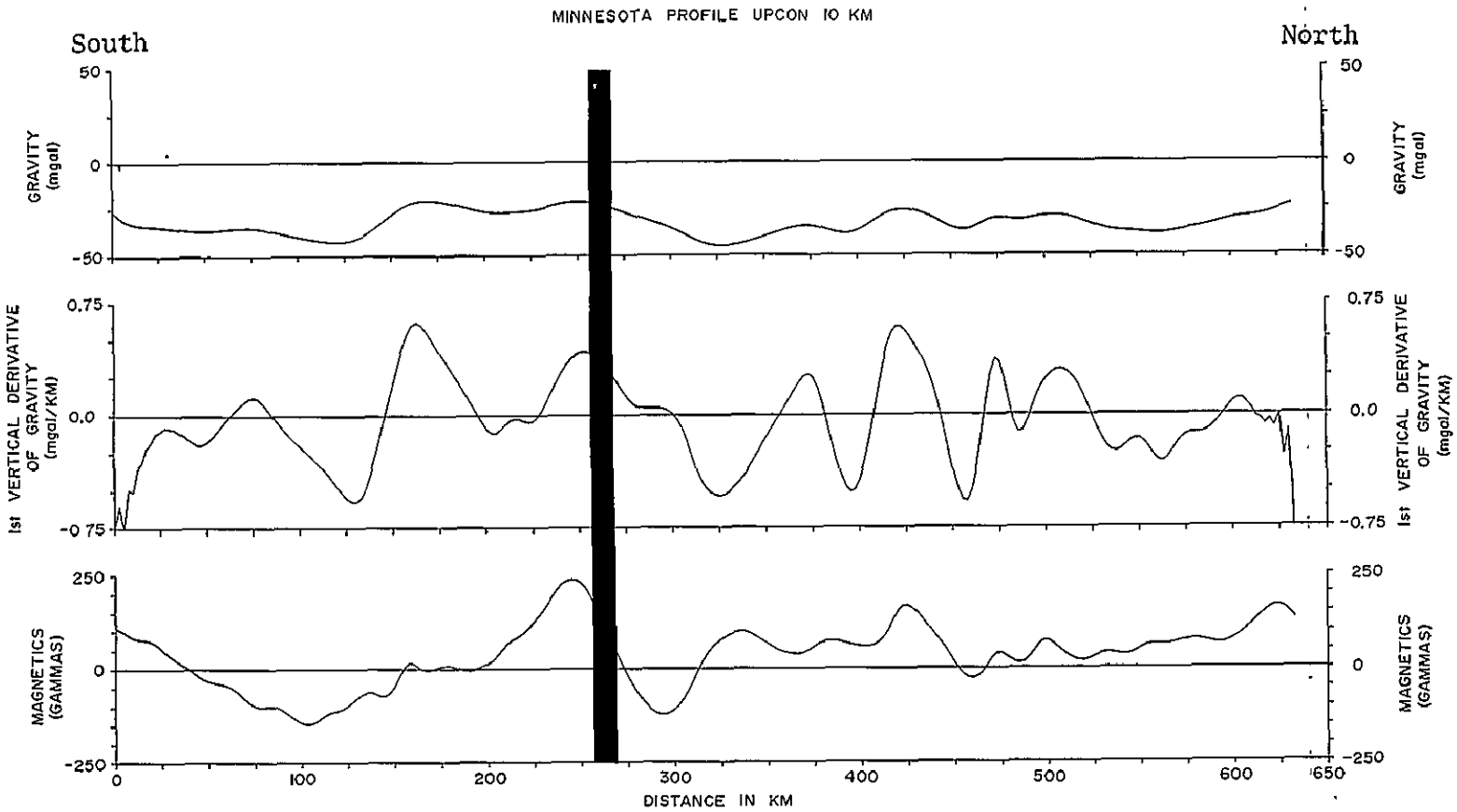

Figure 48. Gravity, first vertical derivative of gravity, and magnetics of western Minnesota profile upward continued to 10 km. Sampling interval is 2.5 km. Heavy dark line is the position of the Morey-Sims boundary.

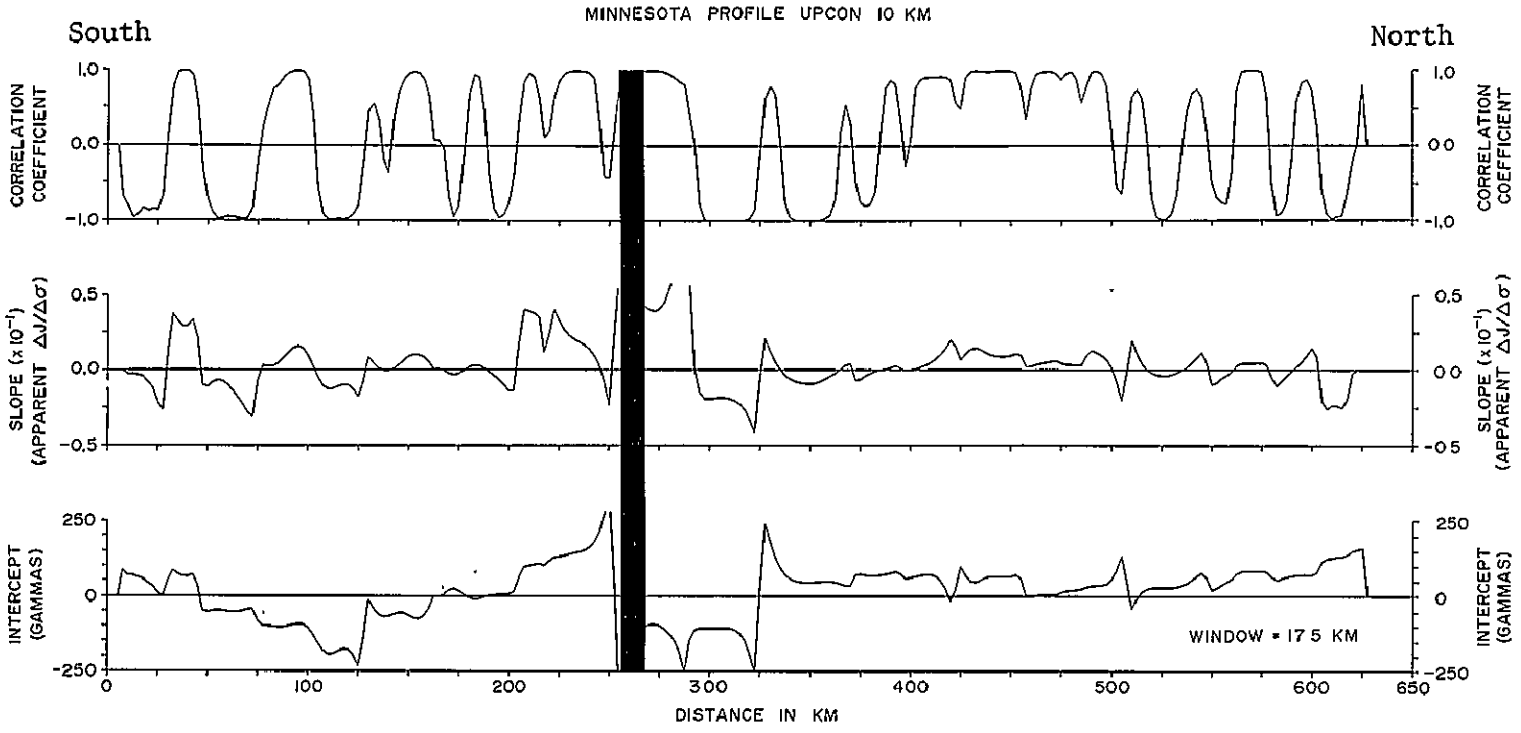

Figure 49. Internal correspondence of western Minnesota profile at 10 km. Window size is 17.5 km. Heavy dark line is the position of the Morey-Sims boundary.

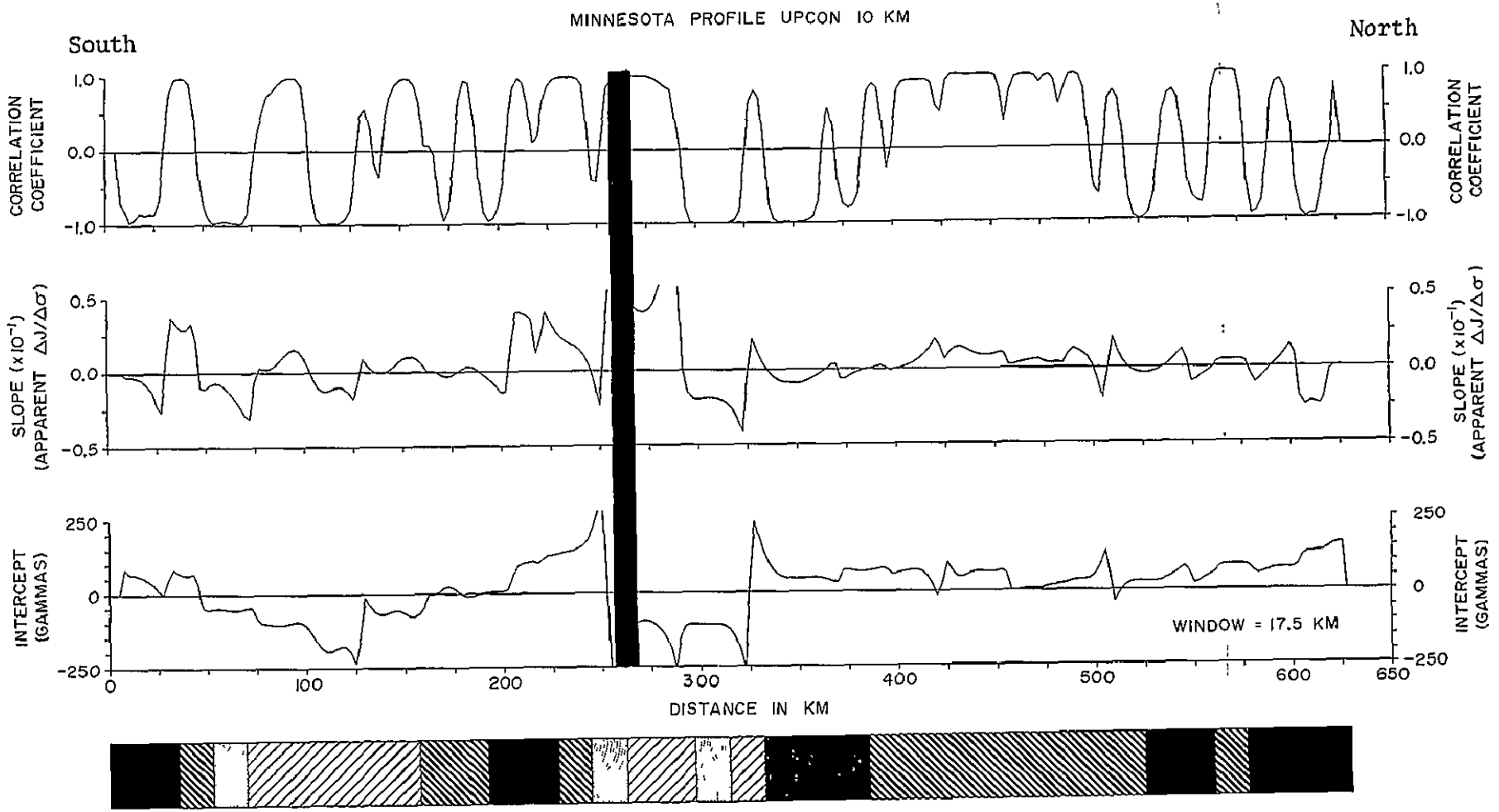

Figure 50. Cluster analysis of western Minnesota profile at 10 km. Subarea size is 17.5 km, similarity measure is a correlation coefficient, clustering cutoff is 0.5, and the variables are the three internal correspondence coefficients.

designated by the heavy ruled lines down to the right occurs predominantly over the greenstone-granite terrain and is characterized by relatively high intercept values, generally positive correlation, and small to moderate magnitude $\Delta J/\Delta\sigma$ estimates. Another cluster, designated by light ruled lines down to the left lies over the ancient gneissic terrain and regions near the proposed Morey-Sims boundary. This cluster is characterized by low intercept values, positive and negative correlations, and moderate to large magnitude $\Delta J/\Delta\sigma$ estimates.

Gravity and Magnetic Data from Eastern South Dakota

This example involves analysis of two-dimensional gridded map data. Modification of ICA from profile to map data is accomplished by converting the moving window to a small square subarea that systematically moves over the entire gridded map space. The ICA coefficients for each window position are determined in the same manner used in profiles and the output consists of gridded correlation, slope, and intercept coefficient maps.

Gravity and magnetic data from eastern South Dakota were digitized on a 10 km grid over a 320 x 320 km area. The magnetics were digitized from a vertical component survey by Petsch (1967) and the gravity data were obtained from the Department of Defense Mapping Agency. The area was chosen for analysis because of the abundance of well control to basement and the presence of several major structural features proposed by previous workers (Lidiak, 1971; Morey and Sims, 1976). To account for uneven control in the data, the broader wavelength anomalies were emphasized by upward continuation of all data to a common elevation of 10 km. The magnetic data were reduced to the pole assuming a regional inclination and declination of 71° and 9°W, respectively. The vertical component of magnetics reduced to the pole is assumed to be equivalent to a vertical total field. The processed data are presented in the form of orthographic projections in Figures 51, 52, and 53.

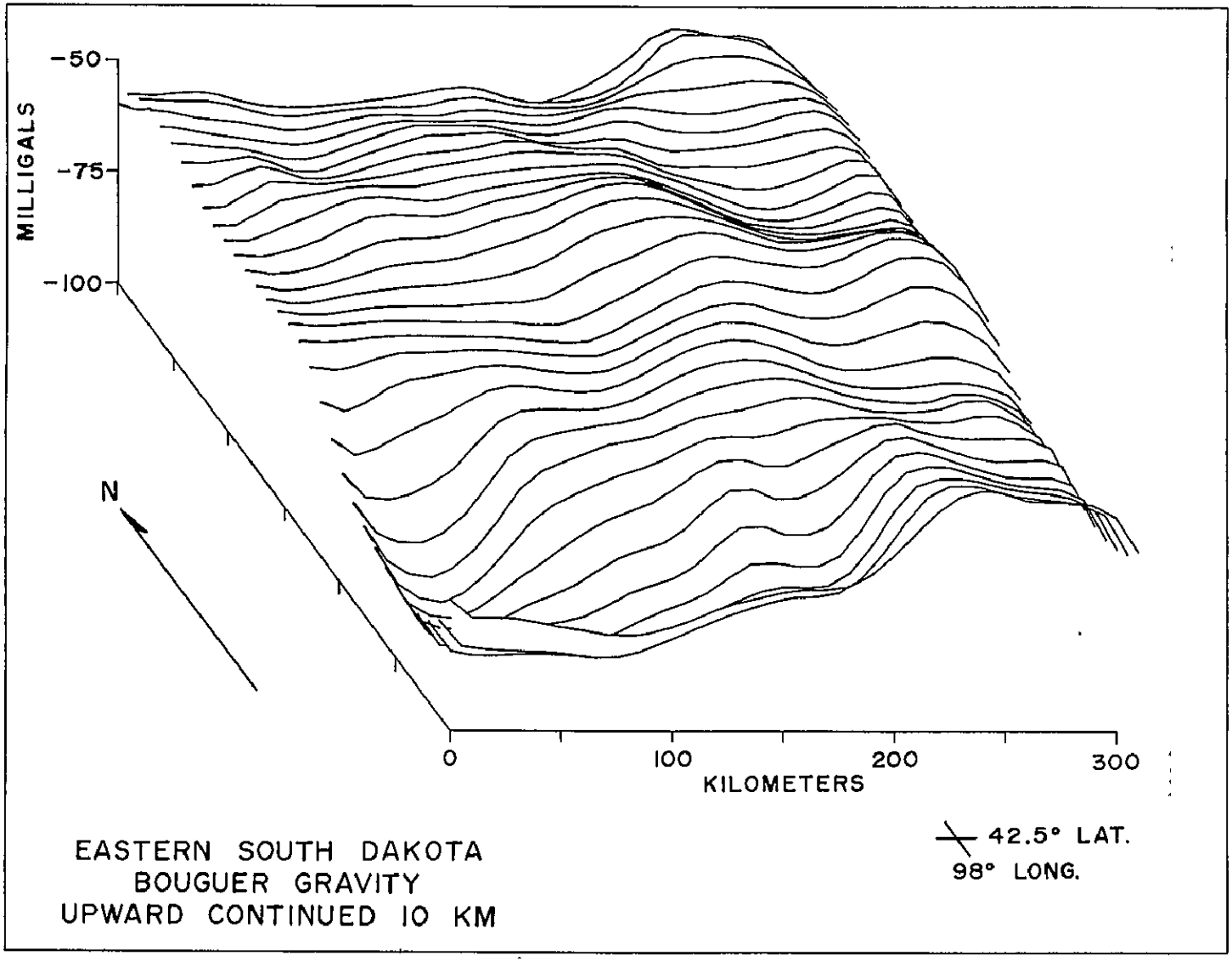

Figure 51. Eastern South Dakota gravity data upward continued to 10 km.

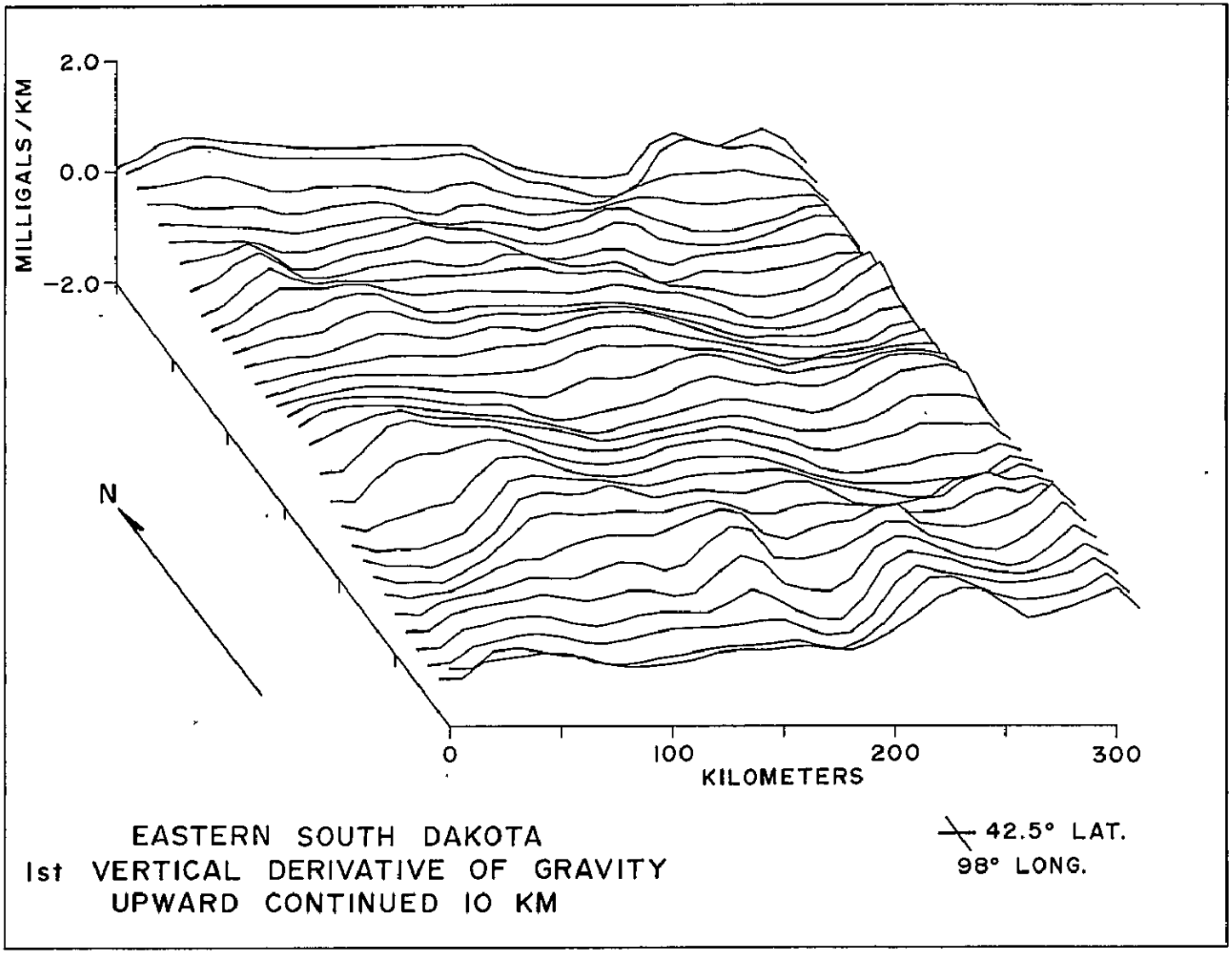

Figure 52. Eastern South Dakota first vertical derivative of gravity upward continued to 10 km.

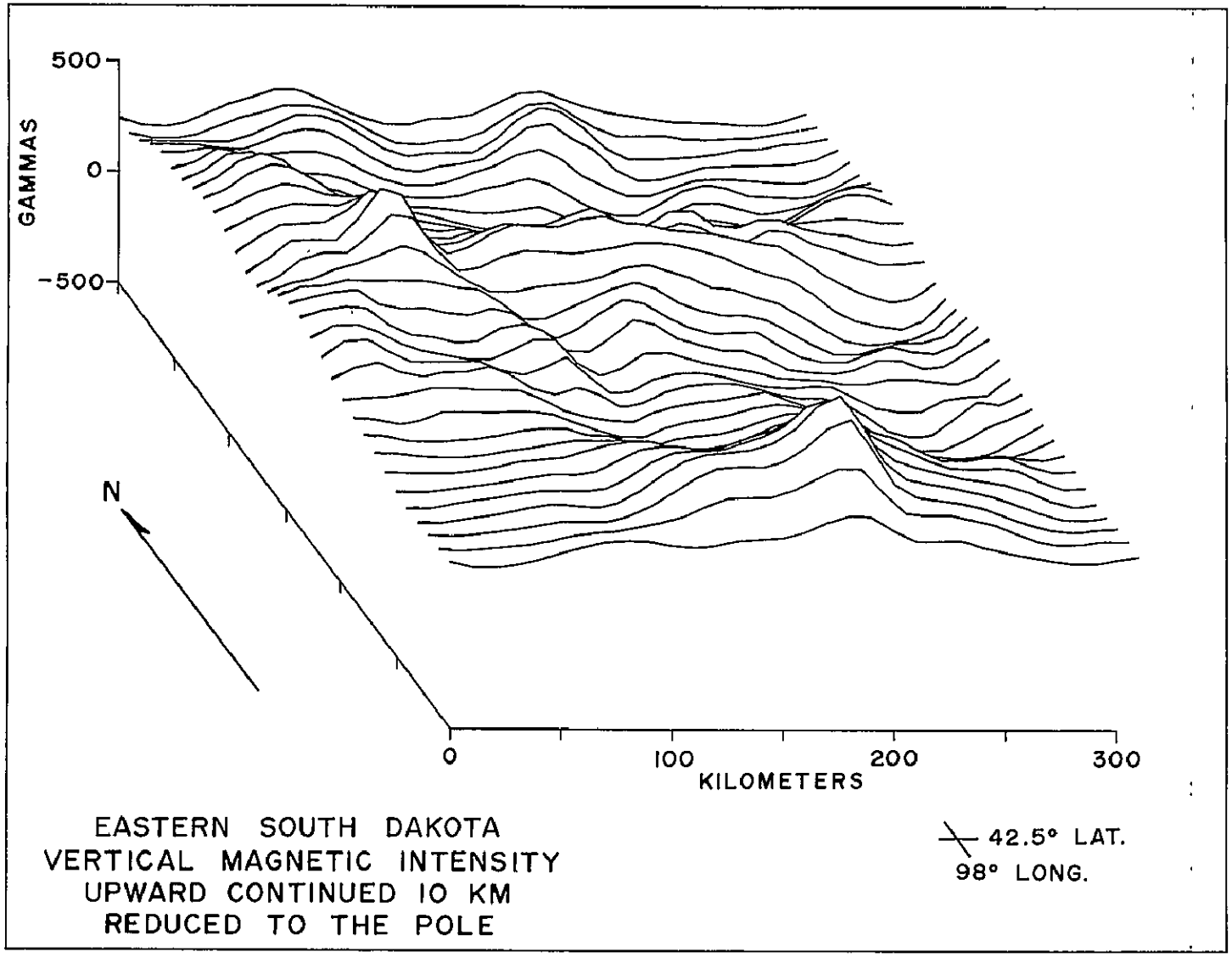

Figure 53. Eastern South Dakota magnetics reduced to the pole upward continued to 10 km.

Analysis of 10 km Level Data

Internal correspondence analysis was conducted on the 10 km level data using a 30 x 30 km moving window. The orthographic projections of the resulting correlation, slope, and intercept data are presented in Figures 54, 55, and 56. In addition to the orthographic projections, line printer contour maps were available for detailed analyses. The regional characteristics of the ICA on the 10 km level data are summarized in Figure 57.

The eastern portion of the summary diagram display several features that appear to correlate with features along the adjacent Minnesota profile previously discussed. The area of low intercept and moderate magnitude $\Delta J/\Delta\sigma$ estimates in the east central portion of the summary diagram may correspond to the ancient gneissic terrain in Minnesota. The northeast corner of the summary diagram exhibits two northeasterly trending belts. The southernmost belt has moderate intercepts and large magnitude $\Delta J/\Delta\sigma$ estimates, while the more northerly belt has low intercept values and moderate magnitude $\Delta J/\Delta\sigma$ estimates. The boundary between these two northeasterly trending zones partially coincides with a southwesterly extension of the Morey-Sims boundary in Minnesota. The ICA coefficients in the northeasterly trending zones in South Dakota are similar in value and behavior to those on the Minnesota profile near the proposed boundary.

The ICA data in the western portion of the study area displays prominent features along a roughly northwest trending zone. This zone, characterized by a long belt of positive correlations and local changes in intercept levels, occurs along a major crustal discontinuity proposed by Lidiak (1971). Lidiak believed that the discontinuity represents the boundary between two major basement provinces; the Churchill to the southwest and the Superior to the northeast.

Analysis of 50 km Level Data

The broader wavelength components of the anomalies were emphasized

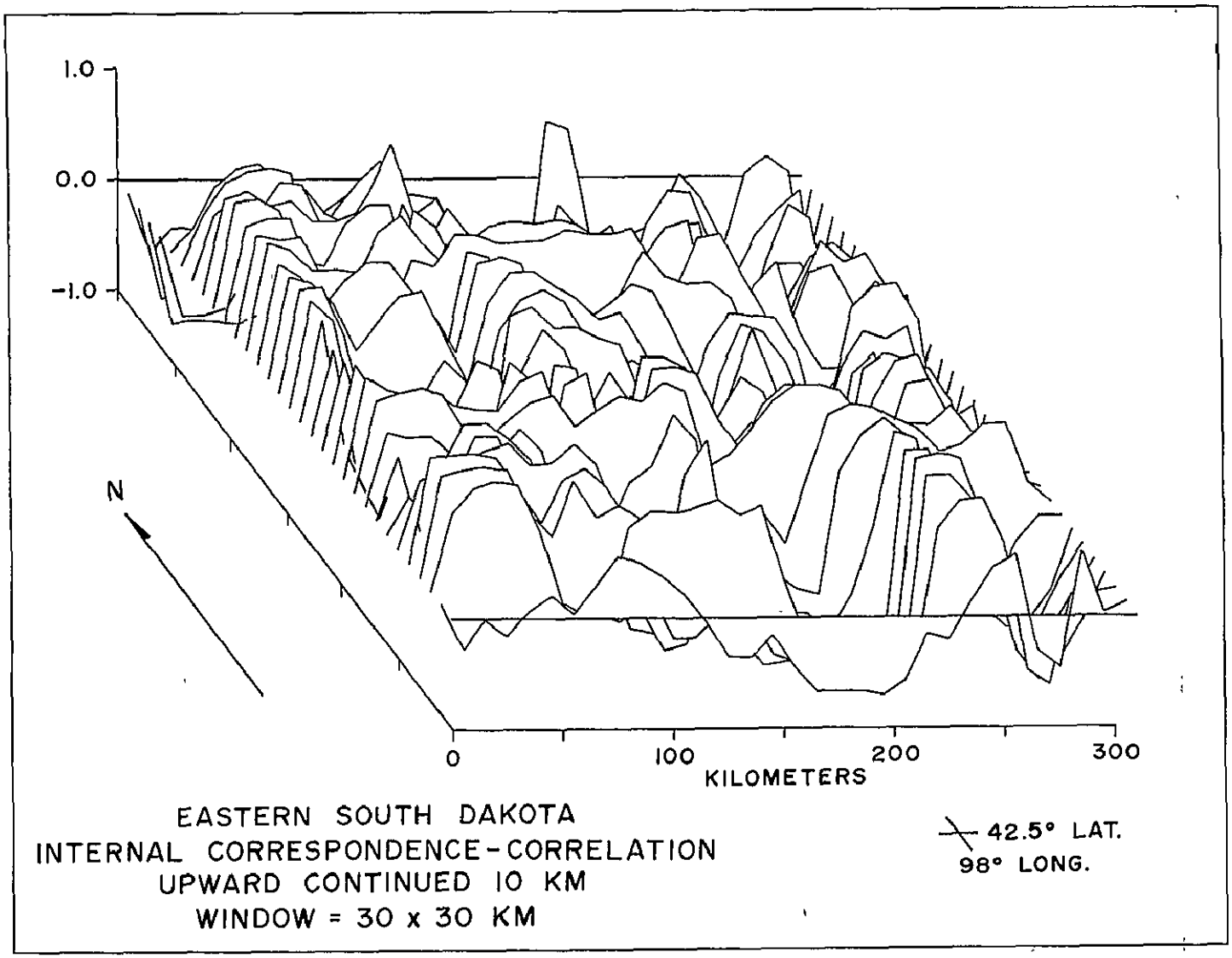

Figure 54. Eastern South Dakota internal correspondence analysis on upward continued to 10 km data: correlation coefficient.

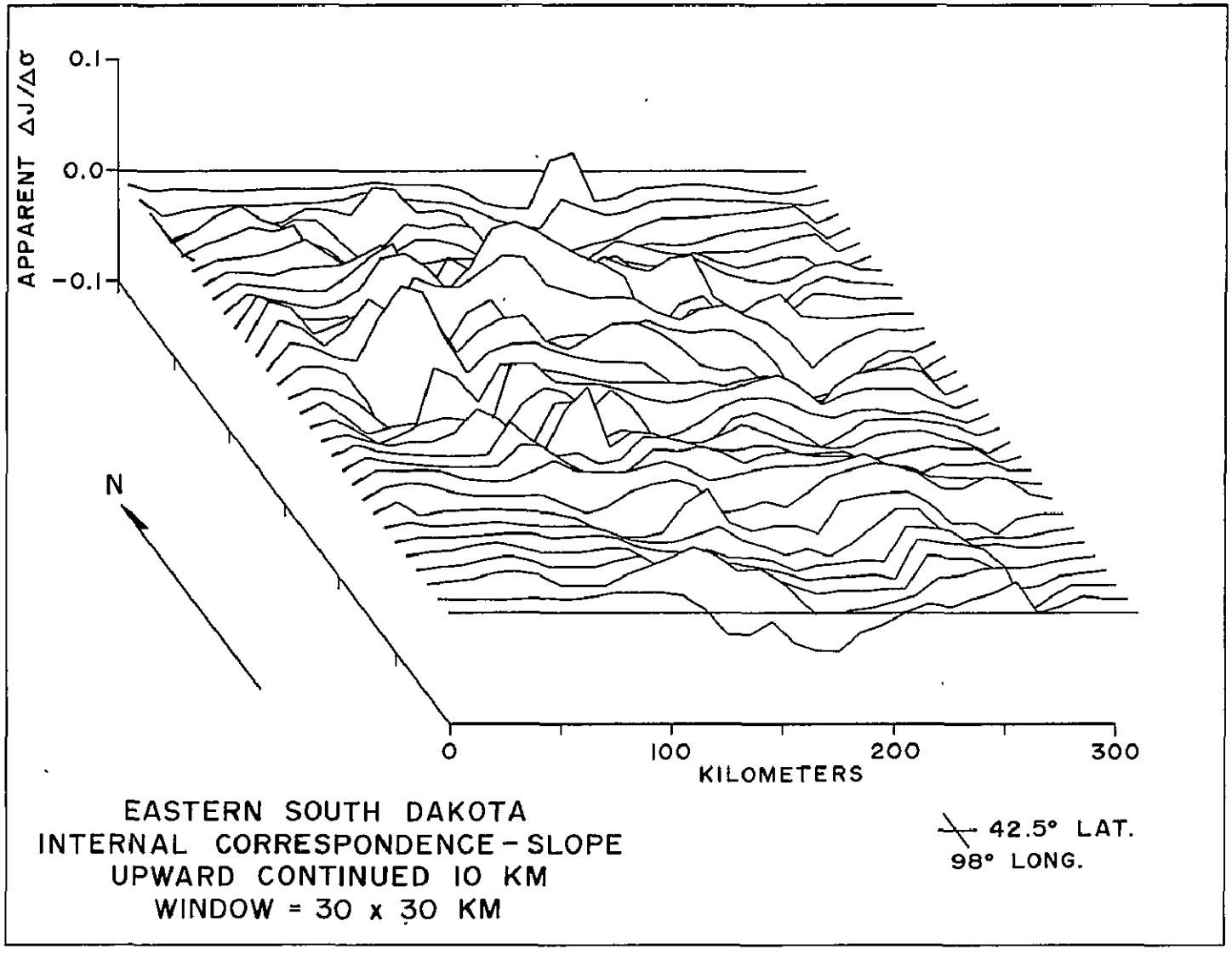

Figure 55. Eastern South Dakota internal correspondence analysis on upward continued to 10 km data: slope ($\Delta J/\Delta\sigma$) coefficient.

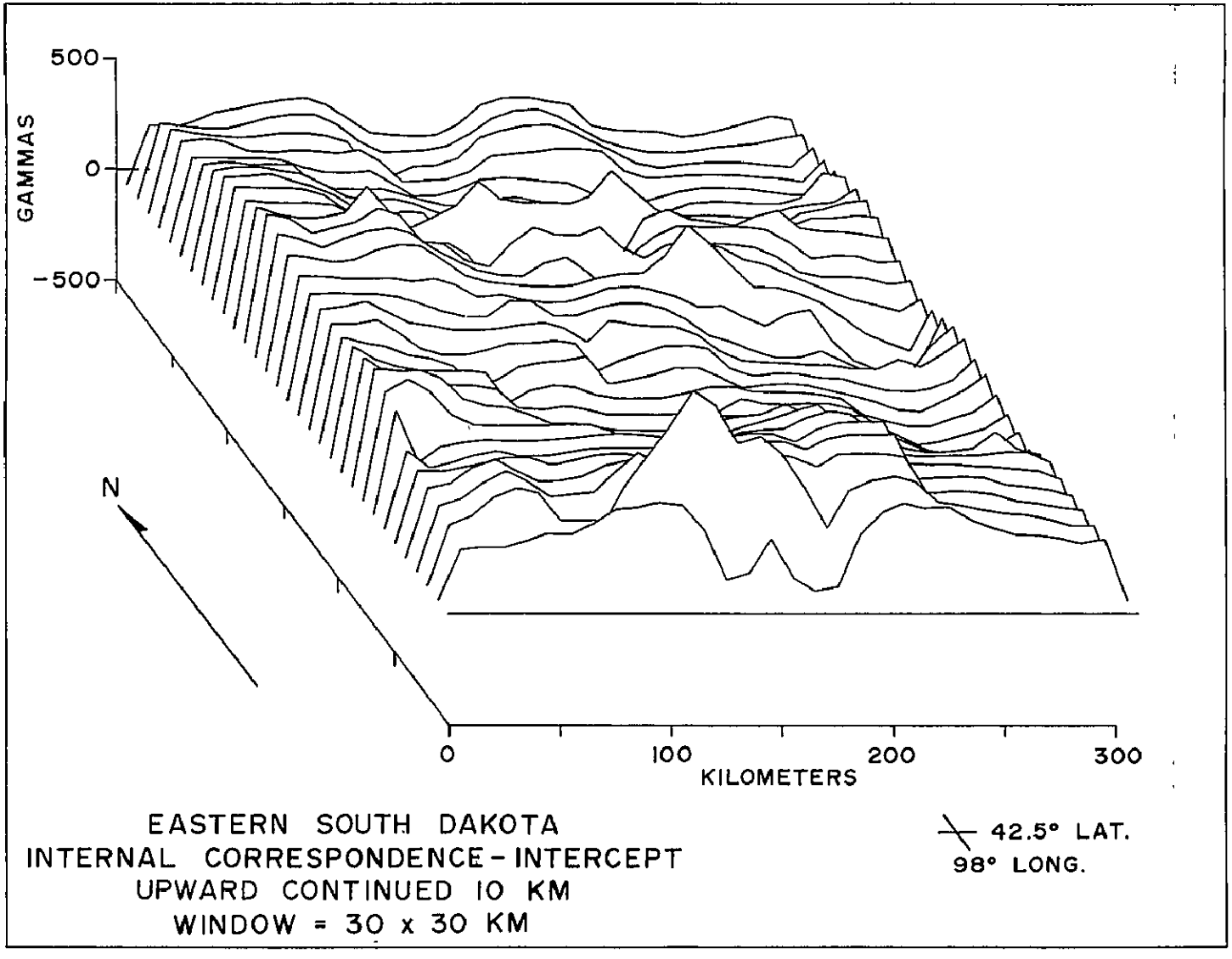

Figure 56. Eastern South Dakota internal correspondence analysis on upward continued to 10 km data: intercept coefficient.

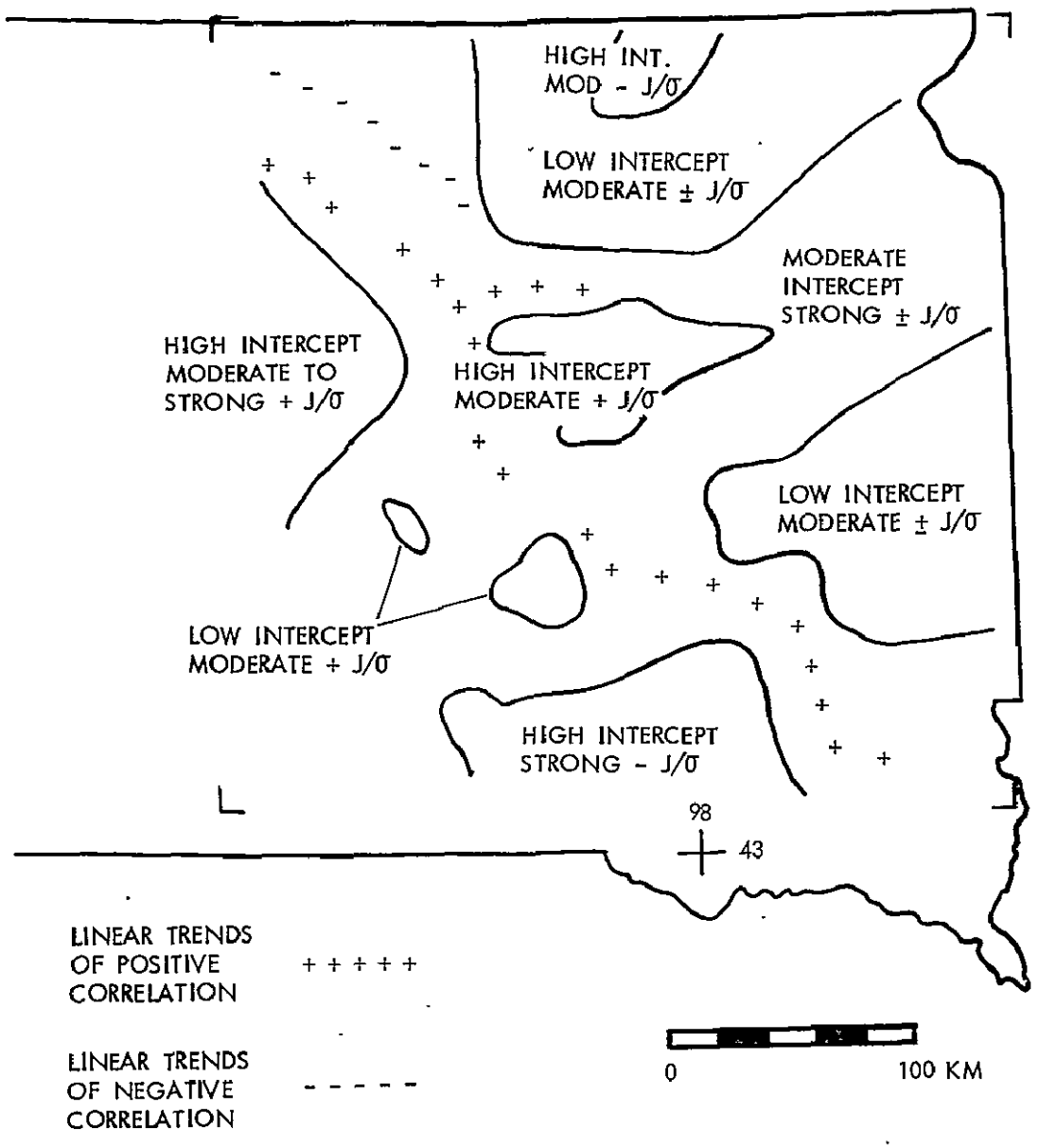

ANALYSIS BASED ON UPWARD CONTINUED 10 KM DATA (30 X 30 KM WINDOW)

Figure 57. Eastern South Dakota internal correspondence analysis summary diagram.

by upward continuation of all data to a common elevation of 50 km. The broad wavelength data, shown in Figures 58, 59 and 60, accentuates the contribution of deep crustal sources. Internal correspondence analysis was conducted using a 30 x 30 km moving window and the resulting correlation, $\Delta J/\Delta\sigma$, and intercept data are shown in Figures 61, 62 and 63. Line printer contour maps of all data were available for detailed analysis.

Several significant observations can be made from the 50 km level ICA data. The ICA coefficient data in the northeastern portion of the area show no strong correlation with the proposed position of the Morey-Sims boundary. This observation suggests that deep crustal structure may be similar on either side of the proposed boundary. The north central region shows a zone of positive correlation and high positive $\Delta J/\Delta\sigma$ estimates. A semi-continuous belt of similar ICA coefficient values appears to extend southeastward to the corner of the area. The most dramatic feature in the ICA data is a zone that extends northwest across the area and is characterized by large magnitude positive and negative $\Delta J/\Delta\sigma$ estimates and a very distinct decrease in intercept values to the northeast. This decrease indicates a significant change in anomaly base levels across the zone. The geographic position of the zone lies very close to Lidiak's proposed Churchill-Superior Province boundary. Thus, Lidiak's proposed boundary shows a relationship to the ICA data in both the 10 km and 50 km level data. The persistence of an apparent relationship during upward continuation suggests the structure has deep as well as shallow crustal significance.

Cluster Analysis

Cluster analysis was conducted on the 10 km level data using a 30 x 30 km subarea with ICA coefficients as variables (Figure 64). Correlation coefficients were the similarity measure and a cluster cutoff value of 0.6 was selected. A general correspondence appears to exist between the cluster indicated by the broad ruled lines and the

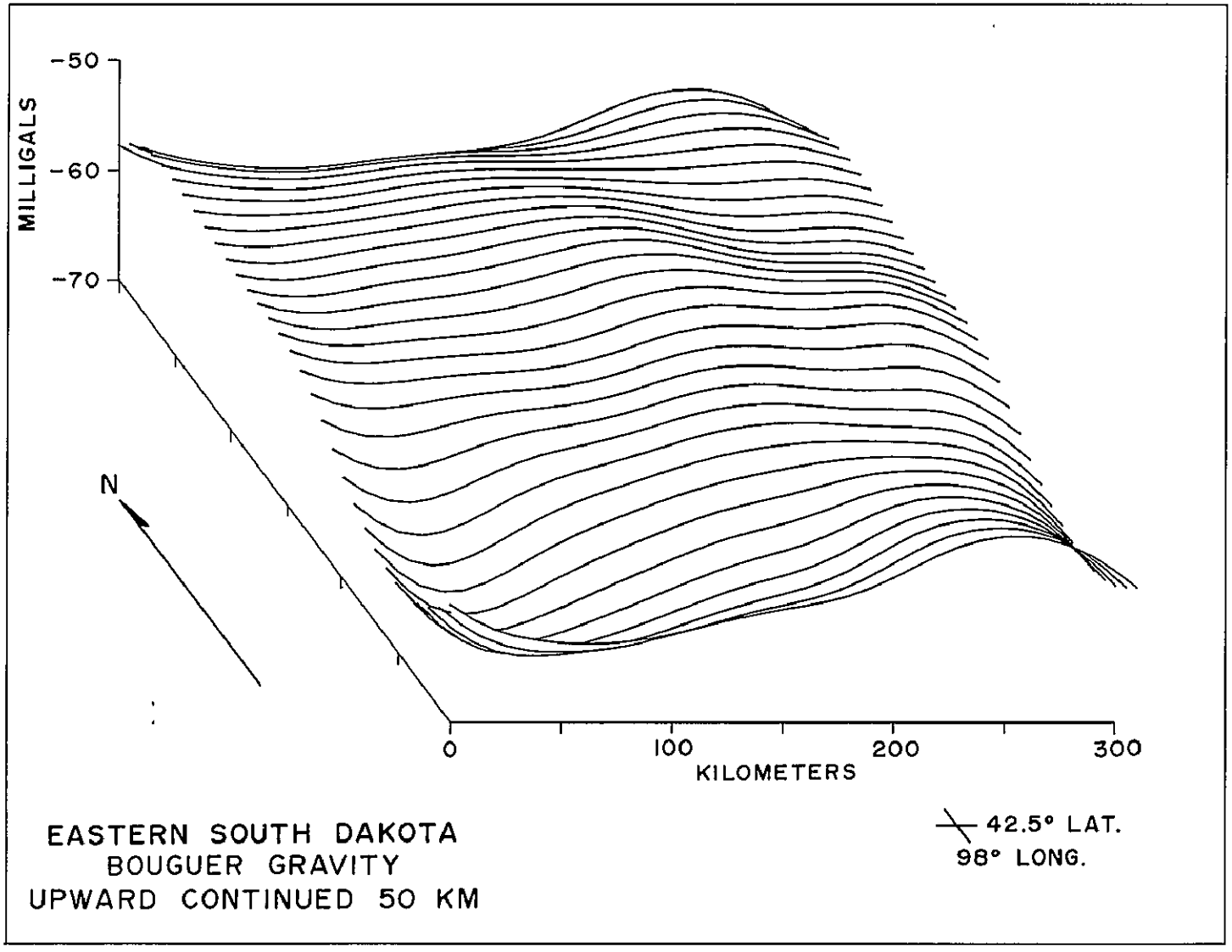

Figure 58. Eastern South Dakota gravity data, upward continued to 50 km.

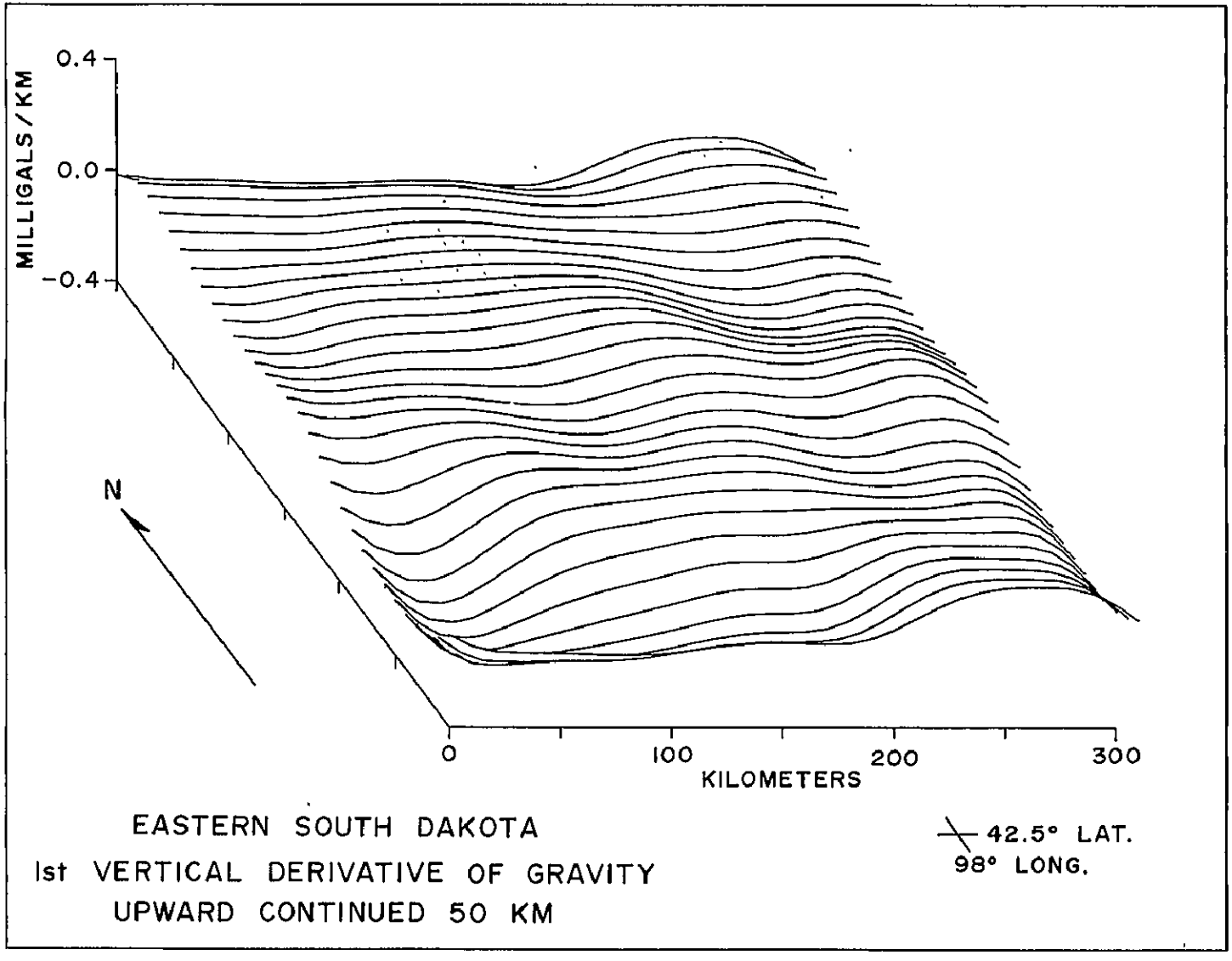

Figure 59. Eastern South Dakota first vertical derivative of gravity, upward continued to 50 km.

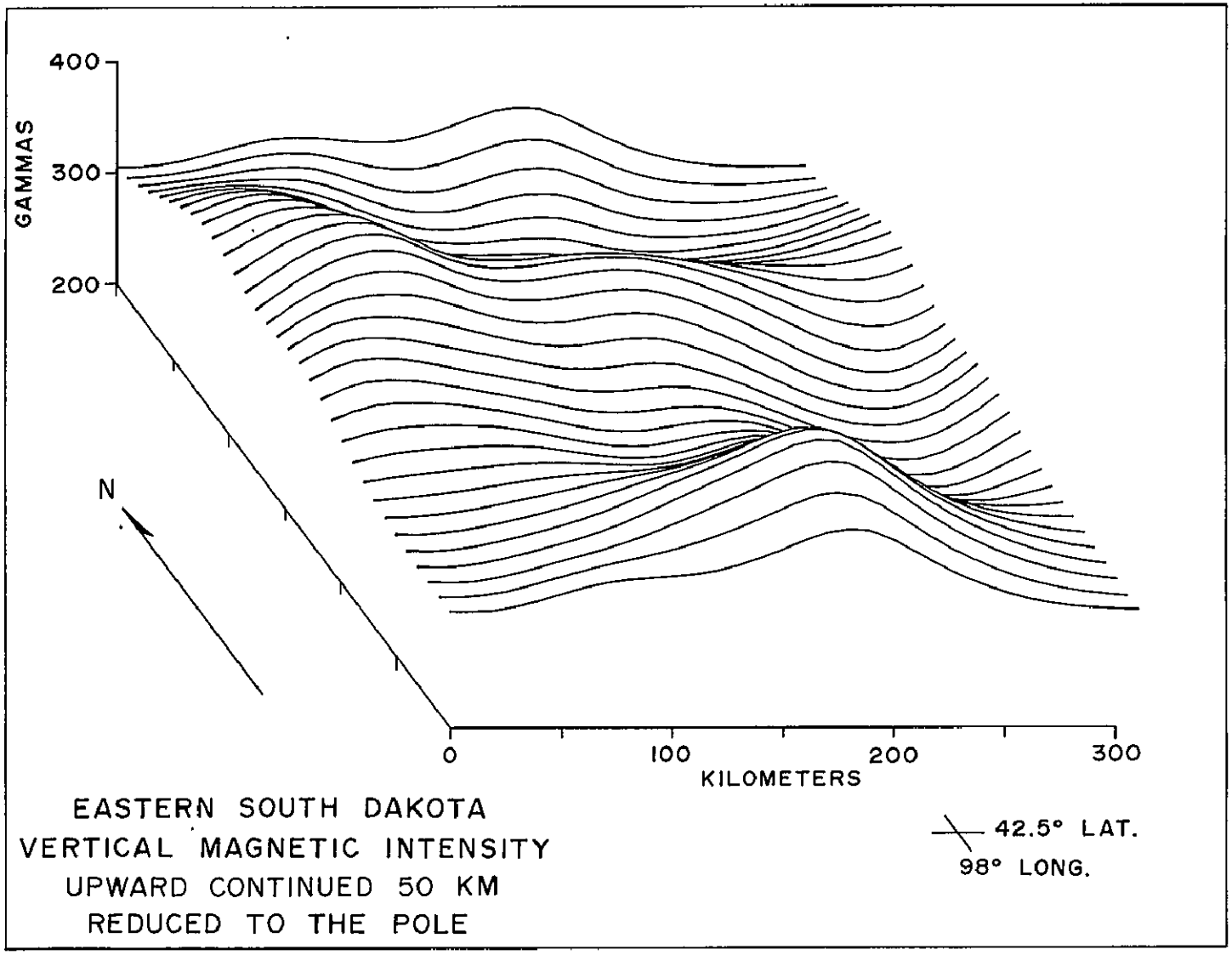

Figure 60. Eastern South Dakota magnetics reduced to the pole, upward continued to 50 km.

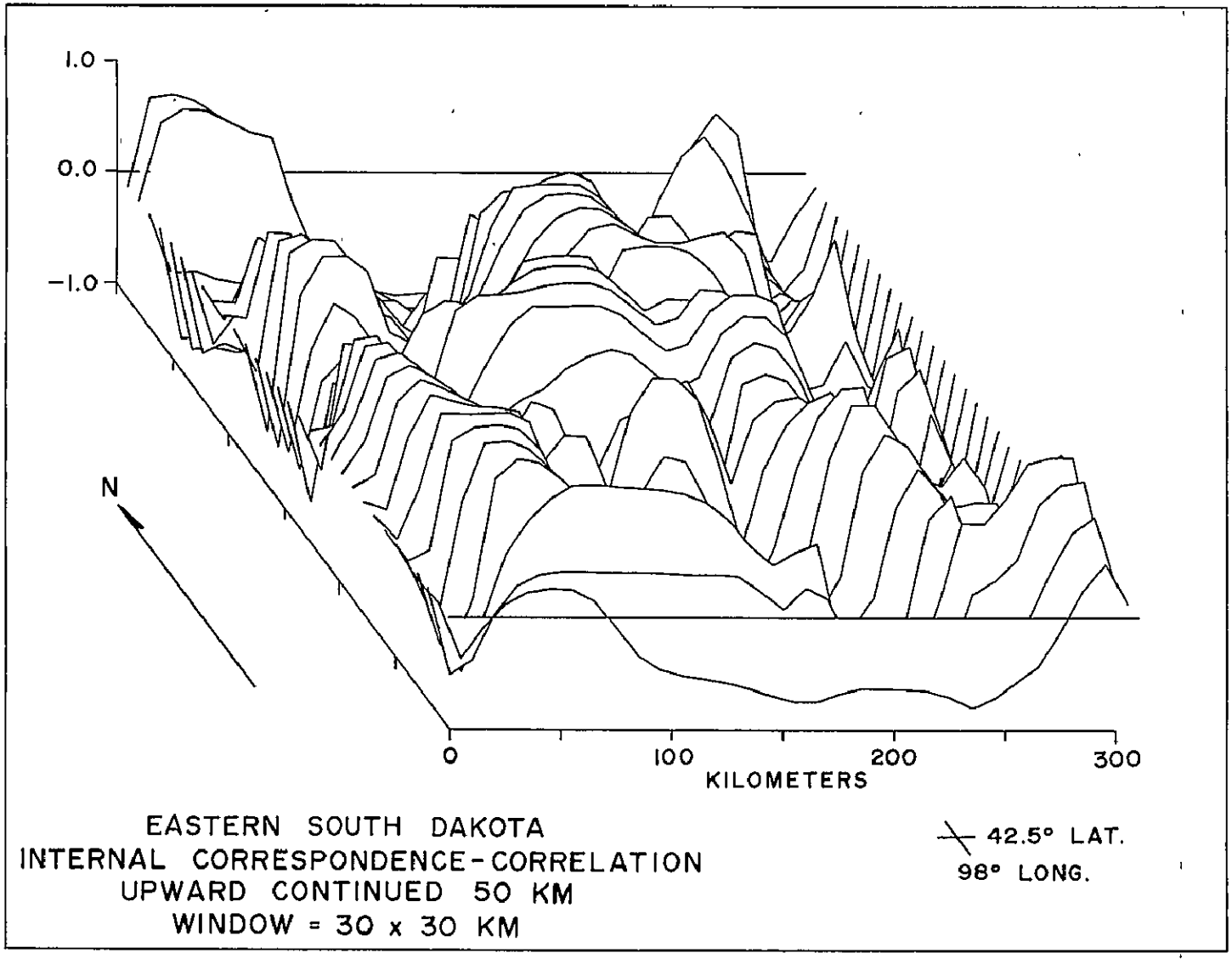

Figure 61. Eastern South Dakota internal correspondence analysis on upward continued to 50 km data: correlation coefficient.

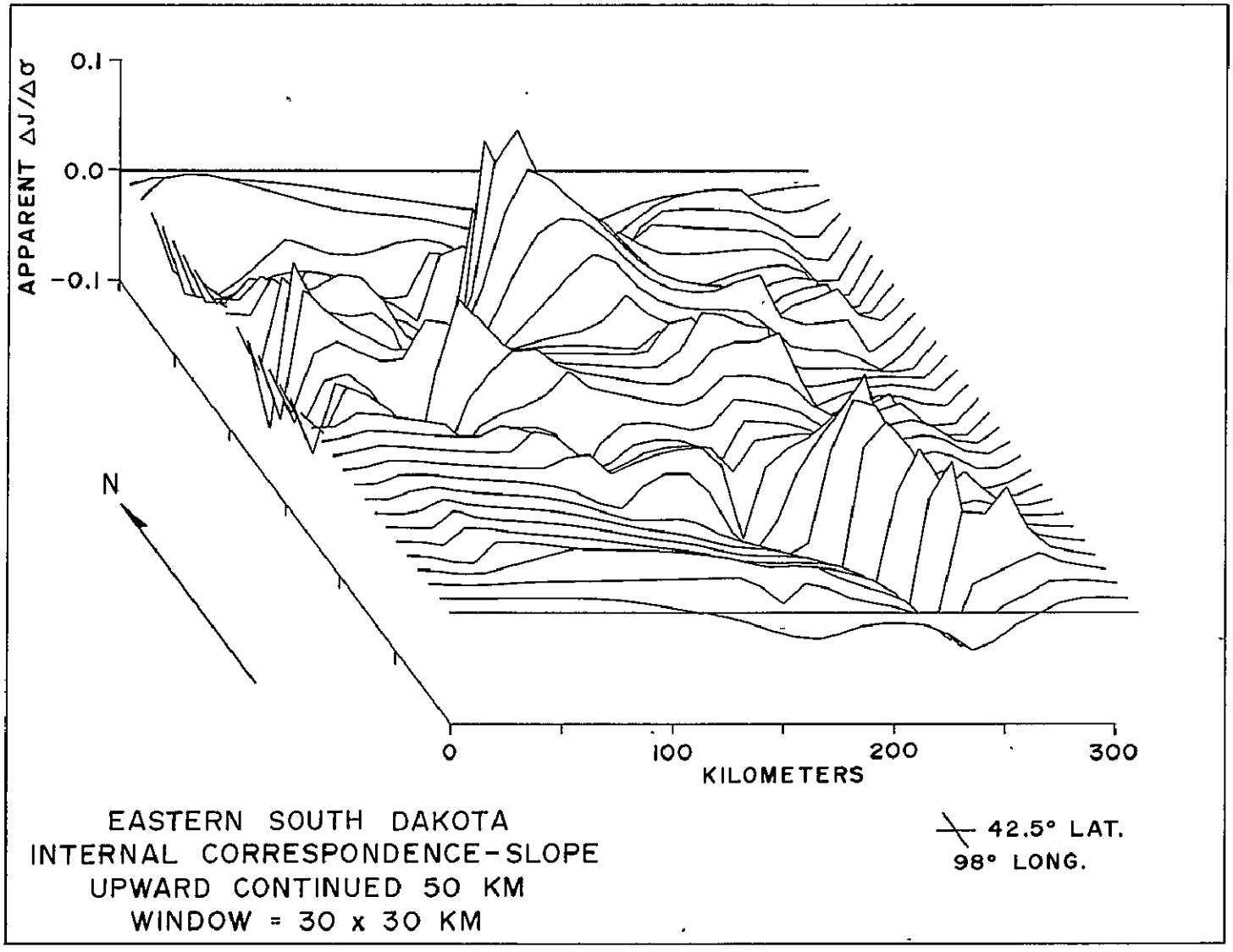

Figure 62. Eastern South Dakota internal correspondence analysis on upward continued to 50 km data: slope ($\Delta J/\Delta\sigma$) coefficient.

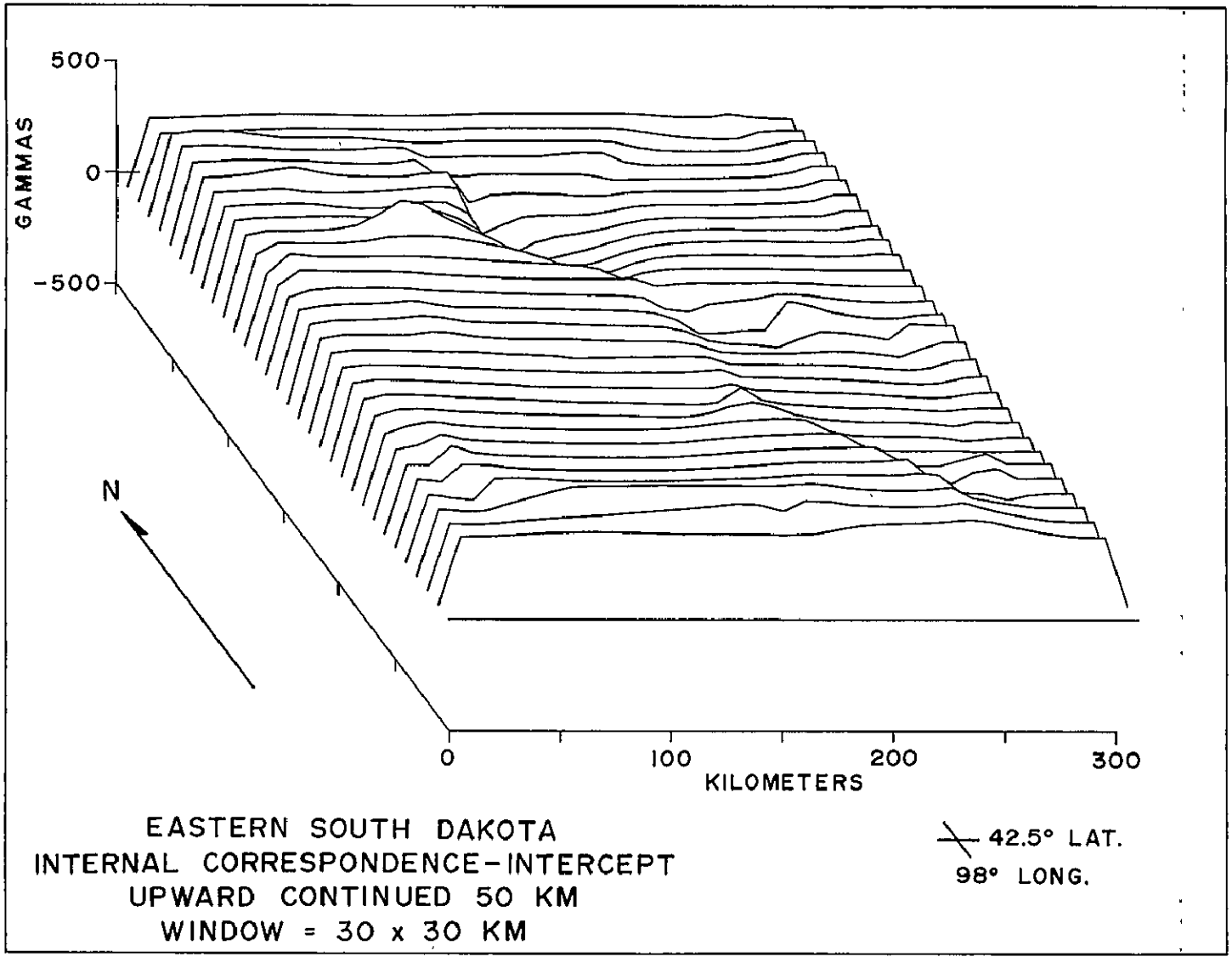

Figure 63. Eastern South Dakota internal correspondence analysis on upward continued to 50 km: intercept coefficient.

proposed Morey-Sims boundary. The subareas of this cluster occur either along or southeast of a line corresponding to an extension of the Morey-Sims boundary from Minnesota. This cluster is characterized by low intercept values, positive correlation, and moderate to large magnitude $\Delta J/\Delta\sigma$ estimates.

Cluster analysis was also conducted on the 10 km level data using a 50 x 50 km subarea size and six variables. The variables selected for this analysis were the mean and standard deviation of the azimuth of the magnetic horizontal gradients, the mean value of the magnetic horizontal gradients, and the three ICA coefficients. To avoid the undesirable effect of correlated variables, the six variables were transformed into six orthogonal, principal component variables using a program from Davis (1973). The results of the cluster analysis using a correlation coefficient similarity measure and a clustering cutoff of 0.25 are shown in Figure 65. Although the results of this clustering are difficult to evaluate, some suggestion of geological correlation is observed. For example, clusters designated by cross-hatching and broad ruled lines occur primarily along and southwest of the proposed Churchill-Superior Province boundary. However, the results are clearly not definitive.

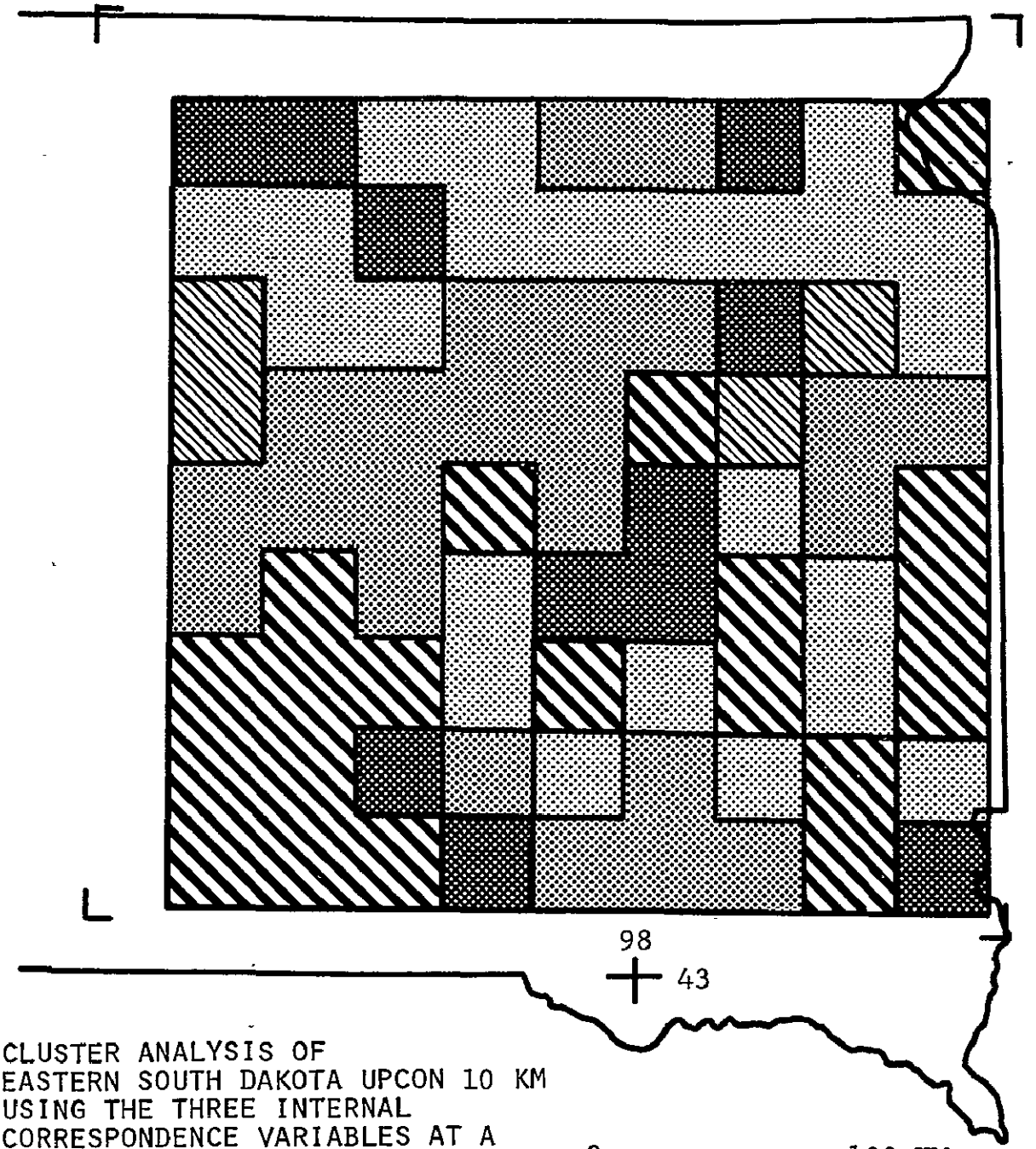

Figure 64. Eastern South Dakota cluster analysis on 10 km level data using the internal correspondence coefficients as variables.

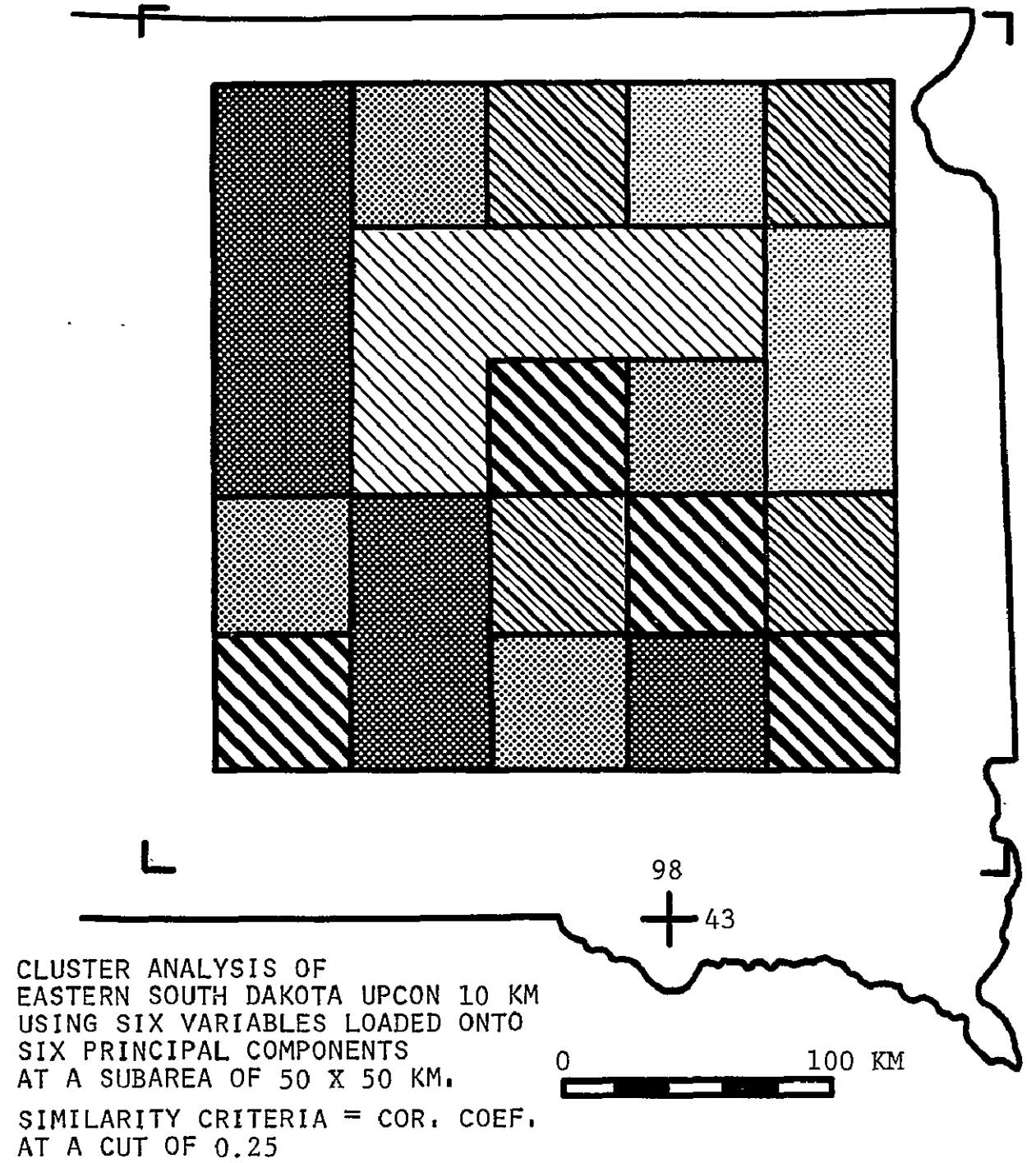

Figure 65. Eastern South Dakota cluster analysis on 10 km level data using the mean and standard deviation of the magnetic horizontal gradient, the average plunge of the magnetic horizontal gradient, and the three internal correspondence coefficients as variables.

CHAPTER VI

SUMMARY & RECOMMENDATIONS

The geological interpretation of gravity and magnetic data often relies heavily on an effective correlation of anomalies. The objectives of correlation can cover a dramatic range of scope, from a localized search for a shallow orebody to a study of regional crustal structure. In the past this correlation has usually been accomplished by subjective visual methods or by very restricted uses of Poisson's theorem. Recent studies have indicated that analytical correlation procedures are a more efficient and effective means of gravity and magnetic correlation. This study has developed two analytical methods, internal correspondence and cluster analysis, and evaluated their effectiveness through use of theoretical and observed data. Both methods resemble visual spatial correlation in that they analyze large, complex data sets simultaneously, but differ in their increased objectivity and quantitative results. Both methods can be used on profile and map data.

Principal attention was given to the internal correspondence analysis approach. This procedure involves Poisson's theorem in a moving window linear regression between the first vertical derivative of gravity and the magnetics at vertical polarization. Three regression coefficients - correlation, slope, and intercept are generated at each window position and yield significant information regarding base levels and the $\Delta J/\Delta\sigma$ estimates of apparent sources.

Analysis of theoretical and observed data indicates that crustal provinces often yield characteristic ICA coefficient values. Upward continuation may enhance this effect because at increased elevation, multi-source crustal provinces often begin to approximate a uniform source with a characteristic $\Delta J/\Delta\sigma$. In addition to recognizing crustal provinces, ICA provides valuable information on the horizontal and vertical variation of physical properties within the crust. Internal correspondence analysis also is capable of validating the presence of long wavelength anomalies and isolating problems of geomagnetic field removal schemes. Finally, it has been demonstrated that a statistical basis apparently exists for an internally based criterion that would aid in isolating valid $\Delta J/\Delta\sigma$ estimates from ICA.

Cluster analysis is a pattern recognition scheme that involves the classification of a data set into groups of similarity. The classification is based upon variables measured on each sample. In the case of gravity and magnetic data, subareas of the data set are treated as samples and variables consist of assorted parameters calculated from data existing in a particular subarea. Although at an embryonic stage, cluster analysis in this study demonstrates a sensitivity to crustal provinces in observed data. One particularly useful approach to clustering is using ICA parameters as variables. This approach delineates regional trends in the ICA data that may not be immediately apparent by visual examination.

Several directions for further investigations are apparent at the close of this segment of the study. In order to continue the current effort toward the analysis of satellite level data, both modeling and upward continuation schemes must be developed for a spherical earth. The regional as well as local effects of remanent magnetization should also be investigated. Future work with ICA would be aided by an automatic scheme that recognizes and determines the sign of a particular anomaly. The development of an automatic criterion that isolates valid ICA $\Delta J/\Delta\sigma$ estimates would prove extremely beneficial to the analysis of areas containing a multitude of interfering anomalies.

Several important problems involving cluster analysis should also be investigated in future work. There is a large selection of variables that can now be used in clustering; studies must be conducted to determine specifically what combination of variables are most critical to crustal province recognition. Due to the limitations of computer core, the current cluster analysis technique is restricted to the analysis of a relatively small number of subareas. This is the major reason that the subareas used in cluster analysis are non-overlapping. If the size of the sample set could be increased to include overlapping subareas, a more highly resolving and continuous portrayal of regional cluster distributions may be possible. This problem could be approached by using the cluster analysis of non-overlapping subareas as a training set to establish the principal clusters. Once the clusters have been

established, a relatively simple classification scheme could be used to assign the overlapping subareas into the clusters. The incorporation of more advanced pattern recognition techniques such as supervised learning and discriminant analyses also may prove very beneficial to the correlation of gravity and magnetic data.

Finally, the geological significance of ICA and cluster analysis must be further investigated by analysis of additional observed data. Gravity and magnetic data from a 1000 x 1000 km area over the North American Great Lakes Region has recently been digitized at a 5 km interval. This area contains several major crustal structures and provinces and the analysis of these data should reveal significant information regarding the crustal structure of the region.

The techniques developed in this study should not be necessarily restricted to the analysis of continental data. The application of the proposed methods to oceanic and plate margin data should also be investigated. The comparison of analyses over continental and oceanic areas may be significant, especially to satellite level data. In addition, the incorporation of oceanic and plate margin data would bring the methods proposed by this study within the vast realm of current plate tectonic studies. The revealing success of the proposed methods in cratonic areas clearly indicates that they should be attempted in this currently dynamic realm.

REFERENCES

Baranov, V., 1957; A new method for interpretation of aeromagnetic maps; pseudogravimetric anomalies: Geophysics, v. 22, p. 359-382.

Bhattacharyya, B.K., 1965; Two-dimensional harmonic analysis as a tool for magnetic interpretation: Geophysics, v. 30, p. 829-857.

Bhattacharyya, B.K., 1972; Design of spatial filters and their application to high resolution aeromagnetic data: Geophysics, v. 37, p. 829-857.

Chandler, V.W., Hinze, W.J., and Braile, L.W., 1975; Preliminary results of combined magnetic and gravity analysis: Transactions, American Geophysical Union, v. 56, no. 9, p. 597.

Craddock, C., Mooney, H.M., and Kolehmainen, V., 1970; Simple Bouguer gravity map of Minnesota and northwestern Wisconsin: Geol. Survey University of Minnesota miscellaneous map series map M-10.

Davis, J.D., 1973; Statistics and Data analysis in Geology: New York, John Wiley and Sons, Inc., 550 p.

Fenneman, N.M. and Johnson, D.W., 1969; Physical Divisions of the United States: U.S. Geological Survey Index Map.

Hinze, W.J., Braile, L.W., Chandler, V.W., and Mazzella, F.E., 1975; Combined magnetic and gravity analysis: Final Report NASA Contract No. S-500 29A Modification No. 8, 87 p.

Lidiak, E.G., 1971; Buried Precambrian rocks of South Dakota: Geol. Soc. America Bull., v. 82, p. 1411-1420.

Mayhew, M.A., and Davis, W.M., 1976; A magnetic anomaly map of North America from satellite data: Proceedings of the Second International Conference on the New Basement Tectonics, Univ. of Delaware.

Morey, G.B., and Sims, P.K., 1976; Boundary between two Precambrian W. terrains in Minnesota and its geologic significance: Geol. Soc. America Bull., v. 87, p. 141-152.

Pakiser, L.C. and Zietz, I., 1967; Transcontinental crustal and upper mantle structure: Rev. of Geophysics, v. 3, p. 505-520.

Petsch, B.C., 1967; Vertical intensity map of South Dakota; Ground magnetometer survey: South Dakota Geol. Survey Mineral Resource Investigations Map no. 4.

Poisson, S.D., 1826; Memoire sur la theorie du magnetisme: Memoires de la l'acadamie royale des sciences de l'Institut de France, p. 247-348.

Riggs, E.A., 1960; Major Basins and Structural Features of the United States: The Geographical Press; C.S. Hammond & Co., Maplewood, N.J.

Robinson, A.H., 1962; Mapping the correspondence of isoarithmic maps: Annals of the Association of American Geographers, v. 52, p. 414-425.

Zietz, I. and Kirby, J.R., 1965; Aeromagnetic and gravity profiles of the United States along the 37th parallel; A contribution to the upper mantle project: U.S. Geol. Survey Geophysical Investigation Map GP-597.

Zietz, I., Bateman, P.C., Case, J.E., Crittenden, M.D., Jr., Griscom, A., King, E.R., Roberts, R.J., and Lorentzen, G.R., 1969; Aeromagnetic investigation of crustal structure for a strip across the western United States: Geol. Soc. America Bull., v. 80, p. 1703-1714.

Zietz, I., and Kirby, J.R., 1970; Aeromagnetic map of Minnesota: U.S. Geol. Survey Geophysical Investigations Map GP-725.